UNIVERSIDADE FEDERAL DE SERGIPE
PRÓ-REITORIA DE PÓS-GRADUAÇÃO E PESQUISA

ANÁLISE MULTITEMPORAL DOS AJUSTES MORFOLÓGICOS NO BAIXO RIO SÃO FRANCISCO (NORDESTE, BRASIL): IMPACTOS DA BARRAGEM DE XINGÓ NA DINÂMICA FLUVIAL

Pedro Victor Oliveira Gomes

Orientador: Dr. Felipe Torres Figueiredo

DISSERTAÇÃO DE MESTRADO

Programa de Pós-Graduação em Geociências e Análise de Bacias

São Cristóvão-SE
2021

Pedro Victor Oliveira Gomes

ANÁLISE MULTITEMPORAL DOS AJUSTES MORFOLÓGICOS NO BAIXO RIO SÃO FRANCISCO (NORDESTE, BRASIL): IMPACTOS DA BARRAGEM DE XINGÓ NA DINÂMICA FLUVIAL

Dissertação apresentada ao Programa de Pós-Graduação em Geociências e Análise de Bacias da Universidade Federal de Sergipe, como requisito para obtenção do título de Mestre em Geociências.

Orientador: Dr. Felipe Torres Figueiredo

São Cristóvão–SE
2021

FICHA CATALOGRÁFICA ELABORADA PELA BIBLIOTECA CENTRAL
UNIVERSIDADE FEDERAL DE SERGIPE

Gomes, Pedro Victor Oliveira
G633a Análise multitemporal dos ajustes morfológicos no baixo rio São Francisco (Nordeste, Brasil) : impactos da barragem de Xingó na dinâmica fluvial / Pedro Victor Oliveira Gomes ; orientador Felipe Torres Figueiredo. – São Cristóvão, SE, 2021.
112 f. : il.

Dissertação (mestrado em Geociências e Análise de Bacias) – Universidade Federal de Sergipe, 2021.

1. Geociências. 2. Barragens e açudes – Brasil, Nordeste. 3. Canais fluviais – Aspectos ambientais. 4. Mudanças climáticas. 5. Usina Hidrelétrica de Xingó. 6. São Francisco, Rio. I. Figueiredo, Felipe Torres, orient. II. Título.

CDU 551.4.04:627.82(282.281.5)

ANÁLISE MULTITEMPORAL DOS AJUSTES MORFOLÓGICOS NO BAIXO RIO SÃO FRANCICO (NORDESTE, BRASIL): IMPACTOS DA BARRAGEM DE XINGÓ NA DINÂMICA FLUVIAL

por:

Pedro Victor Oliveira Gomes
(Geólogo, Universidade Federal de Sergipe – 2019)

DISSERTAÇÃO DE MESTRADO

Submetida em satisfação parcial dos requisitos ao grau de:

MESTRE EM GEOCIÊNCIAS

BANCA EXAMINADORA:

Dr. Felipe Torres Figueiredo [Orientador – PGAB/UFS]

Dr. Cristiano Padalino Galeazzi [Membro Externo – SNU]

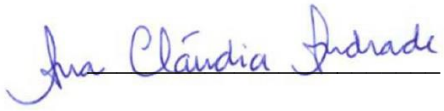

Dra. Ana Cláudia da Silva Andrade [Membro Interno – PGAB/UFS]

Data Defesa: 27/05/2021

RESUMO

Após a sucessiva construção de 6 grandes barragens ao longo do último século, principalmente após a construção da barragem de Xingó, o baixo curso do rio São Francisco (BSF) sofreu reduções na descarga média de água e na sua capacidade de transportar a carga sedimentar em direção a sua foz. Apesar disso, a discussão sobre a avaliação do papel das barragens e do clima nos ajustes morfológicos do rio São Francisco é escassa. Para preencher essa lacuna e avaliar o papel do reservatório de Xingó nos ajustes morfológicoss, esse trabalhou objetivou a caracterização e quantificação dos ajustes que ocorreram no BSF. Para isso foi utilizada uma série temporal de 35 anos, assim como dados de descarga de água e sedimentos ao longo de 17 trechos entre a barragem de Xingó e a cidade de Penedo (estado de Alagoas). Para avaliar a influência das mudanças climáticas ao longo do BSF, realizamos ajustes de regressões lineares confrontando dados de pluviosidade e vazão durante os períodos pré (1941-1961) e pós-Xingó (1995-2018). As imagens de satélite demonstraram um predominância de ajustes morfológicos internos ao canal em relação aos externos, com uma baixa taxa de migração lateral e uma pequena variação da sinuosidade do canal.Após a construção de Xingó, o percentual de barras de meio de canal manteve-se constante nos grupos mais próximo à barragem (G1 e G2), enquanto o G3 apresentou um aumento nas de leito. Entretanto, com a diminuição das vazões devido à redução das chuvas na bacia de drenagem, os sedimentos passaram a ser depositados cada vez mais próximos da barragem. Este processo levou também ao aumento da taxa de entrelaçamento do canal no BSF. Foi com o início desse período de seca prolongada (2013-presente) que as maiores diminuições na largura do canal ocorreram em todos os trechos analisados. Esse período de estiagem foi responsável pela diminuião de 40,4% da vazão no período pós-Xingó, representando o principal controle das vazões de água e dos ajustes morfológicos decorrentes dessa diminuição. Portanto, a redução nas descargas defluentes da barragem de Xingó, assim como as demais localizadas rio acima, é, em grande parte, uma consequência da redução da pluviosidade na bacia do rio São Francisco.

Palavras-chave: Rios barrados, Barragem de Xingó, Morfologia fluvial, Descarga efetiva, Estreitamento do canal, Mudanças climáticas.

ABSTRACT

After successive impoudments of 6 big dams stations troughout the last hundred years, particularly after the facility of Xingó was build , the lower course of São Francisco River (LSFR) suffered a reduction in the average water discharge and is no longer capable to transport most of sandy bed load sediments towards its mouth. Nevertlheless, a discussion assessing the role of dams and climate changes on the São Francisco River morphological ajdustments is scarce. In order to fullfill that gap and evaluate the role of Xingó´s reservoir on morphological adjustments we focused on the characterization and quantification of the morphological adjustments in the LSFR. To do so, a time series of satellite images were chosen, and water, sediment discharges data were used along seventeen reaches. To assess the influence of climate change along the drainage basin we carried out a linear regression aproach using a pre and post-dam time series comparison along. Our satellite images demonstrate a predominance of internal adjustments to the channel in relation to external ones, with low values of lateral migration rate and little variation in channel sinuosity. After the construction of the Xingó dam, the percentage of sand bars remained constant in the groups closest to the dam (G1 and G2), while G3 presented an increase in bed forms. However, with the decrease in water discharges due to the decrease in rainfall in the river basin, sediments started to be deposited closer and closer to the dam. This process is also responsible for increasing the channel interlace rate in the LSFR. It is during this period of prolonged drought (2013-present) that the largest decreases in channel width occurred in all LSFR reaches. This dry period was responsible for the 40.4% decrease in discharges in the post-Xingó period, representing the main control over the decrease in water discharge and the morphological adjustments resulting from this decrease. Thus, the reduction in effluent discharges from Xingó, and from other dams upstream, is largely a consequence of lower rainfall in the drainage basin.

Keywords: Dam rivers, Xingó dam, Fluvial Morphology, Effective Discharge, Channel Narrowing, Cimate Changes

SUMÁRIO

LISTA DE FIGURAS

Capítulo 1 - Introdução

Capítulo 2 – Multitemporal analysis of morphological adjustments in the Lower São Francisco River (Northeast, Brazil): impacts of the Xingó dam on river dynamics

LISTA DE TABELAS

Capítulo 1 - Introdução

Capítulo 2 - Multitemporal analysis of morphological adjustments in the Lower São Francisco River (Northeast, Brazil): impacts of the Xingó dam on river dynamics

Appendix

CAPÍTULO 1 – INTRODUÇÃO

1.1 - Apresentação

Os principais rios do planeta têm um papel central no desenvolvimento de várzeas e no escoamento de água e sedimentos para os oceanos (Gupta, 2007). A maioria deles está sujeita a barreiras naturais e mudanças de declive ao longo da área de drenagem, especialmente em seus trechos mais baixos, que invariavelmente forçam os cursos dos rios a mudanças morfológicas naturais (Schum e Lichty, 1965). No entanto, durante o século XX, a implantação de barragens acrescentou complexidade ao gerenciamento dos ajustes fluviais (Milliman, 1997; Wallick et al., 2007). Os cursos dos rios modificaram severamente sua trajetória espacial, mas o mais importante, também afetaram sua capacidade de preservar as mudanças naturais da bacia de drenagem. Consequentemente, os fluxos do rio a jusante alteraram suas margens e o leito ao longo do tempo (Meade, 1996; Wohl, 2007; Ma et al., 2012). Vários pesquisadores estudaram o efeito de barragens em regimes de estágio de fluxo e morfologia de canal sucessiva desde o século passado (Gregory e Park, 1974; Petts, 1979; Galay, 1983; Williams e Wolman, 1984; Carling, 1988; Jiongxin, 1990a. B ; Thoms e Walker, 1993; Benn e Erskine, 1994; Zhou, 1996; Morris e Fan, 1997; Phillips, 2003, Petts e Gurnell, 2005; Phillips et al., 2005; Magilligan et al. 2008; Bandeira et al. , 2008; Zahar et al., 2008; Ma et al., 2012; Zhou et al., 2015; Wu et al., 2015; Zhou et al., 2017., Li et al., 2018; Kong et al. , 2020; Petts e Gurnell, 2021).

Trabalhos detalhados contribuírampara o entendimento sobre como as descargas de água e sedimentos modificam a dinâmica fluvial em diferentes escalas de tempo: horárias até anuais (Magilligan e Nislow, 2001; Petts e Gurnell, 2005; Vericar e Batalla, 2006; Ma et al., 2012). Um dos ajustes mais rápidos e relevantes é a diminuição das cheias, agora com efluências regulamentadas (Souza Filho et al., 2004; Lehner et al., 2011; Grill et al., 2015; Roman, 2017; Best , 2019; Wang et al., 2021). Outro ajuste esperado diretamente relacionado a obras de engenharia (Harmar et al., 2015; Kesel, 2003) é a redução da carga de sedimentos, que é observada em uma diversidade de rios barrados na América do Norte (Williams e Wolman, 1984, Jacobson et al., 2009; Heimann et al., 2011) e Ásia (Rustomji et al., 2008; Gupta et al., 2012, Yang et al., 2014). A retenção de água no reservatório da barragem leva a um declínio da capacidade natural de escoamento do rio a um aumento da capacidade erosiva, o que impõe ao rio uma série

de ajustes morfológicos (Wallin, 2006; Gupta et al., 2012). A diminuição do aporte sedimentar pode aumentar a capacidade de erosão devido ao de fluxo livres de sedimentos (Nouh, 1990; Chen et al., 2010), o que leva à degradação da margem do rio e do leito (Petts, 1979; Choi et al., 2005; Magilligan e Nislow, 2005; Dai e Liu, 2013). Como consequência adicional, os processos erosivos têm maior probabilidade de se intensificar na foz do rio (c; Syvitski et al., 2005; Syvitski et al., 2009). Por essas razões, muitos pesquisadores concentram seus esforços estudando os ajustes morfológicos indesejáveis mais significativos (Higgs e Petts, 1988; Zhou, 1996; Surian, 1999; Nelson et al., 2013; Kong et al., 2020) e a geração de modelos conceituais para quantificar o impacto em rios barrados (Brandt, 2000; Schimidt e Wilcock, 2008; Skalak et al., 2013; Grill et al., 2015).

Outra questão ainda em debate é se as mudanças climáticas em curso (Nakicenovic et al., 2000; Marengo et al., 2012; Assis et al., 2015; Getirana, 2016; Marengo et al., 2017; Santos et al., 2017; Souto et al., 2019) podem desempenhar um papel significativo nos regimes hidrológicos e sedimentológicos nos sistemas fluviais, apesar da influência da barragem (De Jong, 2018; Dominguez & Guimarães, 2021), e qual poderia ser o principal fator de controle. A mudança climática é a resposta mais frequente, com as alterações resultado do efeito estufa sendo evidênciadas pela diminuição da pluviosidade e o aumento dos períodos de seca nas últimas décadas (Trenberth et al., 2014; Jenkins e Warren, 2015; Yang et al., 2015; Best, 2019). Adicionalmente, alguns autores argumentam que as mudanças climáticas e fatores antropogênicos podem reduzir a produção sedimentar de bacias de captura (Meade e Moody, 2010; Yang et al., 2015; Genz e Luz, 2018; Dominguez e Guimarães, 2021; Wang et al., 2021). Consequentemente, são esperados impactos de abastecimento e ecológicos (Trinity River Flow Evaluation, 1999; Brando et al., 2014; Lesk et al., 2016). Além disso, outros efeitos colaterais afetariam a produção de alimentos (Getirana, 2016) refletindo em prejuízos econômicos como na agricultura, pecuária e indústria que demandam abastecimento de água para operar e gerar energia elétrica (Jekins e Warren, 2015, Sun, 2016, Lucena et al. 2009; de Jong, 2018).

No Brasil, apesar da quantidade de rios barrados e dos efeitos causados tanto na paisagem quanto nas economias locais, poucos trabalhos relacionam os ajustes morfológicos à implantação de barragens de hidrelétricas, a exemplo dos raros trabalhos sobre o rio São Francisco (Borges, 2004; Stevaux et al., 2009; Fontes et al., 2009; Medeiros et al., 2011; Medeiros et al., 2014). O rio atualmente enfrenta problemas semelhantes em seu curso inferior, e a barragem de Xingó é considerada um marco nos

impactos ambientais (Fontes et al., 2009; Cavalcante, 2011; Santos et al., 2012). Este rio é o quarto maior rio da América do Sul e a principal fonte de água doce na região semi-árida do Nordeste do Brasil, o que demonstra a importância de uma boa gestão de caráter nacional desta bacia. Apesar disso, estudos anteriores se concentraram em documentar erosões de margens em pontos específicos (por exemplo, Casado et al.2002; Fontes 2015) e na planície deltaica (por exemplo, Oliveira et al., 2003; Bandeira et al., 2008, Dominguez e Guimarães, 2021). Até o momento, poucos trabalhos investigaram ajustes morfológicos no baixo rio São Francisco (Cavalcante, 2011; Fontes, 2015) ou a interação do clima e regulação de barragens como fatores combinados que governam os ajustes morfológicos (Dominguez & Guimarães, 2021).

Para abordar uma perspectiva mais ampla da influência da barragem de Xingó sobre a morfologia Baixo São Francisco, analisamos 17 trechos de seu baixo curso, localizados entre os estados de Sergipe e Alagoas, no nordeste do Brasil. Nossos objetivos foram caracterizar e quantificar os ajustes morfológicos considerando séries temporais de imagens de satélite antes e depois da construção de Xingó. Além disso, debatemos como as descargas controladas por Xingó afetam o padrão do canal principal descrito na literatura (por exemplo, Silva et al., 2010; Medeiros et al., 2014) ou se as mudanças climáticas influenciam os ajustes morfológicos observados.

Os resultados dessa pesquisa foram organizados e discutidos na forma de um artigo científico intitulado "*Multitemporal analysis of morphological adjustments in the Lower São Francisco River (Northeast, Brazil): impacts of the Xingó dam on river dynamics*", submetido à revista *Geomorphology* (QUALIS CAPES – A2).

1.2 - Objetivos

O objetivo geral da dissertação foi quantificar espacialmente e no tempo e identificar os principais controles das modificações geomorfológicas ocorridas em 17 trechos, em um total de 185 km de extensão de canal no baixo curso do rio São Francisco, entre a barragem de Xingó e a cidade de Penedo nos últimos 35 anos.

Como objetivos específicos pretendeu-se:

- Analisar imagens de satélite nos 17 trechos antes e após a construção de Xingó;

- Quantificar variações de métricas como: sinuosidade do canal, taxa de entrelaçamento, largura, migração lateral e porcentagem de barras de meio de canal e largural do canal em cada trecho;

- Interpretar aqueles trechos com maiores variações de cada uma das métricas acima;

- Apontar os trechos mais críticos dos pontos de vista de degradação e assoreamento do canal;

- Correlacionar as modificações morfológicas mais significativas com diferentes escalas de tempo;

- Discutir as hipóteses de influência da barragem de Xingó, do clima e de aspectos naturais sobre as modificações geomorfológicas interpretadas na escala de décadas.

1.3 - Localização da área

O rio São Francisco se estende por aproximadamente 2.863 km e sua bacia de captação de drenagem totaliza 641.10³ km², dividida em quatro regiões fisiográficas: alto, médio, submédio e baixo, em direção a sua foz no oceano Atlântico (Bernardes, 1951; De Jong et al., 2018). A área de estudo está localizada no baixo curso, que foi dividida em trechos equidistantes de 10 km de extensão, totalizando 185 km entre a barragem de Xingó e a cidade de Penedo (AL) (**Figura 1**).

O baixo curso é marcado por uma declividade média de 0,5 m/km. Próximo a barragem é marcado por uma paisagem de vale fluvial encaixado, onde o rio atravessa rochas ígneas e metamórficas da Faixa de Dobramentos Sergipana. À jusante, o rio expande a área do canal erodido rochas sedimentares da bacia de Sergipe-Alagoas (Fontes, 2015). Nessa mesma área, recebe o aporte sedimentar de pequenos tributários de natureza intermitente e efêmera, altamente dependente das características climáticas locais do semiárido alagoano e sergipano (Medeiros, 2011). Na proximidade das cidades de Propriá (SE) e Penedo (AL) o canal do rio atravessa uma planície aluvial marcada pela interação entre sedimentação continental fluvial e influenciada por processos costeiros eólicos e marinhos.

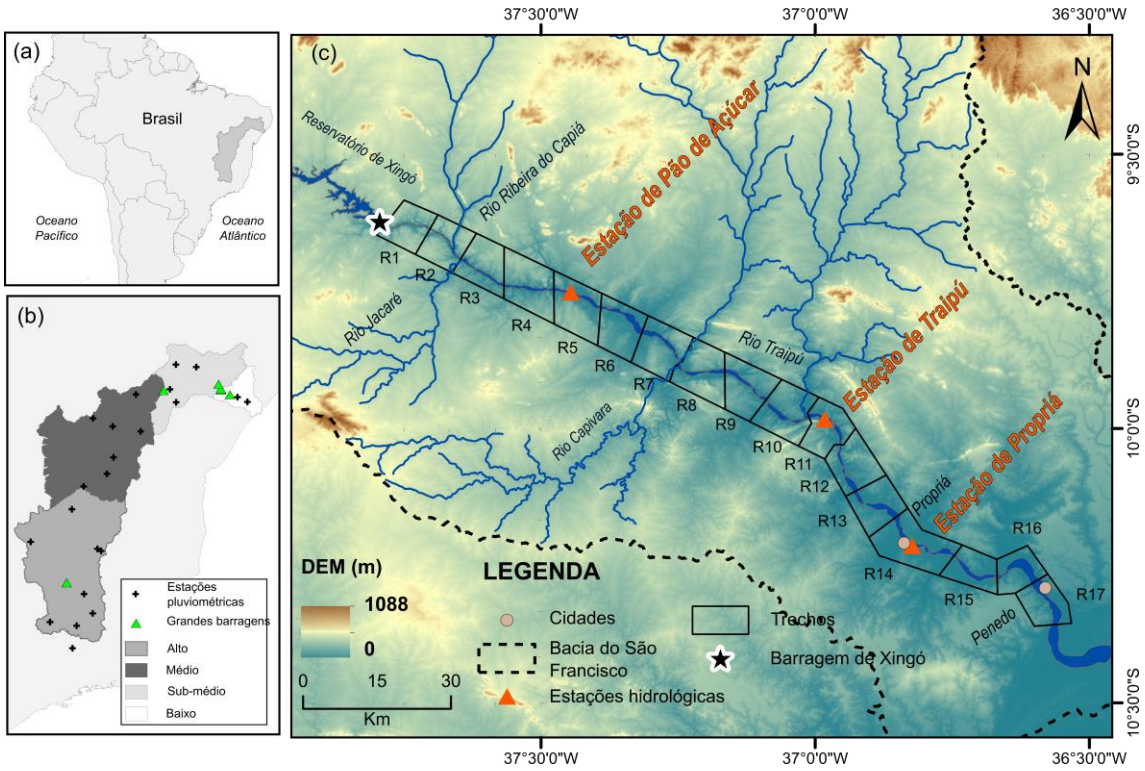

Figura 1. (a) Extensão da bacia do rio São Francisco desde a região Sudeste até o Nordeste do Brasil, (b) Regiões fisiográficas da bacia de drenagem, localização das grandes barragens (triângulos verdes) e estações pluviométricas (cruzes pretas), (c) Localização da área de estudo no Baixo Rio São Francisco entre a barragem de Xingó (estrela preta) e a cidade de Penedo (círculo preto). Os triângulos marrons indicam a localização das estações fluviométricas. Os trechos têm 10 km cada e estão numerados de R1 a R17.

1.4 - Métodos de trabalho

Foram utilizados dois tipos de materiais (imagens multitemporais de satélite e dados de vazão específica), aos quais foram aplicados os métodos descritos adiante.

1.4.1 - Aquisição e seleção de imagens Landsat

Para analisar a distribuição temporal de elementos morfológicos do canal fluvial foi utilizado um conjunto de treze imagens de satélite *Landsat* com resolução espacial de 15 e 30 m (sensores TM, ETM + e OLI), adquirido a partir do *website Earth Explorer* (https://earthexplorer.usgs.gov) da *United States Geological Survey* (USGS), totalizando dados dos últimos 35 anos (1985 e 2020) dos 17 trechos da área de estudo. Em função da

diferença de resolução espacial entre imagens de diferentes anos e excesso de cobertura de nuvens, alguns intervalos temporais foram descartados para que a comparação do tamanho dos elementos morfológicos fizesse sentido. Como primeiro critério de seleção de intervalos de imagens foram utilizados anos-chave anteriores à construção da barragem de Xingó (imagens de 1985 e 1992) e posteriores ao início da regulação de vazão em 1994 (imagens de 1996, 1998, 2001 e 2003). O segundo critério foi a adoção de anos posteriores aos eventos discretos de cheias registrados em 2004 e 2007 (imagens de 2004, 2009 e 2011) e aos períodos de baixa vazão (imagens de 2013, 2018 e 2020).

1.4.2 - Cálculo de métricas e análise de suas variações temporais

Como forma de analisar as variações temporais de cada métrica (porcentagem de barras de meio de canal, sinuosidade do canal, taxa de entrelaçamento do canal, largura do canal, taxa de migração lateral) e investigar trechos com predomínio de assoreamento ou erosão do canal principal foi preciso comparar cada trecho ao longo dos intervalos de interesse mencionados no item anterior. Para isto foi necessário adotar a seguinte rotina que levou em conta o tratamento e interpretação das imagens *Landsat*: *(1) construção de fotomosaicos, (2) composição de bandas, (3) Delimitação de elementos morfológicos, (4) Cálculo de métricas*

(1) Construção de fotomosaicos

Foram selecionadas imagens de cada ano mencionado acima e em seguida todas as imagens de mesmo ano foram integradas para a construção de uma imagem integrada que permitisse a visualização dos 17 trechos da área de estudo.

(2) Composição de bandas

Como forma de destacar os corpos d’água foram selecionadas bandas individuais das faixas espectrais do vermelho, infravermelho próximo e infravermelho de ondas curtas (*SWIR*) para formar composições coloridas (composição RGB543 para Landsat 5 e 7 e RGB654 para Landsat 8). As imagens Landsat 7 e Landsat 8 foram fundidas com a banda pancromática para aumentar a resolução espacial do pixel para 15 m.

(3) Delimitação de elementos morfológicos.

O método adotado para delimitação e medição de elementos fluvio-morfológicos foi baseado nas propostas de Nelson et al. (2013) e Kong et al. (2020). Estes autores propuseram a aplicação de ferramentas em *softwares* GIS como forma de extrair informações de área das barras e a largura média do canal. No presente trabalho foram utilizadas ferramentas de traçado vetorial e poligonal dentro do *software ArcGIS 10.4.1*. Através dele foi possível delimitar, de forma manual, os contornos de barras de meio de canal, área do canal, comprimento do canal principal e dos canais secundários, em cada imagem ao longo da área de estudo. Da mesma forma foi mapeado o traçado que define o limite do canal principal com as margens do rio. As linhas centrais do canal foram traçadas com a ajuda da extensão *River Bathymetry Toolkit* importada dentro do *ArcGis*.

(4) Cálculo de métricas

Algumas métricas como área de canal, de barras de meio de canal e de barras alternadas foram extraídas automaticamente dentro do *ArcGIS* após a etapa de delimitação destes elementos morfológicos. O cálculo de métricas como porcentagem das barras de meio de canal foi realizado dividindo a área de barras pela área do canal. O cálculo da taxa de entrelaçamento de canal e índice de sinuosidade seguiu à proposta de Friend e Sinhá (1993), e a determinação da taxa de migração lateral foi baseada no método de Giardino e Lee (2011).

Cada métrica foi calculada para os trechos pré-determinados (R1 à R17), e a porcentagem de barras de meio de canal e a largura do canal também foram utilizadas para a Análise de Componentes Principais (PCA) a fim de agrupar grupos com evoluções morfológicas semelhantes. As fórmulas utilizadas para a quantificação de cada métrica estão detalhadas na **Tabela 1** e os valores calculados estão nos APÊNDICES deste volume.

Tabela 1. Fórmulas utilizadas para o cálculo das métricas.

MÉTRICA	FÓRMULA	FONTE
Porcentagem de barras de meio de canal	$CB_{\%} = \frac{A_b}{A_c}$	Modificado de Kong et al. (2020)
Sinuosidade do canal	$P = \frac{Lc_{max}}{Lr}$	Friend e Sinhá (1993)
Taxa de entrelaçamento do canal	$B = \frac{Lc_{tot}}{Lc_{max}}$	Friend e Sinhá (1993)
Largura do canal	$W = \frac{A_c}{L_{central}}$	Nelson et al. (2013)
Taxa de migração lateral	$ML = \frac{A_m}{Lc_1} \times t$	Giardino e Lee (2011)

Onde:

A_b: área das barras de meio de canal; A_c: área do canal; Lc_{max}: comprimento do canal principal; Lr: comprimento em linha reta do canal; Lc_{tot}: somatório do comprimento do canal principal e dos canais secundários; $L_{central}$: comprimento da linha central do canal; A_m: área do polígono formado pela migração das linhas centrais entre dois anos; Lc_1: comprimento da linha central na data mais antiga; t: número de anos entre as datas 1 e 2.

Os elementos morfológicos, que por vezes ficavam encobertos pela presença de nuvens, impedia o cálculo e a comparação das áreas. Desta forma algumas imagens utilizadas cuja cobertura de nuvens variava entre 2% e 16%, poderia gerar o cálculo fictício de ausência de barras encobertas durante a extração automática da área. Para evitar isto, o uso de "zero" quando algum elemento estava encoberto foi substituído por um valor médio, calculado a partir de um dado de um ano antes e do primeiro ano subsequente. Valores de entradas "zero" foram considerados apenas para imagens relacionadas aos anos em que as barras não estavam parcialmente subaéreas, ou capturadas pela imagem na forma de uma duna composta sub-aquosa ou barra unitária. Nestes casos, as entradas "zero" foram consideradas representativas, uma vez que o objetivo era quantificar áreas submersas e sua variação ao longo do tempo. Nesse sentido, o conjunto de dados precisava primeiro ser validado e, portanto, comparado. Para tanto, as entradas de zero foram substituídas por pequenos valores próximos a zero (0,001) e a seguir atribuídos como valores mínimos.

Por fim, a taxa de alteração do tamanho da barra ao longo do período de 35 anos foi calculada dividindo os dados de 1985 por valores obtidos em 2020 de cada área. Barras de canal, larguras de canal, ganhos e perdas de áreas de canal também foram comparados por meio de uma análise de anos pareados.

1.4.3 – Descarga efetiva

A descarga efetiva (Qeff) relaciona-se aos principais processos morfológicos formadores do canal e é definida como a vazão, ou intervalo de vazões, capaz de transportar a maior quantidade de sedimentos (Wolman e Miller, 1960). Essa variável desempenha um papel relevante e mais expressivo no que diz respeito ao transporte de sedimentos e erosão das margens do que aquele desempenhado pela descarga d´água durante eventos de grandes cheias. Isto é devido a baixa frequência de recorrência do evento, mesmo quando comparada com a maior carga de sedimentos tais inundações extremas podem carregar (Stevaux e Latrubesse, 2017 ; Latrubesse, 2008).

No presente trabalho, o cálculo da descarga efetiva foi adaptado da metodologia publicada por Biedenharn et al. (1999). O conjunto de dados foi adquirido do repositório da ANA, a partir do qual foram utilizados os valores de carga de sedimento em suspensão e a série histórica de vazões. Para calcular a descarga efetiva, o conjunto de dados vazão foi dividido em vinte intervalos iguais. Em seguida, os dados de sedimentos em suspensão foram convertidos para toneladas por dia, usando a equação de Colby (1957):

$$\boldsymbol{Qs = 0,0864 \times Q \times C}$$

Onde: **Qs** representa a carga diária de sedimentos; **Q** é a vazão medida em m^3/s; **C** é a concentração do sedimento em mg/L; e 86.400 é o tempo por dia, convertido em segundos.

Os valores de carga de sedimentos foram então relacionados aos valores das vazões correspondentes, a fim de obter uma curva de carga de sedimentos aproximada, usando a seguinte fórmula:

$$\boldsymbol{Qts = aQ^b}$$

Onde: **Qts** representa a descarga total de sedimentos; **Q** é a vazão média de uma classe; **a** e **b** correspondem aos parâmetros ajustados em cada estação.

1.4.4 – Quantificação dos impactos das mudanças climáticas sobre a descarga de água

O método proposto por Yang et al. (2015) foi utilizado para a quantificação dos impactos causadas pelas mudanças de pluviosidade na bacia de drenagem. Para isso, estações pluviométricas localizadas ao longo de toda a bacia foram utilizadas (Figura 1b). Dados do período pós-Xingó (1995-2018) serviram como análise do comportamento da descarga de água (Q) em função da precipitação (P) (ver equação abaixo). Esses dados foram usados para prever os valores de vazão do período pré-Xingó (194-1961) baseado no acumulado mensal de chuvas. A diferença entre a vazão obtida através do ajuste da equação linear e a vazão observada nas estações fluviométricas da área de estudo representa o impacto causado pela mudança do regime pluviométrico da bacia.

$$\boldsymbol{Q = 52.441\,P - 2345.3} \quad ; \quad \boldsymbol{R^2 = 0.79}$$

1.5 - Bibliografia

Bandeira, J.V., Salim, L.H., Calisto Acosta, O.E., 2008. Long-term morphological impacts on the coastline of Sergipe State, Brazil, caused by the construction of dams in the São Francisco River Basin. In. In Seventh International Conference on Coastal and Port Engineering in Developing Countries–COPEDEC VII, Dubai, UAE.

Benn, P.C., Erskine, W.D., 1994. Complex channel response to flow regulation: Cudgegong River below Windermere Dam, Australia. Applied Geography. 14, 153–168.

Bernardes, L.M.C., 1951. Notas sobre o clima da bacia do Rio são Francisco. Revista Brasileira de Geografia. 13, 473-489, 1951.

Best, J., 2019. Anthropogenic stresses on the world's big rivers. Nature Geoscience. 12 (1), 7-21. https://doi.org/10.1038/s41561-018-0262-x.

Biedenharn, D.S., Thorne, C.R., Soar, P.J., Hey, R.D., Watson, Ch.C., 1999. A practicalguide to effective discharge calculation (Appendix A). in: Watson, C.C., Biedenharn, D.S., Torne, C.R. (Eds.), Demonstration Erosion Control-Design Manual. U.S.Army Corps of Eng, Vicksburg, pp. 239-274.

Borges, C.Z., 2004. Erosão marginal no rio Paraná após a conclusão do reservatório da UHE Sérgio Motta (Porto Primavera) a jusante da barragem. Master Thesis, Universidade Estadual de Maringá.

Brando, P.M., Balch, J.K., Nepstad, D.C., Morton, D.C., Putz, F.E., Coe, M.T., Silvério, D., Macedo, M.N., Davidson, E.A., Nóbrega, C.C., Alencar, A., Soares-Filho, B.S., 2014. Abrupt increases in Amazonian tree mortality due to drought–fire interactions. Proceedings of the National Academy of Sciences, 111(17), 6347-6352. https://doi.org/10.1073/pnas.1305499111.

Brandt, S.A., 2000. Classification of geomorphological effects downstream of dams. Catena. 40 (4), 375-401. https://doi.org/10.1016/S0341-8162(00)00093-X.

Carling, P.A., 1988. Channel change and sediment transport in regulated UK rivers. Regulated Rivers: Res. Manage. 2, 369–387. https://doi.org/10.1002/rrr.3450020313.

Casado, A.P.B., Holanda, F.S.R. Araújo-Filho, F.A.G., Yaguiu, P., 2002. Revista Brasileira de Ciência do Solo. 26, 231-239.

Cavalcante, A.D.J.B.D., 2011. Impactos nos processos morfológicos do baixo curso do rio São Francisco, decorrentes da construção de barragens. PhD Thesis, Universidade Federal do Rio de Janeiro, Rio de janeiro.

Chen, Z.Y., Wang, Z.H., Finlayson, B., Chen, J., Yin, D.W., 2010. Implications of flow control by the Three Gorges Dam on sediment and channel dynamics of the middle Yangtze (Changjiang) River, China. Geology. 38, 1043–1046. https://doi.org/10.1130/G31271.1.

Choi, S.U., Yoon, B., Woo, H., 2005. Effects of dam-induced flow regime change on downstream river morphology and vegetation cover in the Hwang River, Korea. River Research and Applications. 21 (2-3), 315-325. https://doi.org/10.1002/rra.849.

Colby, B.R., 1957. Relationship of unmeasured sediment discharge to mean velocity. Eos, Transactions American Geophysical Union. 38 (5), 708-717. https://doi.org/10.1029/TR038i005p00708.

Dai, Z., Liu, J.T., 2013. Impacts of large dams on downstream fluvial sedimentation: An example of the Three Gorges Dam (TGD) on the Changjiang (Yangtze River). Journal of Hydrology, 480, 10-18. https://doi.org/10.1016/j.jhydrol.2012.12.003.

De Jong, P., Tanajura, C.A.S., Sánchez, A.S., Dargaville, R., Kiperstok, A., Torres, E.A., 2018. Hydroelectric production from Brazil's São Francisco River could cease due to climate change and inter-annual variability. Science of the Total Environment. 634, 1540-1553. https://doi.org/10.1016/j.scitotenv.2018.03.256.

Dominguez, J.M.L., Guimarães, J.K., 2021. Effects of Holocene climate changes and anthropogenic river regulation in the development of a wave-dominated delta: The São Francisco River (eastern Brazil). Marine Geology. 435, 106456. https://doi.org/10.1016.j.margeo.2021.106456.

Fontes, L.C.S., Latrubesse, E., Holanda, F.S.R., Aquino, S., 2009. Major hydrological changes and bank erosion in the lower Sao Francisco River, Brazil, as a consequence of dams, in: Vionnet, C.A., García, M.H., Latrubesse, E.M., Perillo, G.M.E. (Eds.), River, Coastal and Estuarine Morphdynamics. London, pp. 131-136.

Fontes, L.C.S., 2015. Da fonte à bacia: interação continente-oceano no sistema sedimentar Rio São Francisco, Brasil. PhD Thesis, Universidade Estadual Paulista (UNESP) – Instituto de Biociências.

Friend, P.F., Sinha, R., 1993. Braiding and meandering parameters. Geological Society, London, Special Publications. 75, 105-111. https://doi.org/10.1144.GSL.SP.1993.075.01.05.

Galay, V.J. 1983. Causes of river bed degradation. Water resources research, 19 (5), 1057-1090.

Genz, F., Luz, L.D., 2012. Distinguishing the effects of climate on discharge in a tropical river highly impacted by large dams. Hydrological Sciences Journal. 57 (5), 1020-1034. https://doi.org/10.1080/02626667.2012.690880.

Getirana, A., 2016. Extreme Water Defict in Brazil Detected from Space. Journal of Hydrometeorology. 17 (2), 591-599. https://doi.org/10.1175/JHM-D-15-0096.1.

Giardino, J.R., Lee, A.A., 2011. Rates of Channel Migration on the Brazos River. Final Report Submitted to the Texas Water Development Board. Texas A and M University, pp. 8–9.

Gregory, K.J., Park, C.C., 1974. Adjustment of river channel capacity downstream from a reservoir. Water Resources Research. 10, 870–873.

Grill, G., Lehner, B., Lumsdon, A.E., MacDonald, G.K., Zarfl, C., Liermann, C. R., 2015. An index-based framework for assessing patterns and trends in river fragmentation and flow regulation by global dams at multiple scales. Environmental Research Letters, 10(1), 015001. https:// doi:10.1088/1748-9326/10/1/015001.

Gupta, A., 2007. Introduction, in: Gupta, A. (Eds.), Large Rivers: Geomorphology and Management. The Atrium, Southern Gate, Chichester, pp. 1-6.

Gupta, H., Kao, S.J., Dai, M., 2012. The role of mega dams in reducing sediment fluxes: A case study of large Asian rivers. Journal of Hydrology, 464, 447-458. https://doi.org/10.1016/j.jhydrol.2012.07.038.

Harmar, O. P., Clifford, N.J., Thorne, C.R., Biedenharn, D.S., 2005. Morphological changes of the Lower Mississippi River: geomorphological response to engineering intervention. River Research and Applications, 21(10), 1107-1131. https://doi.org/10.1002/rra.887.

Heimann, D.C., Sprague, L.A., Blevins, D. W., 2011. Trends in suspended-sediment loads and concentrations in the Mississippi River Basin, 1950-2009. US Department of the Interior, US Geological Survey.

Higgs, G., Petts, G., 1988. Hydrological changes and river regulation in the UK. Regulated Rivers: Res. Manage. 2, 349–368. https://doi.org/10.1002/rrr.3450020312.

Jacobson, R.B., Blevins, D.W. Bitner, C.J., 2009. Sedimet regime constraints on river restoration – An example from the lower Missouri River. Geological Society of America Special papers, p. 1-22.

Jenkins, K., Warren, R., 2015. Quantifying the impact of climate change on drought regimes using the Standardised Precipitation Index. Theoretical and Applied Climatology, 120(1), 41-54. https://doi.org/10.1007/s00704-014-1143-x.

Jiongxin, X., 1990. An experimental study of complex response in river channel adjustment downstream from a reservoir. Earth Surf. Processes Landforms. 15, 43–53. https://doi.org/10.1002/esp.3290150105.

Kesel, R. H., 2003. Human modifications to the sediment regime of the Lower Mississippi River flood plain. Geomorphology, 56(3-4), 325-334. https://doi.org/10.1016/S0169-555X(03)00159-.4

Kong, D., Latrubesse, E.M., Miao, C., Zhou, R., 2020. Morphological response of the Lower Yellow River to the operation of Xiaolangdi Dam, China. Geomorphology. 350, 106931. https://doi.org/10.1016/j.geomorph.2019.106931.

Latrubesse, E.M., 2008. Patterns of anabranching channels: The ultimate end-member adjustment of mega rivers. Geomorphology. 101 (1-2), 130-145. https://doi.org/10.1016/j.geomorph.2008.05.035.

Lehner, B., Liermann, C.R., Revenga, C., Vörösmarty, C., Fekete, B., Crouzet, P., Döll, P, Endejan, M, Frenken, K., Magome, J, Nilsson, C., Robertson, J.C., Rödel, R, Sindorf, N., Wisser, D., 2011. Global reservoir and dam (grand) database. Technical Documentation, Version 1.1, 1, 1-14.

Lesk, C., Rowhani, P., Ramankutty, N., 2016. Influence of extreme weather disasters on global crop production. Nature, 529(7584), 84-87. https://doi.org/10.1038/nature16467.

Li, S., Li, Y. Yuan, J., Zhang, W., Chai, Y., Ren, J. 2018. The impacts of the Three Gorges Dam upon dynamic adjustment mode alterations in the Jingjiang reach of the Yangtze River, China, Geomorphology, 318, 230-239, https://doi.org/10.1016/j.geomorph.2018.06.020.

Lucena, A.F.P., Szklo, A.S., Schaeffer, R., Souza, R.R., Borba, B.S.M.C., Costa, I.V.L., Preira Júnior, A.O., Cunha, S.H F., 2009. The vulnerability of renewable energy to climate change in Brazil. Energy Policy, 37(3), 879-889. https://doi.org/10.1016/j.enpol.2008.10.029

Ma, Y.X., Huang, H.Q., Nanson, G.C., Li, Y., Yao, W.Y., 2012. Channel adjustments in response to the operation of large dams: the upper reach of the lower Yellow River. Geomorphology. 147, 35-48. http://dx.doi.org/10.1016/j.geomorph.2011.07.032.

Magilligan, F.J., Nislow, K.H., 2001. Long-term changes in regional hydrologic regime following impoundment in a humid-climate watershed. Journal of the American Water Resources Association 37, 1551–1569. https://doi.org/10.1111/j.1752-1688.2001.tb03659.x.

Magilligan, F.J., Nislow, K.H., 2005. Changes in hydrologic regime by dams. Geomorphology, 71, 61–78. https://doi.org/10.1016/j.geomorph.2004.08.017.

Meade. R.H., 1996. River-sediment inputs to major deltas, in: Milliman, J.D., Haq, B.U. (Eds), Sea-level Rise and Coastal Subsidence: Causes, Consequences, and Strategies. Kluwer, Dordrecht, pp. 63–85.

Meade, R.H., Moody, J.A., 2010. Causes for the decline of suspended-sediment discharge in the Mississippi River system, 1940–2007. Hydrological Processes: An International Journal, 24(1), 35-49. https://doi.org/10.1002/hyp.7477.

Medeiros, P.R.P., Knoppers, B., Souza, W.F.L., Oliveira, E.N., 2011. Aporte de material em suspensão no baixo rio São Francisco (SE/AL) em diferentes condições hidrológicas. Brazilian Journal of Aquatic Science and Technology. 15, 42-53. https://doi.org/10.14210/bjast.v15n1.p42-53.

Medeiros, P.P., Santos, M.M., Cavalcante, G.H., Souza, W.F.L., Silva, W.F., 2014. Características ambientais do Baixo São Francisco (AL/SE): efeitos de barragens no transporte de materiais na interface continente-oceano. Geochimica Brasiliensis. 28, 65-78. http://dx.doi.org/10.21715/gb.v28i1.384.

Milliman, J.D., 1997. Blessed dams or damned dams?. Nature. 386, 325-326. https://doi.org/10.1038/386325a0.

Morris, G.L., Fan, J., 1997. Reservoir Sedimentation Handbook: Design and Management of Dams, Reservoirs, and Watersheds for Sustainable Use. McGraw-Hill, New York, 805 pp.

Nelson, N.C., Erwin, S.O., Schmidt, J.C., 2013. Spatial and temporal patterns in channel change on the Snake River downstream from Jackson Lake dam, Wyoming. Geomorphology. 200, 132-142. https://doi.org/10.1016/j.geomorph.2013.03.019.

Nouh, M., 1990. The flow regime downstream of dams in arid areas: development and effects of channel stability. Hydrology of Mountainous Regions—II: Artificial Reservoirs, Water and Slopes. IAHS Publication, 194.

Oliveira, A.M., Júnior, R.C.S., Hernandez, A.O., Segundo, G.H.C., Araújo, A.E.M. 2003. A morte do Delta do Rio São Francisco. In: Anais do II Congresso sobre Planejamento e Gestão das Zonas Costeiras dos Países de Expressão Portuguesa IX Congresso da Associação Brasileira de Estudos do Quaternário, II Congresso do Quaternário dos Países de Língua Ibéricas.

Petts, G.E., 1979. Complex response of river channel morphology subsequent to reservoir construction. Progress in Physical Geography. 3, 329–362. https://doi.org/10.1177/030913337900300302.

Petts, G.E., Gurnell, A.M., 2005. Dams and geomorphology: research progress and future directions. Geomorphology. 71, 27–47. https://doi.org/10.1016/j.geomorph.2004.02.015.

Petts, G.E., Gurnell, A.M., 2021. Hydrogeomorphic Effects of Reservoirs, Dams, and Diversions, Reference Module in Earth Systems and Environmental Sciences, Elsevier, https://doi.org/10.1016/B978-0-12-818234-5.00034-1

Phillips, J.D., Slattery, M.C., Musselman, Z.A., 2005. Channel adjustments of the lower Trinity River, Texas, downstream of Livingston Dam. Earth Surf. Process. Landforms, 30: 1419-1439.

Roman, P., 2017). The São Francisco inter-basin water transfer in Brazil: Tribulations of a megaproject through constraints and controversy. Water Alternatives, 10(2), 395.

Rustomji, P., Zhang, X.P., Hairsine, PB., Zhang, L., Zhao, J., 2008. River sediment load and concentration responses to changes in hydrology and catchment management in the Loess Plateau region of China. Water Resources Research, 44(7). https://doi.org/10.1029/2007WR006656.

Santos, H.A., Pompeu, P.S., Kenji, D.O.L., 2012. Changes in the flood regime of São Francisco River (Brazil) from 1940 to 2006. Regional Environment Change. 12, 123-132. https://doi.org/10.1007/s10113-011-0240-y.

Schmidt, J.C., Wilcock, P.R., 2008. Metrics for assessing the downstream effects of dams. Water Resources Research, 44(4). https://doi.org/10.1029/2006WR005092

Schumm, S.A., Lichty, R.W., 1965. Time, space and causality in geomorphology, American Journal of Science. 263 (2), 110-119. https://doi.org/10.2475/ajs.263.2.110.

Silva, W.F.; Medeiros, P.R.P.; Viana, F.G.B. 2010. Quantificação preliminar do aporte de sedimentos no baixo São Francisco e seus principais impactos. X Simpósio de Recursos Hídricos do Nordeste. Fortaleza, Brazil, p. 1-14.

Skalak, K.J., Benthem, A.J., Schenk, E.R., Hupp, C.R., Galloway, J.M., Nustad, R.A., Wiche, G.J., 2013. Large dams and alluvial rivers in the Anthropocene: The impacts of the Garrison and Oahe Dams on the Upper Missouri River. Anthropocene. 2, 51-64. https://doi.org/10.1016/j.ancene.2013.10.002.

Souza Filho, E.E., Rocha, P.C., Comunello, E., Stevaux, J.C., 2004. Effects of the Porto Primavera Dam on physical environmental of the downstream floodplain. In: Thomaz, S.M., Agostinho, A.A., Hahn, N.S. (eds.), The Upper Paraná River and its Floodplain: Physical Aspects, Ecology and Conservation. Backhuys Publisher, Lieden, The Netherland, pp. 55-74.

Stevaux, J.C., Martins, D.P., & Meurer, M., 2009. Changes in a large regulated tropical river: The Paraná River downstream from the Porto Primavera Dam, Brazil. Geomorphology, 113(3-4), 230-238. https://doi.org/10.1016/j.geomorph.2009.03.015

Stevaux, J.C. and Latrubesse, E.M., 2017. Geomorfologia fluvial, ed. Oficina de Textos, São Paulo.

Sun, T., Ferreira, V.G., He, X., Andam-Akorful, S.A., 2016. Water Availability of São Francisco River Basin Based on a Space-Borne Geodetic Sensor. Water. 8 (5), 213. https://doi.org/10.3390/w8050213.

Surian, N. (1999). Channel changes due to river regulation: the case of the Piave River, Italy. Earth Surface Processes and Landforms: The Journal of the British Geomorphological

Research Group, 24(12), 1135-1151. https://doi.org/10.1002/(SICI)1096-9837(199911)24:12<1135::AID-ESP40>3.0.CO;2-F.

Syvitski, J.P., Vörösmarty, C.J., Kettner, A.J., Green, P., 2005. Impact of humans on the flux of terrestrial sediment to the global coastal ocean. Science, 308(5720), 376-380. https://doi.org/10.1126/science.1109454.

Syvitski, J.P., Kettner, A.J., Overeem, I., Hutton, E.W., Hannon, M.T., Brakenridge, G.R., Day, J., Vörösmarty, C., Saito, Y., Giosan, L., Nicholls, R. J., 2009. Sinking deltas due to human activities. Nature Geoscience. 2 (10), 681-686. https://doi.org/10.1038/ngeo629.

Thoms, M.C., Walker, K.F., 1993. Channel changes associated with two adjacent weirs on a regulated lowland alluvial river. Regulated rivers: Res. Manage. 8 (3), 271–284. https://doi.org/10.1002/rrr.3450080306.

Trenberth, K.E., Dai, A., Van Der Schrier, G., Jones, P.D., Barichivich, J., Briffa, K.R., Sheffield, J., 2014. Global warming and changes in drought. Nature Climate Change, 4(1), 17-22. https://doi.or/10.1038/NCLIMATE2067.

United States Fish and Wildlife Service and Hooja Valley Tribe, 1999. Trinity River Flow Evaluation, Final Report. June 1999. 307 pp.

Vericat, D., Batalla, R.J., Garcia, C.,2 006. Breakup and reestablishment of the armour layer in a large gravel-bed river below dams: The lower Ebro. Geomorphology, 76(1-2), 122-136. https://doi.org/10.1016/j.geomorph.2005.10.005.

Wallick, R.J., Grant, G.E., Lancaster, S.T., Bolte, J.P. Denlinger, R.P., 2007. Patterns and Controls on Historical Channel Change in the Willamete River, Oregon, USA, in: Gupta (Eds.), Large Rivers: Geomorphology and Management. The Atrium, Southern Gate, Chichester, pp. 491-516.

Walling, D.E., 2006. Human impact on land–ocean sediment transfer by the world's rivers. Geomorphology, 79(3-4), 192-216. https://doi.org/10.1016/j.geomorph.2006.06.019.

Wang, W., Wang, T., Cui, W., Yao, Y., Ma, F., Chen, B., Wu, J., 2021. Change of Flow and Sediment Transport in the Lower Min River in Southeastern China under the Impacts of Climate Variability and Human Activities. Water, 13(5), 673. https://doi.org/10.3390/w13050673.

Williams, G.P., Wolman, M.G., 1984. Downstream effects of dams on alluvial rivers, Washington, DC.

Wohl, E.E., 2007. Hydrology and Discharge, in: Gupta, A. (Eds.) Large Rivers: Geomorphology and Management. The Atrium, Southern Gate, Chichester, 29-44.

Wolman, M.G., Miller, J.P., 1960. Magnitude and frequency of forces in geomorphic processes. The Journal of Geology. 68 (1), 54-74. http://dx.doi.org/10.1086/626637.

Wu, X., Bi, N.S., Yuan, P., Li, S., Wang, H.J., 2015. Sediment dispersal and accumulation off the present Huanghe (Yellow River) delta as impacted by the Water-Sediment Regulation Scheme. Cont. Shelf Res. 111, 126–138. http://dx.doi.org/10.1016/j.csr.2015.11.003.

Yang, S.L., Milliman, J.D., Xu, K.H., Deng, B., Zhang, X.Y., Luo, X.X., 2014. Downstream sedimentary and geomorphic impacts of the Three Gorges Dam on the Yangtze River. Earth-Science Reviews, 138, 469-486. https://doi.org/10.1016/j.earscirev.2014.07.006.

Yang, S.L., Xu, K.H., Milliman, J.D., Yang, H.F., Wu, C.S.; 2015. Decline of Yangtze River water and sediment discharge: Impact from natural and anthropogenic changes. Scientific reports, 5(1), 1-14. https://doi.org/10.1038/srep12581.

Zahar, Y., GhoRbel, A., Albergel, G., 2008. Impacts of large dams on downstream flow conditions of rivers: aggradation and reduction of the Medjerda channel capacity downstream of the Sidi Salem dam (Tunisia). Journal of Hydrology. 351, 318–330. https://doi.org/10.1016/j.jhydrol.2007.12.019.

Zhou, Z., 1996. Impact of reservoirs on fluvial processes and environment of alluvial rivers. Reservoir Sedimentation, Proceedings of the St Petersburg Workshop May 1994, IHP-V., Paris, France, pp. 273–290.

Zhou, Y.Y., Huang, H.Q., Nanson, G.C., Huang, C., Liu, G.H., 2015. Progradation of the Yellow (Huanghe) River delta in response to the implementation of a basin-scale water regulation program. Geomorphology. 243, 65–74, http://dx.doi.org/10.1016/j.geomorph.2015.04.023.

Zhou, M., Xia, J., Lu, J., Deng, S., Lin. F. 2017. Morphological adjustments in a meandering reach of the middle Yangtze River caused by severe human activities, Geomorphology, 285, 325-332. https://doi.org/10.1016/j.geomorph.2017.02.022.

CAPÍTULO 2 – Multitemporal analysis of morphological adjustments in the Lower São Francisco River (Northeast, Brazil): impacts of the Xingó dam on river dynamics

Pedro Victor Oliveira Gomes[a*], Felipe Torres Figueiredo[a,b], Gelson Luís Fambrini[c], Carlos Henrique Grohmann[d], Luiz Alberto Vedana[a,b], Luisa Sampaio Franco[a]

[a] Programa de Geociências e Análise de Bacias, Federal University of Sergipe - Av. Marechal Rondon, s/n - Jardim Rosa Elze, São Cristóvão - Sergipe State, 49100-000, Brazil gomes.pvoliveira@gmail.com ; luisa.sampaiofranco@gmail.com

[b] Departamento de Geociências, Federal University of Sergipe - Av. Marechal Rondon, s/n - Jardim Rosa Elze, São Cristóvão - Sergipe State, 49100-000, Brazil ftfigueiredo@gmail.com

[c] Geology Department (Integrated Laboratory of Technology in Petroleum, Natural Gas and Biofuels (LITPEG), Federal University of Pernambuco – Av. da Arquitetura, 953-995 – Cidade Universitária, Recife -Pernambuco State, 50740-540, Brazil gelson.fambrini@ufpe.br

[d] Instituto de Geociências – Rua do Lago, 562, University of São Paulo, Cidade Universitária, São Paulo – São Paulo State, Brazil carlos.grohmann@gmail.com

***** corresponding author

Abstract

After successive big dams were built throughout the last hundred years, and particularly after the facility of Xingó became operational, the lower course of the São Francisco River (LSFR) suffered a reduction in the average water discharge and is no longer capable of transporting most of the sandy bedload downstream. Nevertheless, assessing the role of dams or climate change on the São Francisco River morphological adjustments is difficult and scarce in the literature. In order to fulfill that gap and evaluate the role of Xingó's reservoir on morphological adjustments, we focused on the characterization and quantification of the morphological adjustments in the LSFR. A time series of satellite images, water, and sediment discharge data were used along seventeen reaches between Xingó and Penedo. To assess the influence of climate change along the drainage basin, we carried out a linear regression approach using a pre and post-dam time series comparison. Our satellite image analysis demonstrates a predominance of internal adjustments to the channel over external ones, with low values of lateral migration rate and slight variation in channel sinuosity. After the construction of the Xingó dam, the percentage of sandy bars remained constant in the groups closest to the dam (G1 and G2), while G3 presented an increase in bedforms. However, with the decrease in water discharges accompanied by rainfall in the river basin, sediments settled closer to the dam. This process is also responsible for increasing the channel interlace rate in the LSFR. During the prolonged drought (2013-present), the most significant decreases in channel width occurred in all LSFR reaches. This dry period was responsible for a 40.4% decrease in discharges in the post-Xingó period, representing the primary control over the decrease in water discharge affecting fluvial morphological elements downstream of Xingó. Thus, the reduction of Xingó's and other upstream dam outflows is essentially a consequence of lower rainfall in the whole drainage basin.

Keywords: Dam rivers, Xingó dam, Fluvial Morphology, Effective Discharge, Channel Narrowing, Climate Changes

1. Introduction

Major rivers on the planet have a central role in developing floodplains and draining water and sediments to the oceans (Gupta, 2007). Most of them are prone to natural barriers and slope changes across the drainage area, especially in their lower reaches, which invariably force river courses to natural morphological shifts (Schum and Lichty, 1965). However, during the twentieth century, the implementation of dams added complexity to the management of fluvial adjustments (Milliman, 1997; Wallick et al., 2007). River courses had not only severely modified their spatial trajectory, but most importantly, it affected their capacity to preserve natural changes of water drainage. Consequently, the downstream river flows altered river banks and riverbed over time (Meade, 1996; Wohl, 2007; Ma et al., 2012). Several researchers have studied the effect of dams on flow stage regimes and successive channel morphology since the last century (Gregory e Park, 1974; Petts, 1979; Galay, 1983; Williams e Wolman, 1984; Carling, 1988; Jiongxin, 1990a. b; Thoms e Walker, 1993; Benn e Erskine, 1994; Zhou, 1996; Morris e Fan, 1997; Phillips, 2003, Petts e Gurnell, 2005; Phillips et al., 2005; Magilligan et al. 2008; Bandeira et al., 2008; Zahar et al., 2008; Ma et al., 2012; Zhou et al., 2015; Wu et al., 2015; Zhou et al., 2017., Li et al., 2018; Kong et al., 2020; Petts e Gurnell, 2021).

Detailed works contributed on how water discharges and sediments modify fluvial dynamics in different time scales: hourly to yearly (Magilligan and Nislow, 2001; Petts and Gurnell, 2005; Vericar and Batalla, 2006; Ma et al., 2012). One of the quickest and most relevant adjustments is the reduced number of high peak discharges, now discharged as regulated outflows (Souza Filho et al., 2004; Lehner et al., 2011; Grill et al., 2015; Roman, 2017; Best, 2019; Wang et al., 2021). Another expected adjustment directly related to engineering projects (Harmar et al., 2015; Kesel, 2003) is the reduced sediment load, which is observed in a diversity of barried rivers in North America (Williams and Wolman, 1984, Jacobson et al., 2009; Heimann et al., 2011), and Asia (Rustomji et al., 2008; Gupta et al., 2012, Yang et al., 2014). Retained water at the dam reservoir leads to a decline in the river's natural flow capacity to transport and erode, which

imposes the river to a series of morphological adjustments (Wallin, 2006; Gupta et al., 2012). The stabilization of sedimentological at low-flow stages can increase the rate of free flow sediments erosion (Nouh, 1990; Chen et al., 2010), followed by the river bank and degradational bed processes (Petts, 1979; Choi et al., 2005; Magilligan and Nislow, 2005; Dai and Liu, 2013). As an unintended consequence, erosive processes are more likely to intensify at the river mouth (c; Syvitski et al., 2005; Syvitski et al., 2009). For that reasons, many researchers focus their efforts, either studying the most significant undesired planform morphological adjustments (Higgs and Petts, 1988; Zhou, 1996; Surian, 1999; Nelson et al., 2013; Kong et al., 2020) and the generation of conceptual models to quantify the impact in dam rivers (Brandt, 2000; Schimidt and Wilcock, 2008; Skalak et al., 2013; Grill et al., 2015).

Another question still under debate is whether ongoing climate changes (Nakicenovic et al., 2000; Marengo et al., 2012; Assis et al., 2015; Getirana, 2016; Marengo et al., 2017; Santos et al., 2017; Souto et al., 2019) can play a significant role upon hydrological and sedimentological regimes downstream, despite the dam's influence (De Jong, 2018; Dominguez & Guimarães, 2021), and which one could be the best candidates to controlling factors. Climate change is the most frequent answer, and greenhouse the driving engine as evidenced by the diminished pluviosity rates and the outnumbered register of droughts in the last decades (Trenberth et al., 2014; Jenkins and Warren, 2015; Best, 2019). Prolonged drought periods have caused declining water (Yang et al., 2015). However, some authors argue that climate change and anthropogenic factors can reduce the sedimentary yield of capture basins (Meade and Moody, 2010; Yang et al., 2015; Genz and Luz, 2018; Dominguez and Guimarães, 2021; Wang et al., 2021). Consequently, a direct impact would be expected on water supply and ecology (Trinity River Flow Evaluation, 1999; Brando et al., 2014; Lesk et al., 2016). Moreover, other side effects would affect the food chain production (Getirana, 2016) reflected in damaging economies based on agriculture, livestock, and industry that demand water supplies to operate and generate electric power (Jekins and Warren, 2015, Sun, 2016, Lucena et al. 2009; de Jong, 2018).

In Brazil, despite the number of dam rivers and the effects caused to both landscape and local economies, few works link the unintended morphological adjustments to the implementation

of electric power dams except for the case of the São Francisco River (Borges, 2004; Stevaux et al., 2009; Fontes et al., 2009; Medeiros et al., 2011; Medeiros et al., 2014). The river is currently facing similar issues on its lower course, and the Xingó dam is considered a milestone in environmental impacts in lowland areas (Fontes et al., 2009; Cavalcante, 2011; Santos et al., 2012). This river is the fourth largest river in South America and the primary source of fresh water in the semi-arid region of northeastern Brazil, which denotes the importance of the national management of this basin. Despite this, previous studies have focused on documenting bank erosions at specific points sites (e.g., Casado et al.2002; Fontes 2015) and in the deltaic plain (e.g., Oliveira et al., 2003; Bandeira et al., 2008, Dominguez and Guimarães, 2021). To date, few works investigated morphological adjustments in the lower São Francisco River (LSFR) (Cavalcante, 2011; Fontes, 2015) or the interplay of climate and dam regulation as combined factors governing morphological adjustments (Dominguez & Guimarães, 2021).

To address a major perspective of the direct influence of the Xingó Dam operation over geomorphological building blocks of the Lower São Francisco River, we aimed for 17 reaches of its lower course, located between Sergipe and Alagoas States, in northeast Brazil. Our goals were to characterize and quantify the morphological adjustments by considering two time series of satellite images before and after Xingó's construction. Moreover, we debated whether the controlled discharges from the Xingó reservoir entirely affect the main channel pattern described in the literature (e.g., Silva et al., 2010; Medeiros et al., 2014) or if climate changes still influence the downstream morphological adjustments observed.

2. Regional setting

2.1. Study area

The São Francisco River is the fourth largest river in South America, with an extension of roughly 2,863 km long and a capture basin that totalizes 641 x 103 km2 (Fig. 1a), divided into four physiographic regions: upper (USFR), middle (MSFR), sub-middle (SMSFR), and lower (LSFR) courses (Fig. 1b), towards its mouth in the Atlantic Ocean (Bernardes, 1951; De Jong et al., 2018).

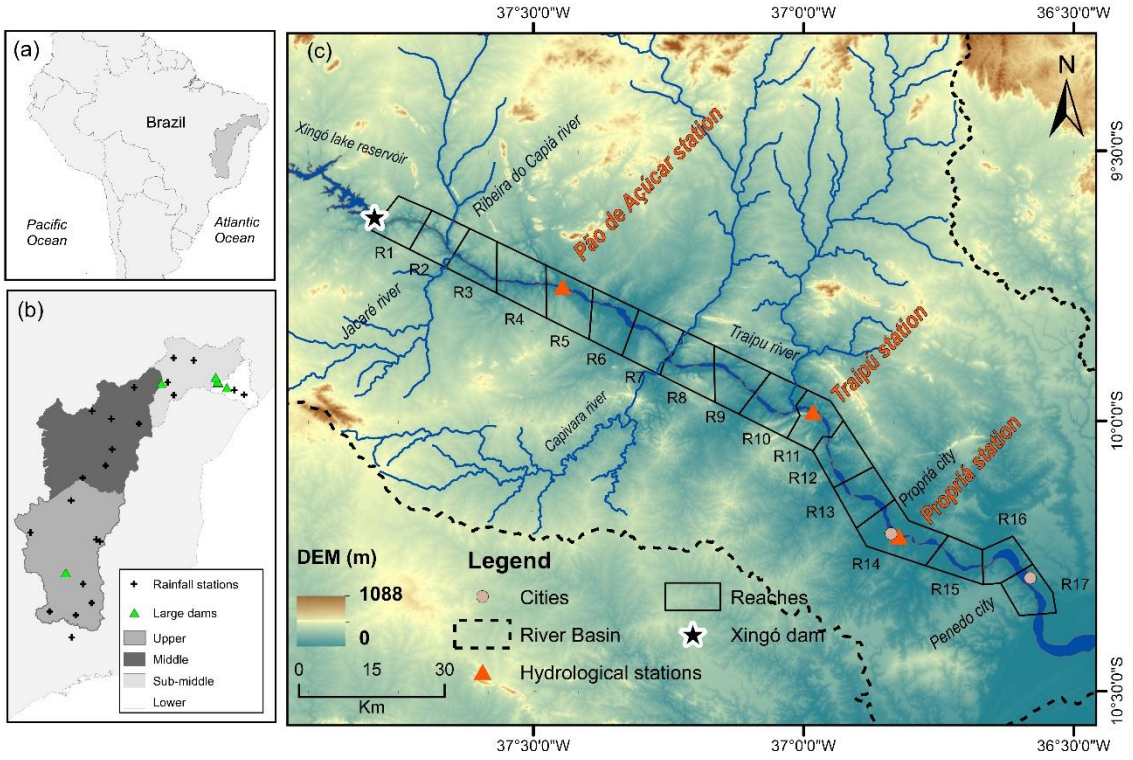

Fig. 1. (a) São Francisco River Watershed in Southeast and Northeast Brazil. (b) Four physiographies domains across the river course are divided into upper regions: the Canastra Hills, where the headwaters are, middle, sub-middle, and lower courses at the coastal plain, where main depositional processes occur. (c) Digital Elevation Model of the São Francisco River basin and the distribution of the seventeen studied reaches across the lower river course, from the Xingó Lake to the City of Penedo.

A series of dams were constructed in the last hundred years, severely modifying the fluvial geomorphology (e.g., Oliveira et al., 2003; Santos et al., 2012). The first dams began with the Rio das Pedras and Pararúna installations in 1908 and 1927 in Minas Gerais. In the coming decades, six big dams were to become operational in the upstream catchment areas, among them: Paulo Afonso (1954), Três Marias (1962), Apolônio Sales (1977), Sobradinho (1979), Luiz Gonzaga (1988), and the most downstream recent barrier imposed on the river is Xingó dam, which became fully operational in 1994 (Fig. 1b). It is considered a milestone concerning environmental impacts on the lower reaches of the river.

The study area is located at the Lower São Francisco River (LSFR), in a stretch of approximately 185 km between the Xingó dam and the Penedo city, which was subdivided into

reaches of ~10 km (R1-R17) (Fig. 1c). In this region, the main channel has a north-west-south-east direction that defines the boundary between Sergipe and Alagoas states towards its mouth, in northeastern Brazil. LSFR has a variable trajectory from a north-west-southeast trend to an east-west direction, behaving primarily as a braided style, although various degrees of sinuosity may occur (Fontes 2003).

2.2. Regional morphology and geology

The current active channel passes through different geological terrains that control the geomorphology and sinuosity of the channel (Fontes 2015). The river valley cuts through the upstream sections (R1 to R5). It runs through igneous and metamorphic rocks of the Pre-Cambrian Age of the Sergipano Belt along a pediplane surface geomorphic unit (França, 1979), tributed by Jacaré and Ribeira do Capiá rivers, on the São Francisco River Canyon. In this region, the landscape is dominated by a single, straight and narrow channel, mainly composed of igneous and metamorphic substrates, rocky islands, and rare stretches of deltaic sand. From Pão de Açúcar to the Propriá stations, Ipanema, Capivara, and Traipu rivers feed São Francisco River, which flows through a pediplane surface unit that transitions to a hill zone geomorphic unit (reaches R8 to R14). From the city of Propriá eastwards, the river expands the channel belt and the flood plain areas, as it crosses the sedimentary rocks of the Sergipe-Alagoas Basin, sculping through a coastal tableland beach ridges towards the city of Penedo (reaches R14 to R17).

2.3. Climatology and hydrology

The São Francisco watershed has undergone long-term rainfall changes, dating back to the early Holocene period, as evidenced by Stríkis et al. (2011) and Novello et al. (2012). When it comes to a century time-scale, pluviometrical numbers have declined by 25% since 1961 in the basin (De Jong et al., 2018). In the 1990s, the downward trend increased, especially in the headwaters of the São Francisco River (De Jong, 2018). The dry period worsened after 2013 when the entire watershed significantly reduced accumulated annual precipitation (Fig. 2a). Therefore, reservoir volumes in the dam cascade were impacted. Historically, these reservoirs have high intra-annual variability, between 50% and close to their maximum capacity, respectively, in the

seasonally dry and wet periods. However, in 2013, the volume of the reservoirs remained below 30%, reaching critical values of 5% in 2015 and 2017 (Fig. 2b).

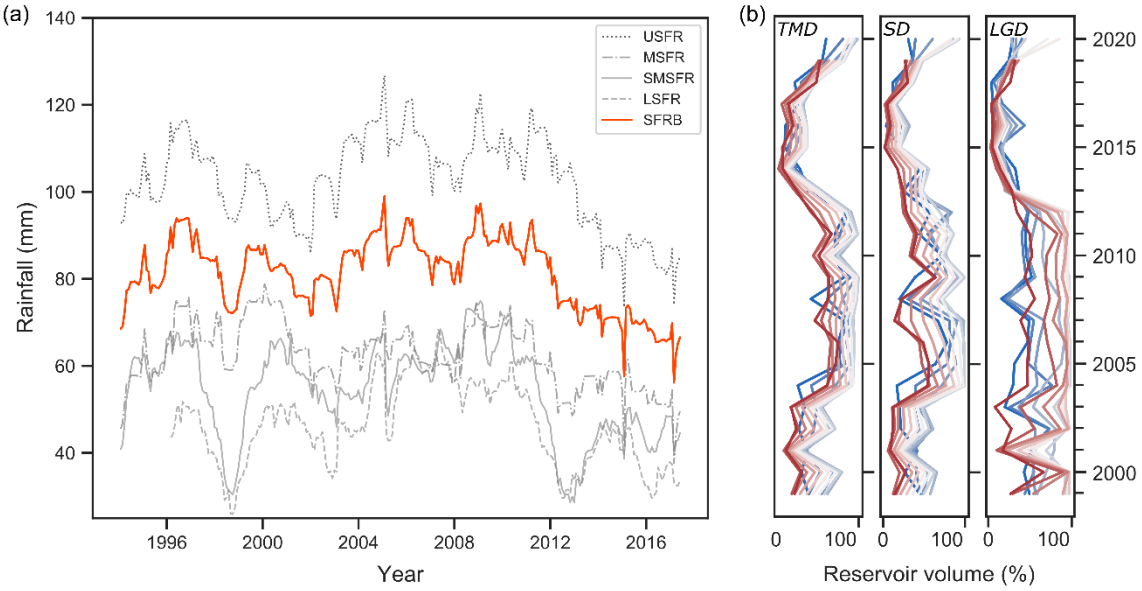

Fig. 2. (a) Moving average of 24 months of precipitation in the Sao Francisco River Basin from 1995 to 2018 (orange line). b) Monthly reservoir volumes for the Tres Marias (TMD), Sobradinho (SD) and Luiz Gonzaga (LGD) dams from 1999 to 2020. The blue lines represent the change between January and June, and the red lines indicate reservoir volumes from July to December. Data source: ONS (2020) and ANA (2020).

Today, the river basin is sensitive to microclimatic regimes that differ in course. On the one hand, the upper river course runs across the Canastra Hills, located in the highlands of Minas Gerais State, southeast of Brazil, where a humid climate, controlled by altitude prevails, and rainy seasons are concentrated in few months of the year, commonly associated to the summer of the southern hemisphere, reaching average marks of up to 1,500 mm per year. On the other hand, downstream regions located in the coastal plains, in the lower river course are influenced by a much drier climate condition, making this number be reduced to 500 mm/year, except for a small strip close to the coast, with rainfall reaching 1,000 mm/year (Gens and Luz, 2012; Dominguez and Guimarães, 2021). Such a contrast with the control of rainfall is evident across the basin, contributing to different quantities of the total flow into the basin. The upper river course drains approximately 70% out of its total streamflow across the entire basin, while the middle and sub

middle regions account for 20%, and the lowlands of the lower course, up to the river mouth, contributes with 10% (Bandeira et al., 2008; Bandeira et al., 2013; Viviroli e Weingartner, 2004). Along the river, a series of dams affect outflows into the lower reaches of the basin. The largest reservoirs in the basin are those with the regulatory capacity for discharges (e.g., Três Marias, Sobradinho, and Luiz Gonzaga dams), respectively, with reservoir volumes around 21, 34, and 11 km³ (Traini et al., 2012; Dominguez and Guimarães, 2021). Over the last 26 years, since the construction of the Xingó power plant, the lower reaches of the main river have been dramatically affected. Fontes et al. (2009) reported that flow rates have been highly controlled after the whole operation of Xingó, which led to a decrease from 3,169 m³/s by the beginning of the 1990s to 1936 m³/s by the end of the 2000s decade. Medeiros et al. (2014) also provided similar evidence, which documented a reduction of 3 136 m³/s to 2 204 m³/s during the same period.

In 2001, a significant reduction in flow occurred to stabilize water volumes within reservoirs to ensure efficient electricity generation during Brazil's worst electricity crisis. In the years of 2004 and 2007, however, the flow rate increased as a result of two anomalous rainfall events, a combination of natural tributary flows into the trunk river and the release of water volumes after Xingó reached its maximum operational limit during this flood event (Cavalcanti, 2004a, 2004b, 2007a, 2007b; Medeiros et al. 2011,). In 2013 a second major discharge rate reduction, forced by a prolonged drought in the catchment area, lowered flow rates below 1,000 m3/s for the first time in a century, according to the Brazilian Water National Regulatory Agency – ANA (Fig. 3). From 2013 to 2019, the same organization authorized the continued reduction of releases to a lower operating limit of 550 m3/s. In 2020, the increasing amount of precipitation on the lower watershed overflowed the tributaries near Propriá. Consequently, high turbidity levels in river water were recorded by two discharge control stations (Pão de Açúcar and Propriá). In order to bring the levels back to normal, discharge rates rose to 1,600 m³/s in July 2020.

It is worth mentioning that after Sobradinho Dam was constructed in 1985 and before Xingó Dam was operational in 1994, the lower São Francisco River basin suffered from flooding events (Fig. 3a) which contributed to the decrease in the intensity and frequency of recurrences between floods. During the onset of Xingó's operation in 1994 and 2012, the mean monthly

discharge remained constant, and high flow stage events became rare, except for the two flood events registered in 2004 and 2007 (Fig. 3b).

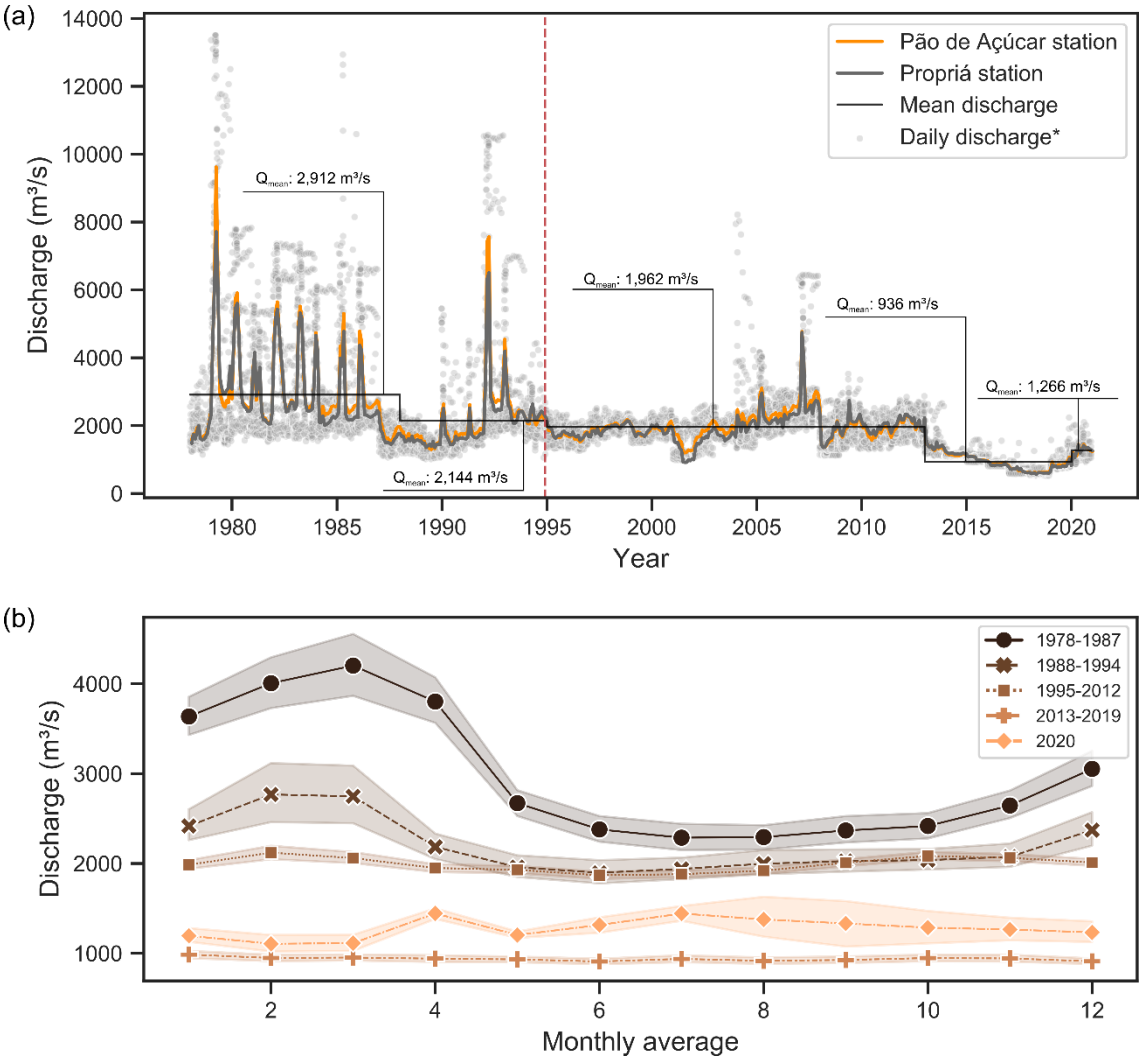

Fig. 3. Measured flow changes at Propriá and Pão de Açúcar stations over the past four decades in the lower reaches of the São Francisco River. The arrows indicate the dates the satellite imagery was acquired. The red dashed line shows the date on which the Xingó Dam became fully operational in December 1994. (b) Variation of the monthly average of discharge at the Pão de Açúcar Station. Data source: ANA (2020).

2.4. Fluvial sedimentary processes

The full operation of powerplants along the São Francisco River course has also affected sedimentary yield throughout the years, as a response to the increased volume of sediment accumulation at the upstream reservoirs, especially in the Três Marias and Sobradinho lakes

(Lima et al., 2001; Bandeira et al., 2008, Syvitski et al., 2009; Silva et al. 2016, Best, 2019). Besides, most of the suspended load that reaches the trunk river has low production rates in the lower course (Medeiros, 2003; Knoppers et al., 2005). It is estimated that the São Francisco's river suffered a sediment yield reduction from approximately 6×106 ton/year in 1975 to less than 0.5×106 ton/year after 1994 (Fontes et al., 2009; Silva et al., 2010).

According to Fontes et al. (2009), morphological changes occurred due to bank erosion in the extension between Xingó and the river's mouth, and erosive sites being mostly concentrated downstream from Propriá. Similarly, Cavalcante (2011) showed that erosive processes had taken place, with rates rising primarily on the banks of the south channel. In addition to this, it is possible to observe through the cross-sections of the repository of the Brazilian Water National Regulatory Agency that the channel has been suffering bed erosion, causing bed degradation (Fig. 4). Cavalcante (2011) observed some lateral shifts in the main channel, contradicting the floodplain's expected river configuration. In both publications, erosion rates were considered to be dependent on sedimentological and geotechnical features of the riverbank and the actual dynamics of river flows. Based on lithological, topographical, and structural features, the lower reaches of the São Francisco River were divided into five segments (Fontes 2003).

Given these aspects, the sections closest to the Xingó dam are more susceptible to bank and bed erosion caused by a decrease in suspended load input. The eroded sandy sediments would, in turn, be transported and deposited across sections further downstream near the town of Propriá. At these sites, the channel would have more mesoform, increasing braiding rates and eroding river banks due to diverging river flows.

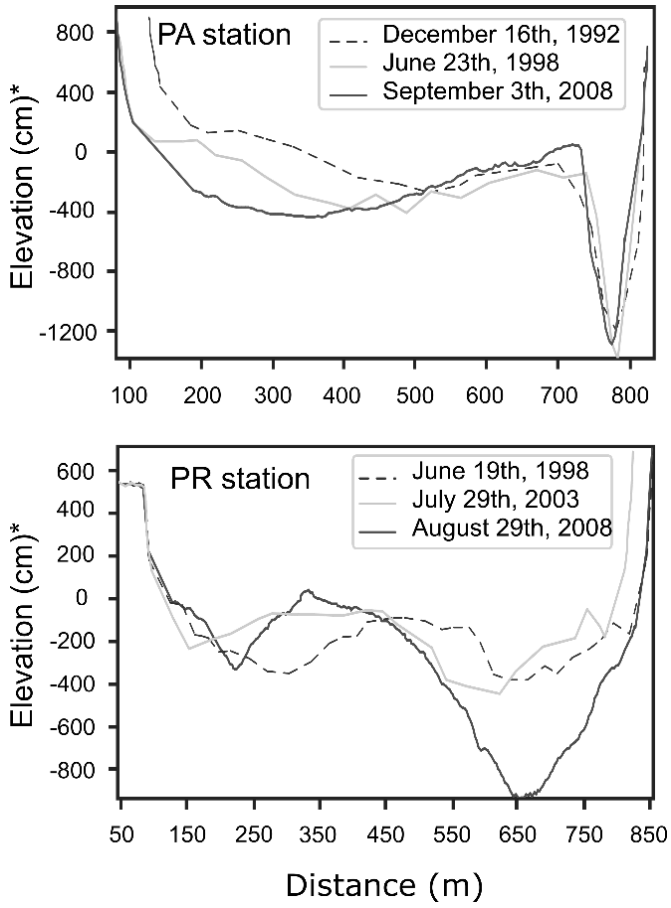

Fig. 4. Elevation of the channel bed at Pão-de-Açúcar (PA station) and Propriá stations (PR station). Cross-section measurements indicate that channel degradation predominated until 2008. * Elevation is relative to an arbitrary datum—data source: ANA (2020).

3. Material and methods

3.1 Channel mask and metrics

Channel morphological variation was analyzed using thirteen Landsat satellite images (TM, ETM, and OLI sensors), downloaded from the USGS Earth Explorer home page (https://earthexplorer.usgs.gov), totaling a thirty-three-year imaging dataset. Set 30 m spatial resolution images for the same area along the whole time and the recognition of critical years before (1985 and 1992) and after Xingó dam operation (1996, 1998, 2001, and 2003), after the great floods of 2004 and 2007 (2004, 2009 and 2011) and periods of low flow discharge (2013, 2018 and 2020) were used as criteria to the selection of images. The images used reflect periods

of low flow each year. This criterion was adopted to maintain the comparative factor during the time studied because images of high seasonal water flows could mask the analyzed morphological adjustments (Table 1).

Table 1. Year, sensor (TM: Thematic Mapper, ETM+: Enhanced Thematic Mapper Plus, OLI: Operational Land Imager), cloud cover, and mean daily discharge from São Francisco River within the selected satellite images. (*) The last satellite image was obtained in October 2020. Discharge data for that date are not yet available in the Brazilian Water National Regulatory Agency's repository. However, communications from the company that manages the dam reported an increased discharge of 2,000 m³/s on October 5th, 2020.

Year	Sensor	Cloud cover	Discharge (m³/s)	
			Pão de Açúcar station	Propriá station
1985	TM	8.0	2,327	1,924
1992	TM	10.5	2,267	1,929
1996	TM	14.0	1,588	1,546
1998	TM	8.0	2,108	2,000
2001	ETM+	5.0	1,572	1,318
2003	ETM+	5.0	1,951	1,799
2004	TM	13.0	1,580	1,474
2009	TM	14.0	1,697	1,865
2011	TM	16.0	1,806	1,691
2013	OLI	4.6	1,217	1,305
2018	OLI	2.5	795	890
2020	OLI	3.3	>2,000*	>2,000*

Images from the same year were joined to build a photomosaic. Red, near-infrared, and short-wave infrared bands were used to build up colored composite layered bands so that water bodies could be highlighted (composition RGB543 for Landsat 5 and 7 and RGB654 for Landsat 8). Landsat 7 and Landsat 8 images were submitted to a band fusion with the panchromatic band to enhance the spatial resolution to 15 m pixels (**Fig. 5**). Photomosaics were later organized in seventeen areas for each chosen year, from the nearest to Xingó dam to the most distant ones, more than halfway to the river mouth, around the city of Penedo.

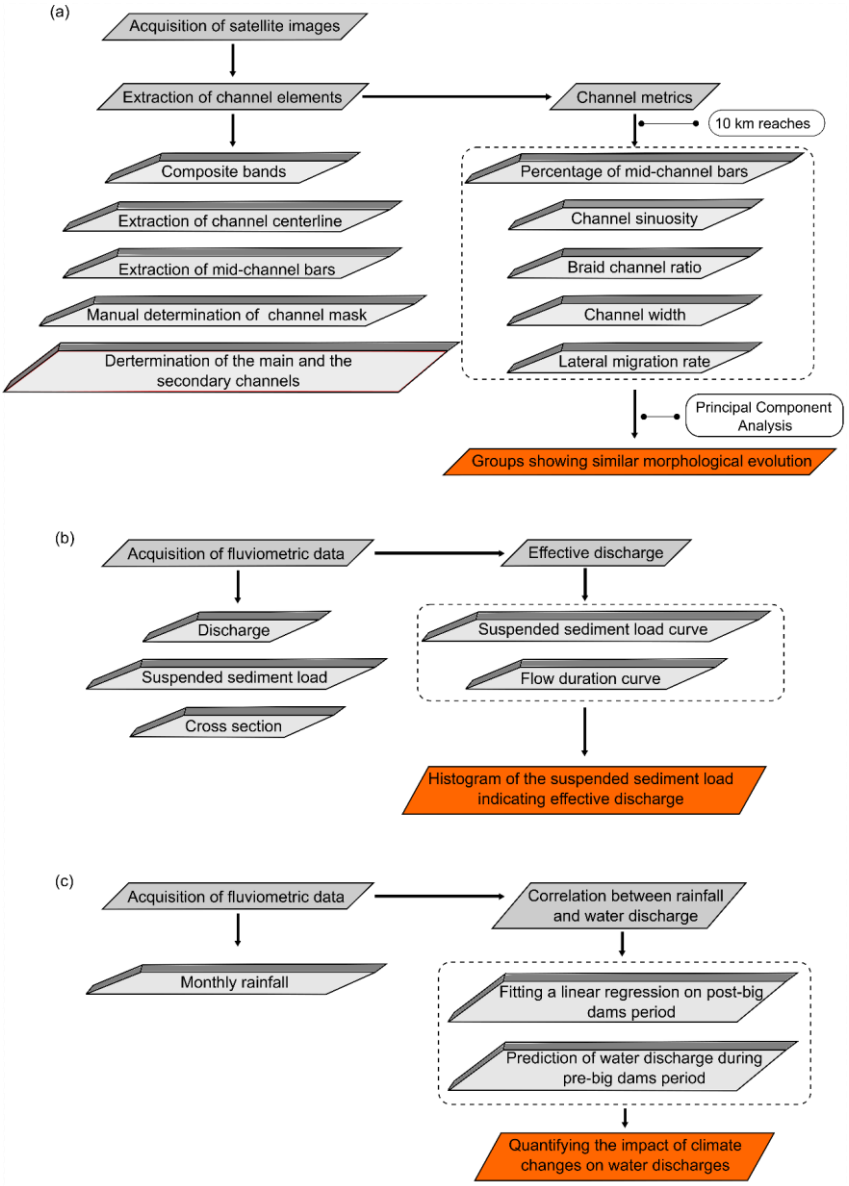

Fig. 5. *Flowchart of methodological steps. (a) Procedures for the quantification of morphological adjustments from satellite images. (b) Data used from the fluviometric database*

made available by ANA and procedures for the identification of effective discharge. (c) Rainfall data used to quantify the impacts caused by reduced rainfall on water discharge.

The structure contour of morphological elements such as bars and channel bank were manually traced on each image across the river course, with the help of a tracing tool using a GIS program (ArcGIS 10.4.1), as the automatic extraction did not present reliable results for the study area. That allowed to draw polygons, then later used to extract the size of each mid-channel bar and the channel width, the last one according to the methodology proposed by Nelson et al. (2013). The area of the mid-channel bars was later divided by the area of the channel mask to obtain the percentage of mid-channel bars. Likewise, river bank lines were mapped. On the one hand, the length of the main channel and the secondary channels were also extracted manually.

On the other hand, middle channel lines were traced with the help of the River Bathymetry Toolkit from the arc toolbox. Both were combined so that other metrics could be calculated, such as braid-channel ratio and sinuosity index (Friend and Sinhá, 1993), lateral migration rate (Giardino and Lee, 2011. Initially, the metrics were analyzed individually for each reach (R1-R17) to quantify the morphological adjustments. In order to avoid bias in the grouping, Principal Component Analysis (PCA) was applied using the independent variables of the percentage of mid-channel bars, and channel width for clustering reaches with similar morphological evolutions.

Morphological elements were sometimes covered by clouds, which prevented the calculation and comparison of areas. In this work, the cloud cover varies between 2% and 16% (Table 1). In order to avoid the use of "zero entries" that would not reflect their real sizes instead, each "zero value" was replaced by an average value, calculated using a datum from one year before and from the first year after with a valid value. Zero entries were only considered for images related to years when bars were not partially subaerial or captured in the image in the form of a subaqueous compound dune or unit bar. In these cases, zero entries are representative since the goal is to quantify subaerial areas and their variation through time. In this sense, the dataset needed first to be validated and thus compared. In order to do so, zero entries were replaced by

small values close to zero (0.001) and then attributed as minimum values. Eventually, bar size-changing rates over the 35 years were calculated by dividing data from 1985 by values obtained in 2020 of each area. A paired years analysis also compared channel bars, channel widths, channel area gains, and losses.

3.2 Effective discharge

Effective discharge (Qeff) relates to the main morphological formative channel processes, and it is defined as the flow rate or the interval of flow rates capable of transporting the greatest amount of sediments (Wolman and Miller, 1960). This variable plays a relevant role, which is greater than extreme flooding events when it comes to sediment transportation and bank erosion, once, despite the greatest sediment load extreme flooding can carry, it is conditioned to a low recurrence frequency (Stevaux and Latrubesse, 2017; Latrubesse, 2008).

In the present work, the effective discharge was adapted from the methodology proposed by Biedenharn et al. (1999). The data set was acquired from the ANA database, from which the suspended sediment concentration values were collected. The used data set was organized between the years pre-dating the construction of the Xingó power station, between 1978 and 1994, and for the post-dam period from 1995 to 2018. To calculate the effective discharge, the flow rates data set was primarily divided into twenty equal intervals. Then, the suspended sediment concentration data were converted to tons per day by using the equation of Colby (1957):

$$Qs = 0.0864 \times Q \times C \quad \text{(eq. 1)}$$

where: Qs represents diary sediment load; Q is the measured discharge in m^3/s; C is the sediment concentration in mg/L, and 0.0864 is the conversion factor of seconds per day.

Sediment load values were then related to the corresponding flow rate values to obtain an approximate sediment load curve by using the following formula:

$$Qts = aQ^b \quad \text{(eq. 2)}$$

Where: Qts represents the total sediment discharge; Q is the mean flow rate of a class; *a* and *b* correspond to parameters adjusted on each station.

Total sediment discharge of each flow rate class was obtained with the application of equation 2. The obtained value was multiplied by the number of days in which flow rates were registered for each class. Furthermore, the effective discharge measured represents a class of flow rate capable of transporting the greatest amount of sediments.

3.3 Quantifying the impacts on water discharge as a function of changes in rainfall

The methodology proposed by Yang et al. (2015) was used to quantify the impacts caused by changes in rainfall on water discharge in the LSFR. For this, rainfall stations throughout the basin were used as data input (see Fig. 1b). Data from the post-Xingó period (1993-2018) were used to analyze water discharge data (Q) as a function of precipitation (P) (eq. 3). These data were used to predict the flows of the period before the construction of large dams (1941-1961) based on accumulated monthly rainfall (Fig. 5c). The difference between the water discharge obtained through the adjusted linear equation and the data observed in the fluviometric stations in the LSFR in the pre-large dam period represents the impact caused by climate change.

$$\ldots\ldots\ldots\ldots\ldots\ldots Q = 52.441\,P - 2345.3 \quad ; \quad R^2 = 0.79 \qquad \text{(eq.3)}$$

4. Results

Principal Component Analysis (PCA) allowed individualizing three groups according to their mid-channel bars and channel width (Fig. 5a). Thus, group 1 (G1) puts together the most upstream reaches from R1 to R5, group 2 (G2) clusters the medium course reaches, from R6 to R12, and group 3 (G3) clusters the most downstream reaches, from R13 to R17 (see Appendix – Table 1 and 4). G1 is characterized by steep banks composed of basement rocks, where the channel is narrow and forms a canyon shape (Fig. 5b). At this point, the river is sourced by sediments at the confluence of small tributaries that form a fan-like deposit (Fig. 5c). Group 2, in turn, exhibits weaker bank angles along the banks of the river, more frequent underwater bed forms, and larger mid-channel bars (Fig. 6d). Finally, Group 3 extends along an alluvial plain, where large vegetated islands are found, and the main channel widens. (Fig. 6e).

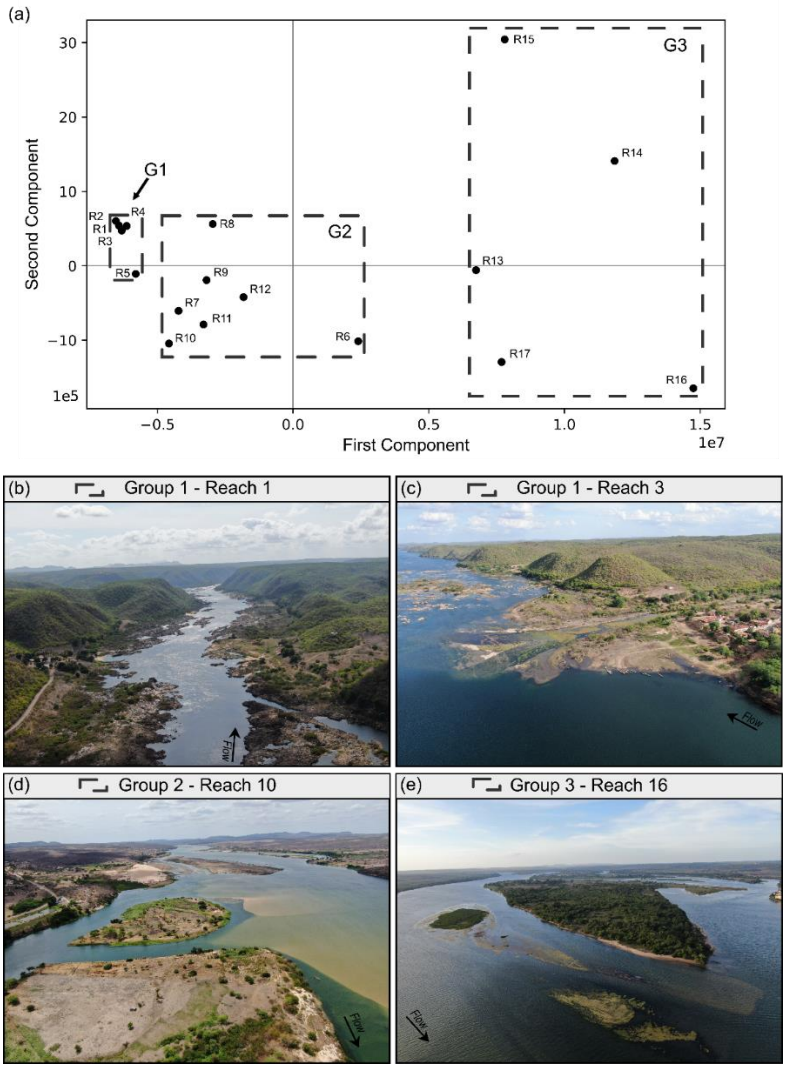

Fig. 5. (a) Principal Component Analysis Clustering Group 1 (G1), Group 2 (G2), and Group 3 (G3), based on the calculated percentage of mid-channel bars and channel width. b) Canyons of the São Francisco River near the Xingó Dam, a morphological feature of Group 1. c) Fan Deposition at the confluence with the Jacaré River d) General view of the main channel and mid-channel bars in Group 2. e) Large vegetation islands on the main channel and floodplain to the left of Group 3. Images of the river were acquired from remotely piloted aircraft (RPA) in February 2021.

4.1 Percentage of mid-channel bars

Mid-channel bars and vegetation-stabilized islands were measured on seventeen sections of the lower Sao Francisco River. During 35 years (1985 to 2020), the area in the main river channel, occupied by mid-channel bars, varied from none in reach 2 and 10 (G1) to a maximum of 51.4% in reach 16 (G3). A minimum mean value was found in sections near the dam (G1), increasing to more downstream zones (G2 and G3, respectively) (see Appendix – Table 1).

G1 comprises the slightest mid-channel bars variation. From 1985-1996 there were no register and in 2018 reach 5 registered 13.7%, exibiting a mean value of 1.7% in G1. G2 clusters the reaches where the bar sizes were more variable in time downstream of the Xingó dam, showing a mean value of 13.0%, from not detected in reach 10 (1985) to 34.7% in reach 6 (2018). G3 clusters have a significant proportion of mid-channel bars with an average value of 32.9%. The low cut line is about 16.5% (2018), and the high cut line is about 51.4% (2020), respectively, at 15 and 16.

Compared to a temporal scale, G1 and G2 showed a discrete average trend in the growth of middle channel bars until 2009. Both groups showed a considerable increase from that year and at a higher rate in G2. Nevertheless, the G3 had a moderate growth pattern, as evidenced by discrete area losses in 1992 and 2004 and gains in 1996, 2003, 2009, and 2020 (Fig. 7).

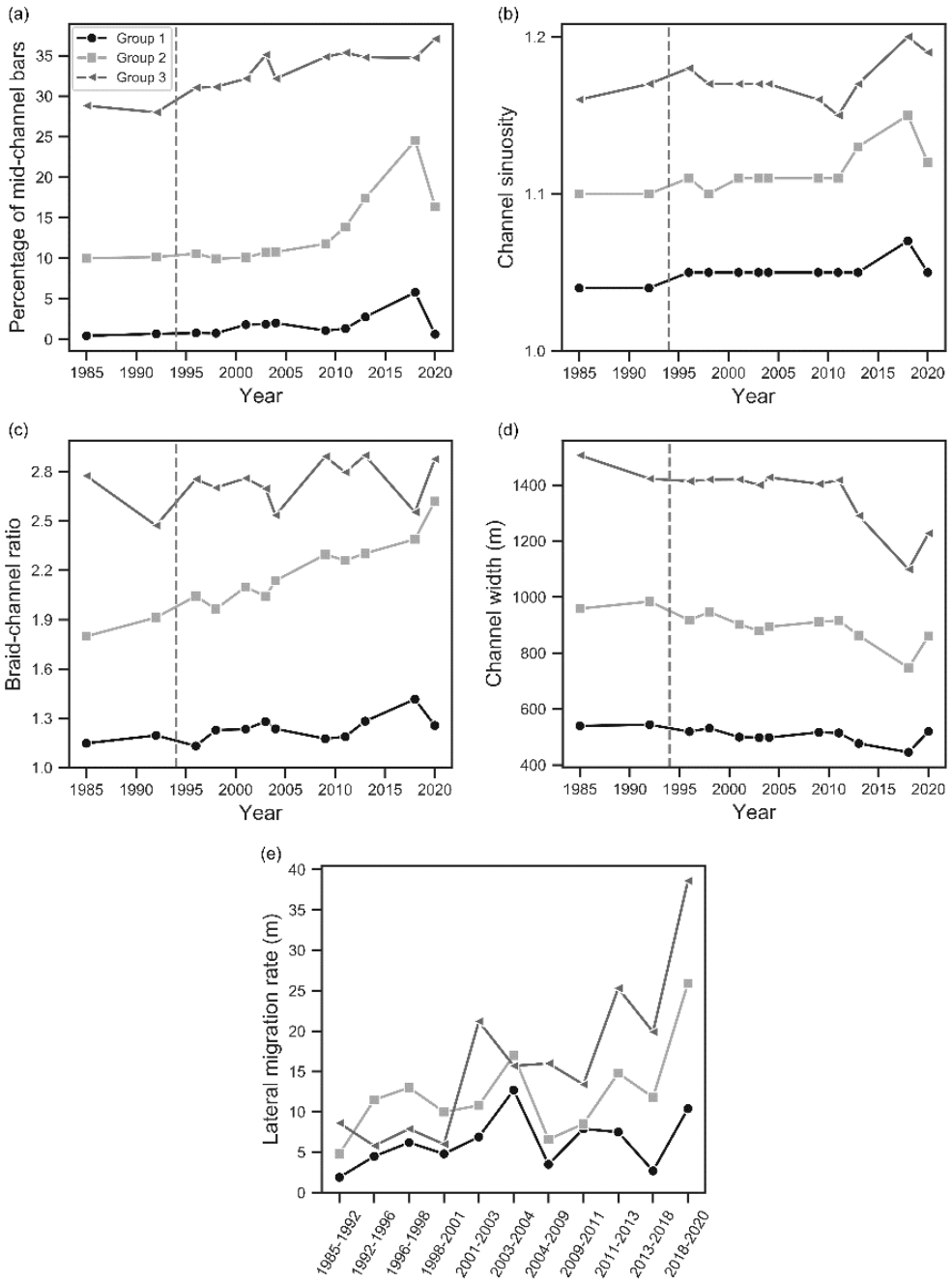

Fig. 6. The temporal scale evolution of metrics at the upstream (G1), medium (G2), and downstream courses (G3): (a) mid-channel bars index, (b) channel sinuosity, (c) braid-channel ratio, d) channel width variation, e) lateral migration rate. The dotted vertical line shows the start of the Xingó dam operation in 1994.

G1 and G2 could be divided into three-time intervals: *(1)* from 1985 to 2009 when the percentage of mid-channel bars was low and stabilized, respectively, around 1.2% and 10.5%; *(2)* from 2011 to 2018, when mid-channel bars had the fastest increasing rates pushed by reaches 1

and reach 5 (G1) and by reaches 9, 10 and 11 (G2). Thus, although the exposure area of the middle channel bars rose slightly between 1992 and 2009 (Fig. 7), the number of exposed bedforms underwent a substantial increase until 2018 (Table 2), followed by a slight reduction after the increasing number of outflow rates operated by the Xingó Dam in 2020; and *(3)* from 2018 to 2020, when channel bars occupation rates decreased from 5.8% to 0.6% in G1 and from 24.5% to 16.4% in G2.

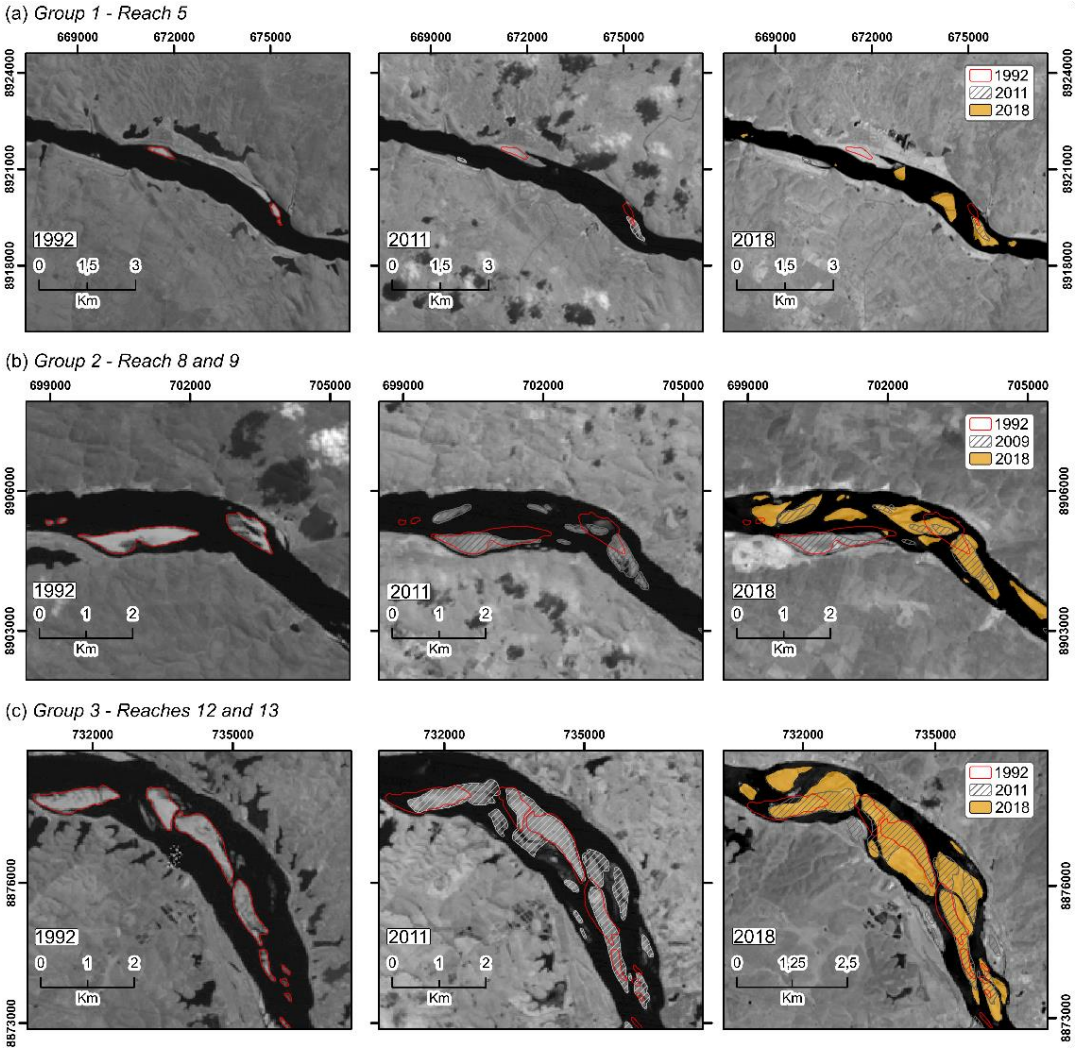

Fig. 7. Contrasting growth modes of the midchannel and alternating bars separated by G1, G2, and G3. (a) G1 showed that mid-channel bars growth is primarily controlled by the exposure of newly underwater dune forms. (b,c). Growth refers to the lateral and downstream expansion of pre-existing or rarely alternating middle channel bars (c). All images were taken under the same flow regime.

Table 2. Evolution of midchannel bars (mean and count size) from 1985 to 2020 in G1, G2, and G3. The average bar count is not a whole number as it is the average of the reaches that constitute each group.

Year of satellite imagery	G1		G2		G3	
	Km²	Average counting	Km²	Average counting	Km²	Average counting
1985	0.1	2.8	3.6	4.7	4.1	9.8
1992	0.2	2.6	3.7	5.6	4.5	9.2
1996	0.3	1.6	2.4	9.0	3.3	12.8
1998	0.2	3.0	2.2	8.4	2.9	11.8
2001	0.5	3.2	2.7	9.0	3.0	13.8
2003	0.6	3.4	2.8	8.9	3.1	10.2
2004	0.6	2.8	2.9	10.1	3.4	10.0
2009	0.3	1.8	2.6	10.4	3.1	11.6
2011	0.4	2.2	2.9	11.3	3.4	12.0
2013	0.8	4.6	3.3	11.1	4.5	13.8
2018	1.6	5.8	5.1	11.7	6.8	12.4
2020	3.0	3.4	3.5	16.3	4.5	14.2

G3, on the other hand, represents at the same time the significant number of channel bars preserved on each year and the most prolonged period of bars stabilization (2003 to 2018), revealing two well-defined periods of growing tendencies, from 1996 to 2003, from 2018 to 2020. In contrast, the following periods (1985-1992, 2003-2004, 2011-2018) registered a slight decrease

in the number of mid-channel bars. Unlike the behavior observed for G2 in which mid-channel bars respond to the accumulation of newly exposed bedforms inside the main channel (Fig. 7a), the size growth of the exposed bars for G3 results from sediment aggradation on pre-existing sedimentary mesoforms, which expand laterally and downstream.

Reaches that had increased mid-channel bars alternate with those where bars decreased before the Xingó Dam became operational. Nevertheless, when individual reaches are taken into account, the rates of eroded bars are much lower than rates of newly exposed or accretion bars (Fig. 8a). There is a predominance of sections in which channel bars increased after the Xingó regulation, compared to six sections in which the total size of bars in the area declined. The total area of bar sizes on individual reaches has increased by more than 95% in four of them (2, 10, 11, and 12), and the others have grown above 15% (Fig. 8b).

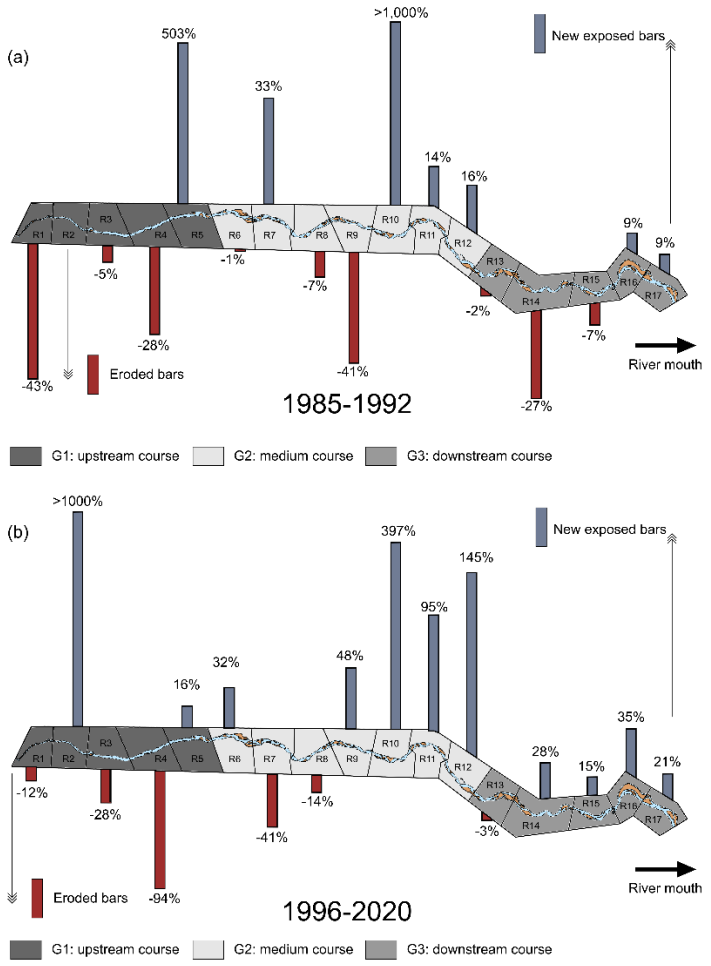

Fig. 8. Distribution of gains and loss rates of bar sizes. (a) Before and (b) after Xingó Dam became operational.

4.2 Channel sinuosity and braid-channel ratios

The Channel Sinuosity Index varied from a minimum of 1.02 in Segment 4 (G1) upstream to a maximum of 1.38 in Segment 16 downstream (G3) of the River Course. However, from 1985 to 2020, sinuosity showed few variations, showing a discrete growing tendency from 2011 to 2018 in every reach, indicating that the main channel banks were preserved across the river profile, even after the construction of Xingó's reservoir (Fig. 6b, see Appendix – Table 2).

The Braid-Channel Index indicated growing downstream values, divided into three groups ranging from the lowest to the highest. G1 has a braid ratio of 1.2. Within this group, reach 2 presented the lowest value (1.0), whereas reach 5 showed the highest (1.9). G2 showed intermediate braid rate values, with an average of 2.2 and a high value in reach 6 (3.3). G3 showed, on average, the highest braid ratio values (2.7), varying from a minimum of 2.2 and a maximum rate of 3.4, both in reach 14 (see Appendix – Table 3). A temporal analysis from 1985 to 2020 showed small changes for each group (Fig. 6c). G1 is the least variable, and G2 is the highest braid-channel ratio in the lower Sao Francisco River, with a steady growth trend between 1985 and 2020. Like the G1, there were no significant temporal changes to the G3.

4.3 Channel width changes

Channel width values varied from a minimum of 171 m in reach 1 (in 2018) and a maximum of 1638 m in reach 16 (2011), an average width of 929 m. G1 (ranges 1 - 5) showed the lowest average widths, reaching a minimum of 171 m in reach 1 and a maximum of 787 m in reach 5 (1992). G2 (reaches 6 – 12) downstream the longitudinal profile revealed the lowest width values in reach 8 (661 m em 2008) and the highest widths in reach 6 (1308 m in 1992). G3 (reaches 13-17) showed the highest width values, varying from 769 m in reach 14 and 1638 m in reach 16 (Fig. 6d).

All analyzed groups of reaches showed an overall channel width decline, which remained constantly declining after the Xingó Dam was fully operational in 1994, except for the period from 2012 to 2020 when the main channel narrowing rates were higher, affecting mainly the most downstream areas (Fig. 6d, see Appendix – Table 4). From that time onwards, the channel width was reduced by about 60 m in G1, 160 m in G2, and 315 m in G3. The higher rates observed since 2018 are interpreted as the response of the main channel to the incremental output values permitted by the ANA. It is imperative to highlight that satellite images representing only the pre-dam period were obtained under a low seasonal discharge regime, which means that the main channel probably flooded a larger floodplain area during the bankfull stages, which suggests the narrowing process might have been more significant in magnitude.

Before the construction of Xingó's reservoir, channel width variation was almost unperceptive within the groups, registered in the form of a discrete channel widening in G2 and a channel narrowing in G3 (Fig. 9a). However, channel widths have been decreasing after the entire operation of Xingó in 1994, highlighting the importance of monitoring the intermediate and downstream reaches of G2 and G3, where the channel width is shrinking faster in the last years (Fig. 9b).

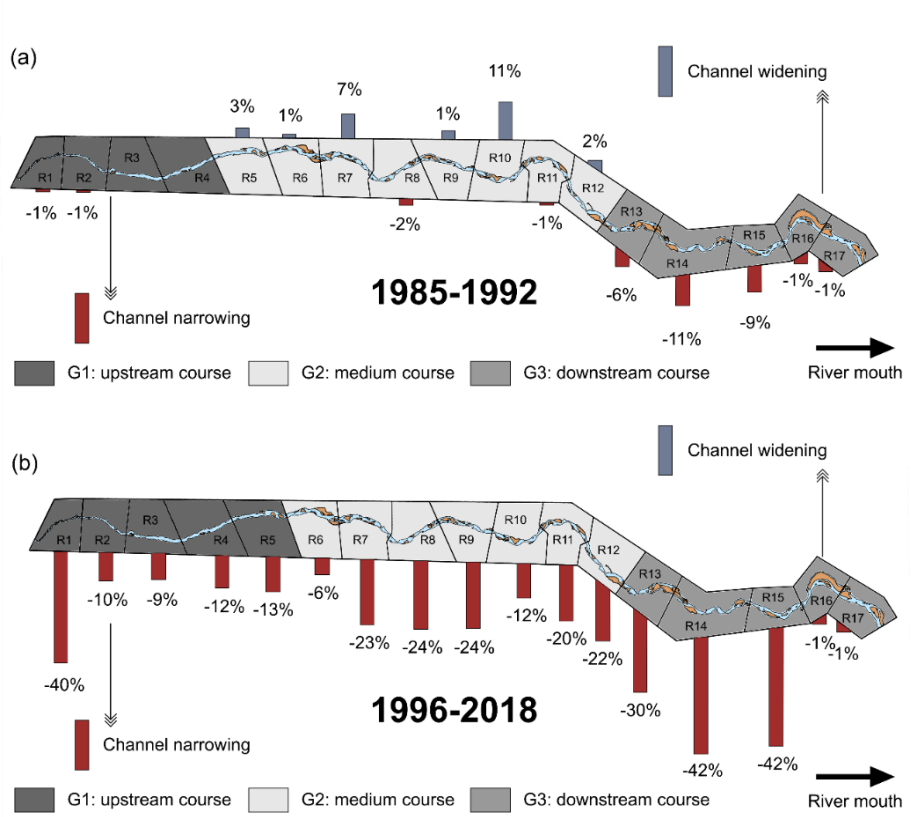

Fig. 9. Distribution of increasing and decreasing channel widths by each reach a) before and b) after the Xingó Dam construction.

4.4 Lateral migration rate

The mean lateral migration rate varied in time and across the river profile (Fig. 6e). In this regard, the groups showed a 1 m/y variation in reaches 3 and 4, and 74 m/y, in reach 15. G1, located by the Xingó Dam, had an average rate of 6 m/y, the least average lateral migration rate. The rates varied from a minimum of 1 in reaches 3 and 4 to a maximum of 18 m/y in reach 5. G2 showed intermediate lateral migration rates with a mean value of 12 m/y. A minimum rate value of 2 m / y was observed in reach 6, and a maximum value of 41 m/y was calculated to reach 12. G3 presented the most significant migration rates with an average of 16 m/y. The values varied from a minimum of 2 m/y in reach 13 and a maximum of 74 m/y in reach 15. These data suggest an increased channel migration towards the river mouth in recent years (Fig. 6e, see Appendix – Table 5).

Regarding the studied interval, groups showed a low lateral migration rate. In G1, we obtained the lowest and the least variable values over time, with a migration rate below 15 m/y during the last 35 years. Despite G2 and G3 migration rates are slightly higher in some years, they also showed average rates below 30 m/y (spatial resolution of Landsat images). Only in 2020, values exceeded this mark (39 m/y - G3) in the outflow discharge from the Xingó dam (Fig. 6e).

4.5 Effective flow rates and suspended load transport

Effective discharge rates showed an apparent contrasting behavior between the two analyzed stations. At the Pão de Açúcar station, on the one hand, we observed a slight decrease of 4% in terms of Q_{eff}, which diminished from 1,955 m^3/s to 1,873 m^3/s after the Xingó dam was built (Fig. 10a). On the other hand, the Propriá station registered an increase of 28%, from 1,746 m^3/s to 2,238 m^3/s (Fig. 10b).

Both stations showed a multimodal behavior concerning the pre-dam period, revealed by different discharge values carrying considerable amounts of suspended sediment. However, during the post-dam period, a more unimodal behavior was observed. Furthermore, the lowest classes of discharge carry a higher percentage of sediment than the higher discharge classes. Therefore, it is suggested here that classes with higher discharge rates played a less important role than ephemeral high peak discharge events in sediment transport along the reaches of the LSFR.

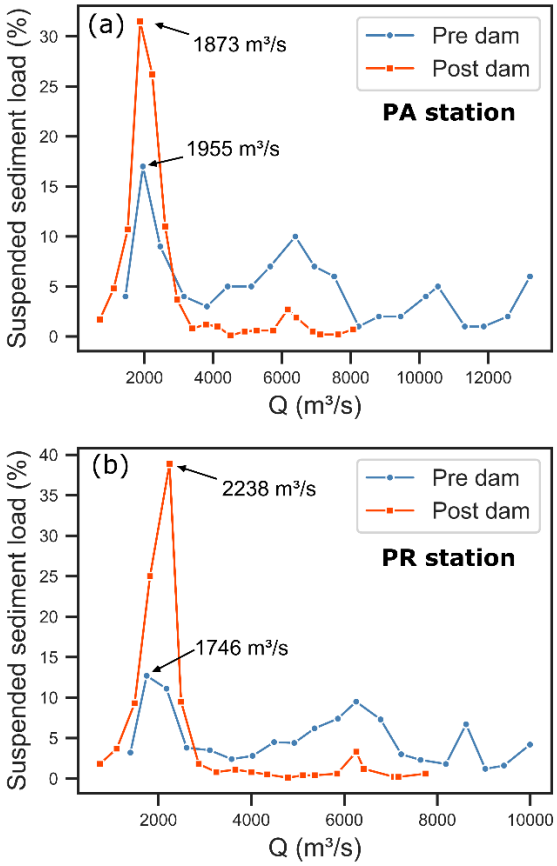

Fig. 10. Total percentage of suspended sediment load transported by each flow class at (a) Pão de Açúcar station (PA station) and (b) Propriá station (PR station). The arrows indicate effective discharge.

4.6 Impacts of rainfall changes on the LSFR

The average monthly rainfall in the SFRB between 1941 and 1961 was 70 mm, and 68 mm in the post-Xingó period (1995-2018), totalizing a decrease of 2 mm (3%) (**Fig. 2**). In the post-Xingó period, rainfall decreased at 36 mm/year, reaching the lowest values in 2015 and 543 mm of annual rainfall accumulated. Similar values were registered during 2001 and 2003, varying, respectively, from 654 mm/year and 655 mm/year. Despite high rainfall events in different basin regions in 2004 and 2007, these episodes were rare, and the dry period quickly prevailed. This scenario aggravated when we analyze the decrease in the prolonged drought

period (2013-2018), where the average monthly rainfall was 57 mm (or 699 mm/year), 18% less than 1941-1961.

Our results showed the basin-wide rainfall and LSFR water discharge are directly related. (Fig. 11a). Both periods (pre and post-Xingó) fit the equations, as demonstrated by square correlation coefficient values of 0.94 and 0.83. Between 1941-1961 the monthly average water discharge was 3,235 m²/s at Traipú station, later reduced to 1,813 m³/s, as measured by the Pão de Açúcar station in the post-Xingó period, and finally to 1,141 m³/s after the 2013 prolonged drought. Using the linear regression data from the post-Xingó period, we calculated the predicted discharge (Qp) between 1941 and 1961, revealing a reduction of 40.4% due to the decrease in the accumulated rainfall throughout the basin (Fig. 11b).

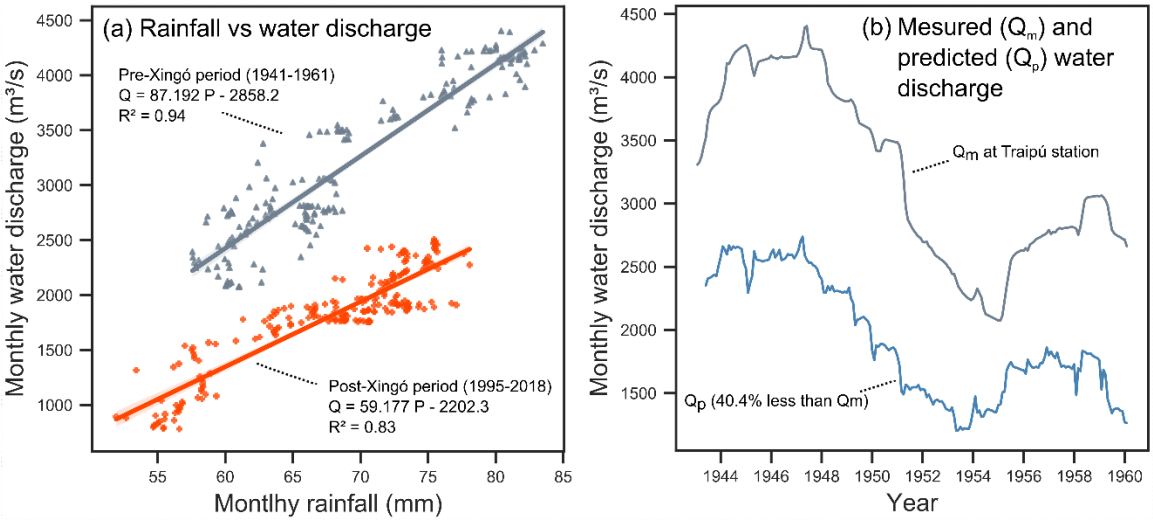

Fig. 11. (a) The forty-eight monthly rolling mean of water discharge at LSFR versus a forty-eight rolling mean of monthly rainfall at basin-wide from the pre-Xingó period (1941-1961) and post-Xingó period (1995-2018). (b) Measured and predicted water discharge in the LSFR at Traipú station.

5. Discussion

5.1 Influences of the Xingó Dam on the fluvial morphology

The full operation of the Xingó power station in 1994 fostered severe impacts on streamflow in the lower São Francisco River Course (Bandeira, 2005; Cavalcante, 2011; Holanda et al., 2005; Fontes et al., 2009), which remained lower than 2,000 m^3/s until 2003 and 1,000 m^3/s after 2013. The latter is due to the beginning of the prolonged drought that hit the basin, except for two discrete high peak discharge events in 2004 and 2007 (Fig. 3a). One direct impact caused by low discharge rates to both incised river canyon (G1) and the alluvial plain (G2 and G3) was the reduction in seasonal floods and the decline in average discharges (Fig. 3b). As a result, one could argue that the river could have suffered an overall base level reduction, making the main channel more dependent on sporadic precipitation over the catchment basin of intermittent tributaries during the last three decades than before Xingó Lake Dam was built. This is corroborated by field data acquired in the 2000s and the first half of the 2010's decades by recognizing an increased number of narrowed spots (e.g., Casado et al. 2002). Our satellite imagery analysis (from 1985 up to 2020) confirms that field data.

5.1.1. Channel style, accretionary and degradational reaches

Low values of the lateral migration rate and low variation of the channel sinuosity suggest that lateral shifts, the creation of chute channels, or the development of crevasse splays are rare morphological elements across the landscape of the LSFR sedimentary record. One way to explain that is possible because the natural morphology restricts the main channel to a valley with higher adjacent areas, decreasing the channel's freedom to migrate laterally (see DEM in Fig. 1c). On the one hand, aerial photographs from the 1960's decade evidence that such morphological elements were previously stabilized in the landscape (Cavalcante, 2011). On the other hand, the trunk river showed discrete adjustments regarding the number and size of mid-channel bars and chute channels over bar tops even before Xingó was operational. From 1985 to 2020, the LSFR

showed a progressive increase in the braid-channel ratio and a slight variation regarding channel sinuosity. Our work suggests a dominant braided style in the area, with a progressive tendency of increased braiding towards the delta plain (Group 3). Compared to Friend and Sinhá (1993) classification, the river has become progressively more braided over the past 35 years (Fig. 12a). G1 suffered morphological changes due to the incised valley and the low discharges that outflowed the Xingó Lake Dam. G2 revealed the most significant variation of braid-channel ratios compared to other groups and among different periods. G3 suffered a decrease in the braid-channel ratio regarding the pre-dam period; however, its braid ratio suffered a slight increase in the post-dam period (Fig. 12b).

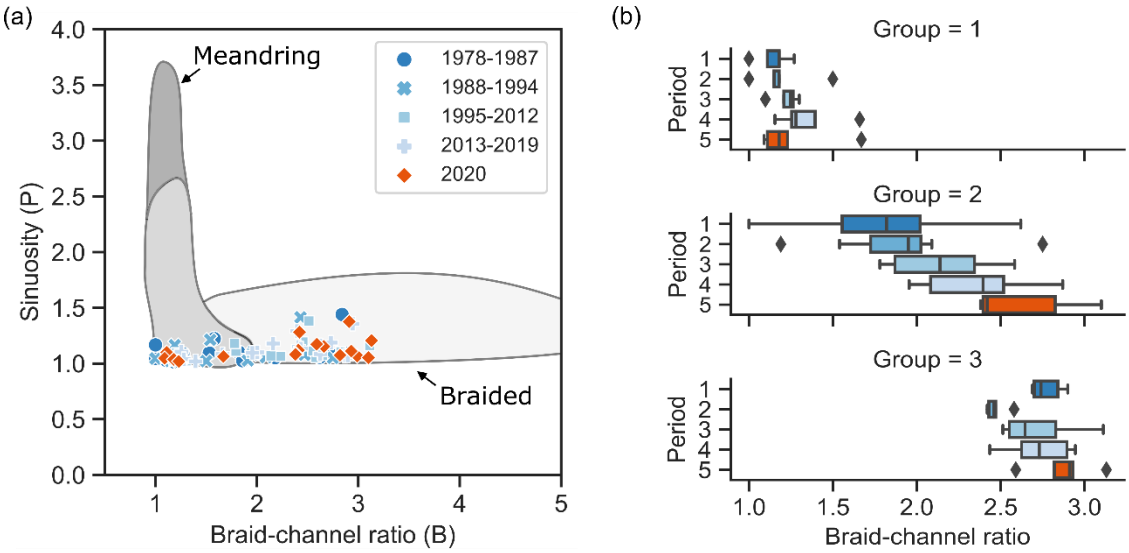

Fig. 12. Compared analysis of sinuosity and braid-channel ratio metrics in the lower São Francisco River with the fluvial morphological fields defined by Friend and Sinhá (1993).

After the Xingó dam was completed in 1994, the percentage of mid-channel bars was increased throughout the LSFR course from Xingó's dam to the city of Penedo, although they differ from one group to another (Fig. 6a). These data contrast Silva et al. (2010) that showed bars were locally reduced in size. That variation in the percentage of mid-channel bars is asynchronous and shows a clear relationship to the new hydrological regime controlled by Xingó. From 1992 to 2009, groups 1 and 2 show similarities in the distribution of mid-channel bars in the main

channel, which remained unchanged until 2009. From 2009 to 2013, we interpret slight accretionary processes on exposed mid-channel bars and abruptly increased accretion from 2013 until 2018 (Fig. 6a, 9) might be related to effective discharge changes before and after the impoundment. At the Propriá Station (reach 14 – G3), effective discharge rates were increased, varying from 1,746 m³/s to 2,238 m³/s, suggesting sediment particles were subjected to less transport at this reach. This interpretation corroborates the results shown by Kong et al. (2020) regarding the alluvial plains of the Yellow River, where the greater is the effective discharge, the greater is the difficulty for the river to carry sediments downstream with a consequent increase in the sandbars deposits. Despite that, the effective discharge measured at the Pão-de-Açúcar Station was slightly lower than the values calculated for the pre-dam period (1,955 m³/s to 1,873 m³/s), which may indicate the opposite effect downstream. It is worth mentioning that the average flow rates measured between 2013 and 2018 were approximately 943 m³/s (Fig. 3), much lower than the established values for the effective discharge at that station (1,873m3/s). These low values tend to carry less amount of suspended sediment load (Fig. 10), showing that the successive reduction of average water discharge, as well as the reduced frequency and intensity of floods in the post-dam period, played a significant role in the retention of sediment in these reaches across the river course. Therefore it is suggested here the flooding events in 2004 and 2007 were punctual and had a low capacity of transporting sediments downstream.

Another relevant process that took place in groups 1 and 2 was the increment of the river flow capacity to erode, which is the result of the free sediments flow derived from the building of barriers along with natural river courses (Nouh, 1990; Merrit and Cooper, 2000; Skalak et al., 2013). Skalak et al. (2013) observed one direct impact in the Missouri River is a rapid channel bed degradation in areas adjacent to the dam, which progressively diminishes downstream. Similar processes were documented in other barried rivers, such as the Colorado River, USA (Williams and Woman, 1984), in the Yangtze River, China (Dai and Liu, 2013), and in the Low Yellow River China (Kong et al., 2020). In the Lower São Francisco River, this process was described by Fontes (2003) between the cities of Pão de Açúcar and Propriá, where the reaches became susceptible to bank erosion and deposition at the most downstream reaches, near the city

of Penedo. Cross-sections measured across the river bed from 1992 to 2008 at the stations of Pão de Açúcar e Propriá corroborate the existence of bed degradational processes taking place in the considered period for reaches R4 and R14, as channel deepened 8 m in the thalweg (Fig. 4).

The increasing percentage of mid-channel bars in G3 occurred through specific time intervals and equally due to different processes. From 1992 to 2003, the occupation of meso and macro forms rose from 28% to 35% in the main channel's area, and from 2003 to 2018, the areal occupation of bars remained constant. This increase after the dam construction results from sediment erosion in the channel itself from areas upstream, as Fontes et al. (2003) described. However, this work predates 2013 to present prolonged drought and the decrease in the average flow, which reduced the river's competence to transport the sediments to this region, now trapping the sediments in the groups closest to the dam (see Fig. 6a).

5.1.2. Modes of channel narrowing

During the last 35 years, a significant narrowing (approximately 20%) was observed associated with the main channel course. From 1996 to 2018, all 17 studied reaches recorded narrowing processes, which contrast most of the field works carried out in the last two decades, suggesting an erosion of channel banks and widening process predominate over narrowing of the main channel (Cavalcante, 2011; Fontes, 2015). In 2020, with a slight increase in water discharge outflow of the Xingó dam, the channel width increased again, however with values still much smaller than the pre-Xingó period.

Different processes were observed that led to the narrowing of the channel, which acted at different times and positions in the LSFR, they are: (1) as the result of unconfined flows from tributaries that widens as a fan-like deposit transversely to the main channel (Schmidt and Rubin, 1995; Grams and Schmidt, 2005), (2) the water discharge decreases, the thalweg deepens, and the channel occupies the deepest parts of the valley (Brandt, 2000) (3) by overall sedimentary accretion, as minor secondary (chute) channels are abandoned or filled up, or by the

superimposition of migrating dunes that laterally accretions mid-channel bars, and progressively expands and attaches to the floodplain area (Miall, 1996; Bridge, 1993; Ashworth et al., 2011),

The first model best explains our results for the most upstream reaches of group 1. This group that extends from the canyons immediately downstream of Xingó Dam to the proximity of the city of Pão de Açúcar, where small rivers carry more water volumes and sediment to the main channel and form the fan-like deposits, that are no longer remobilized downstream (Fig. 13a-e). The actual situation points out that G1 deserves more attention, as it was observed when the river at the higher flow stage could no longer remobilize bedload sediments from tributaries nor deepens the thalweg as a function of a bedrock mainly composed of igneous and metamorphic.

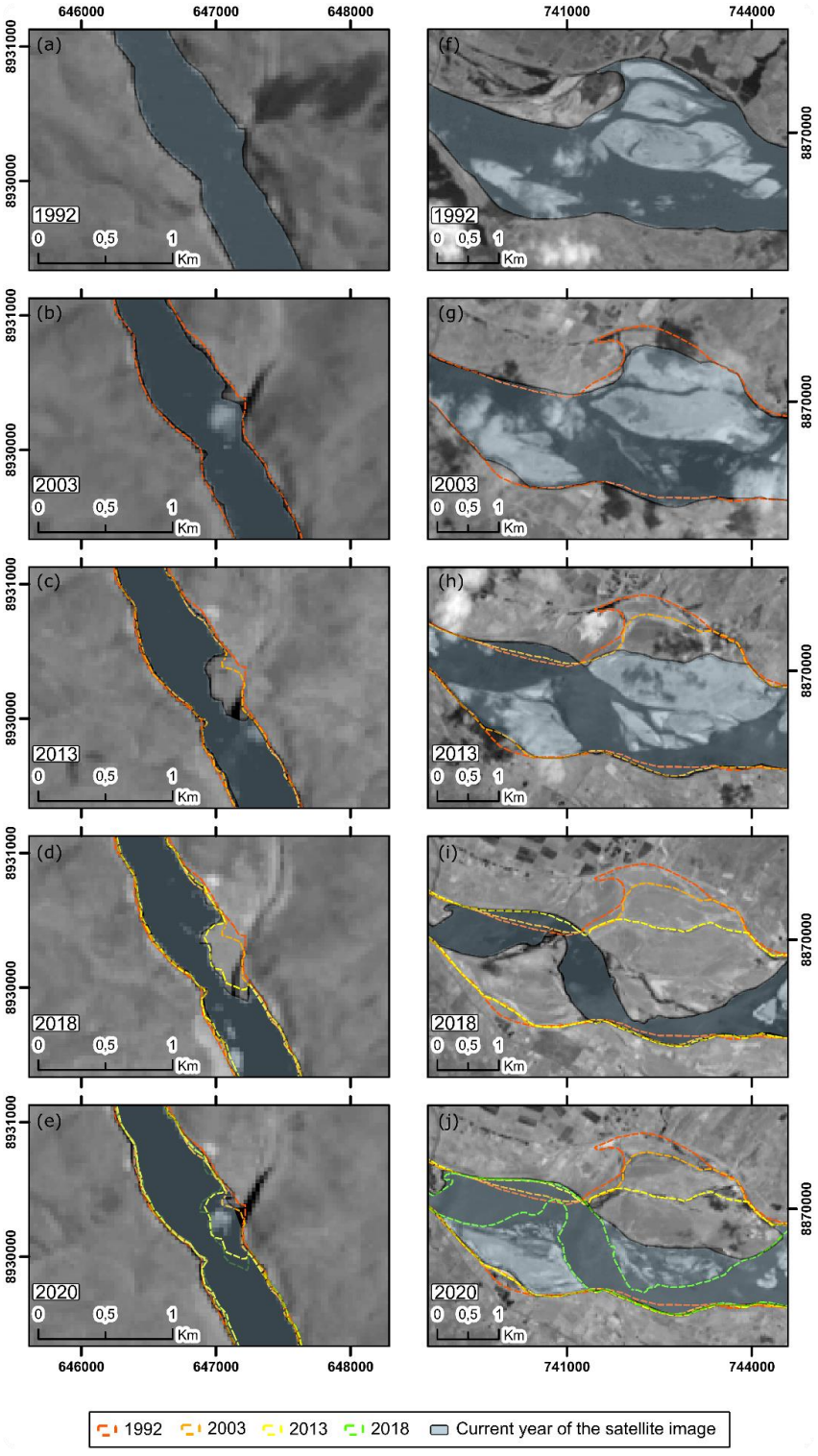

Fig. 13. Channel width changes between 1992 and 2020 near the city of Propriá (Group 3 – reach 14). In 2018 the width was reduced due to the expansion and attachment of bars to channel banks. In 2020, increased discharges made the base level rise, lower areas were flooded, some secondary channels were activated, and the width of the channel increased. The red line indicates the channel bank position in 1992.

An alternative channel narrowing process (model 2) was interpreted for groups 2 and 3; with the reduction of flows and only the deepest parts of the river valley being occupied by the main channel, there is an abandonment of the minor secondary channels and the consequent anchorage of the mid-channel bars to the banks, transforming them into a floodplain. In addition, most of the new accretion areas are sourced by eroded sediment from the river bank and shallower areas within the channel, where active subaqueous dunes are remobilized in a similar way described by Ashworth (1996) and Ashworth et al. (2000). Thus, the expansion of deposits (mainly in group 3) and filling secondary channels, as described in model 3, combined with model 2, would be the main process responsible for decreasing channel width. These processes suggest bank erosion is local and part of the fluvial dynamic, prevailing the transformation of riverbed into floodplains.

Conversely, channel widening was only observed in the last years before Xingó Dam was built from 1985 to 1992 (Fig. 12). In the last decade, from 2013 to 2020, morphological changes have intensified in the lower São Francisco River, with a direct impact upon reaches that suffered erosion in both river banks, at sites where different stages of bank erosion were evidenced, mainly near the cities of Propriá and Penedo (Cavalcante, 2011; Fontes, 2015).

The erosion that occurs preferentially of the channel bed instead of the margins, disfavoring the channel widening, take place due to the absence of processes that prevent the degradation of the bed, such as armoring effect (Sherrard and Erskine, 1991; Gupta, 2007) or sediment yield downstream of the dam (Sherrard and Erskine, 1991; Choi et al., 2005). Previous works do not evidence that gravel sediments can contribute to the onset of armoring effect (Casado et al., 2002; Fontes, 2003; Fontes et al., 2009). Despite that, detailed research regarding the lack of bedload armoring in the LSFR is still needed. Furthermore, higher velocity flows occupy the deepest and central parts of the channel, and erosion occurs preferentially in the channel bed instead of eroding the banks (Miall, 1996).

5.2. Impacts caused by climate controls in the LSFR course

Other natural controls such as climate and hydrological changes measured in the LSFR course can contribute to the effects caused by human activity downstream of Xingó reservoir. The first control is the hydrological dependence that arid regions have on the "water towers" located at the headwaters of the catchment basin, discussed by Viviroli and Weingartner (2004). The authors have demonstrated that lowland rivers that run through dry climate regions account for up to 50% of their water discharges at the highlands (e.g., Ebro, Indus, Niger, Po, Senegal, and Tigris rivers). In cases where extreme arid conditions were documented, the interdependence from highland discharges can reach up to 90% of the total amount (e.g., Amu-Darya, Colorado, Euphrates, Negro, Nile, and Orange rivers). In Brazil, the São Francisco River basin is an example of the dependence that the dry lower course (semi-arid region of Northeastern Brazil) has on the flow from the rainy highlands, which contribute to approximately 70% of the flow originating in the upstream São Francisco River (Viviroli e Weingartner, 2004; Bandeira et al., 2008; Bandeira et al., 2013; Fontes, 2015).

In the last decades, the São Francisco River Basin has been suffering from the increased frequency and intensity of dry periods (Knight et al., 2006; Marengo et al., 2012; Assis et al., 2015; De Jong et al., 2018; Kuwajima et al., 2019), especially at the highlands (Getirana, 2016; Sun et al., 2016; Santos et al., 2017; Santos et al., 2018) (Fig. 2a). Our results demonstrated that the decrease in rainfall resulted in 40.4% less frequent water discharges into the LSFR (Fig. 11). This fact has directly impacted water availability for human consumption, agriculture, livestock, and hydropower generation. These prolonged drought events worsened after 2012, registering one of the most severe droughts on a century-scale (Sun et al., 2016; De Jong, 2018). As a result, there was a significant decrease in reservoirs volume in large dams such as Três Marias, Sobradinho, and Itaparica, which have remained below 50% since then (Fig. 2b). This drawdown caused a decrease in the effluent water discharges from the reservoirs to maintain the minimum operating volumes. As a result, the amount of water reaching the Lower São Francisco River has decreased significantly in recent decades, since the magnitude of the flow reduction is greater than the decrease in rainfall in the basin due to the different uses of water in the basin (Milliman et al.,

2008; De Jong et al., 2018). This decrease in the amount of water made available to the lowlands was responsible for the lowering of the river level and the abandonment of small secondary channels leading to the anchoring of mid-channel bars to the banks of the, one of the main processes of transformation of areas occupied by floodplain channel, resulting in the narrowing of the channel.

In addition, since 2013 and the consequent outflow reduction in the last decade, this extreme drought event was one of the factors responsible for the increase in bedforms in the Lower São Francisco River. As the mean monthly discharges were reduced, from high peak discharges (1,900 m^3/s) between 1995 and 2012 to 930 m^3/s between 2013 and 2019, flowrates today are about 51% and 43% of the effective discharge at the gauge stations of Pão de Açúcar and Propriá, respectively. As a result, the river can no longer transport sediments downstream, increasing the percentage of mid-channel bars that double-folded in G2, making the river even more braided since 1995 (see Fig. 12).

The climate mentioned above and the reduced rainfall in the drainage basin also influenced the sedimentation of the São Francisco delta at the river mouth. Dominguez and Guimarães (2021) pointed out a progressive decrease in flow rates has a more significant impact than the trapping of sediments in the reservoirs of large dams upstream. The authors suggest that the increasing flow values and the transport of sediments downstream of the Xingó dam could decrease erosion processes and keep the coastline constant for some decades. This interpretation supports our argument that the river has greater difficulty transporting sediments downstream, thus becoming trapped closer to the dam, even those sourced downstream of Xingó. In addition, the value of the effective discharge in the post-Xingó period may indicate a minimum flow to be practiced in order to prevent the processes of accumulation of sediments in the river system from occurring and these sediments reaching the mouth, maintaining the dynamic balance and decreasing the anthropic effects in the region.

5.3. Areas of concern in the short-term

The LSFR has suffered from the accumulation of sediments as mid-channel bars (or anchorage bars areas that have become a floodplain) and reduced channel width in response to the decrease in water discharge due to the accumulation in the the upstream dams reservoirs. However, natural changes as a decrease in rainfall seem to significantly reduce average water discharge.

G1 is the least variable among all groups and has not shown channel width variations from 1996 to 2020 (Fig. 6d). However, when the discharge values reached their minimum in 2018, the group presented a 14% reduction. In this regard, the most upstream area (reach 1) inside this group deserves more attention since it showed a significant reduction of 40% in the same period (Fig. 9b). Additionally, the percentage of mid-channel bars showed a definite upward trend in response to the decrease in channel transport capacity throughout the lowest drought discharges since 2013. Similar behavior is observed for group 2, where it moved from a sediment source area to a downstream area of accumulation after 2013 (see Fig. 6)

The groups further downstream (G2 and G3) show a low variation in the pre-dam period, with an average variation of less than 10% in channel width. However, after the impoundment, the scenario became critical. G2 showed a mean reduction of 22 % in 33 years (1985-2018), strongly pulled by reaches 7, 8, 9, 11, and 12, which had their channel width reduced by more than 20 % between 1996 and 2018 (Fig. 9b). G3 is the most critical group, specifically in reaches 13, 14, and 15 (Fig. 9b) that together with reach 1 (G1), suffered the highest channel width reductions (30 %, 42 %, and 42 %) after the Xingó was built. Whereas few variations were noted in reaches 15 and 16, revealing the reduced influence of the dam's entire operation upon these areas. From 2018 to 2020, it is remarkable how flow rates above 1,000 m3/s released in 2020 could double fold the channel width and promote the inundation of exposed bars in two years. Such an inundation event was evidenced by activating secondary chute channels running through mid-channel bars and alternate bars (Fig. 13j).

With the combination of forecasts predicting reduced rainfall across the São Francisco River Basin (Nakicenovic, 2000; De Jong et al., 2018) and the growing demand for water

resources for various purposes, further reductions in average water discharges may occur (De Jong et al., 2018). With this, the river will seek a new dynamic balance due to its imposed changes. Therefore, a reduction in the flow transport capacity and an even more significant accumulation of sediments in bars in groups 1 and 2 are expected if the predicted scenarios are not changed. Furthermore, the reduction in rainfall will further reduce the amount of sediment in the basin, making the LSFR more dependent on the low sediment load of its lower course (Moura et al., 2007).

6. Conclusions

Dammed river systems may exhibit significant variations in their hydrological and sedimentological regimes and reveal a high complexity for quantification and comparison of these adjustments. Therefore, this work aimed to analyze the processes and outcomes of the significant water discharge control factors and how this has impacted LSRF. Our satellite image analyses showed a predominance of adjustments internally to the main channel (decrease in width and increase in the percentage of mid-channel bars) instead of external adjustments to the channel (low lateral migration rate and a slight variation of channel sinuosity).

The channel narrowing (approximately 20%) in the main channel has prevailed instead of widening over the past 35 years. In this regard, G1 has undergone a 40% reduction, mainly due to fan deposition by tributaries. G2 and G3 exhibited the worst-case scenario. The transformation of the active channel into floodplains is due to the abandonment of secondary channels that responded faster after Xingó was built to expand the mid-channel bars and the attachment of these bars to the channel banks. Channel narrowing processes in G2 suggest bank erosion is local and part of the fluvial dynamic, prevailing the transformation of riverbed into floodplains, corroborated by the mean width reduction of 22 % in 33 years (1985-2018). G3 (reaches 13, 14, and 15) suffered the highest channel width reductions (30 %, 42 %, and 42 %) after the Xingó was built and is the most critical group.

The depositional modes that best explain the accumulation of sediments in LSFR indicate that new accretion areas are sourced by eroded sediment from the channel bed and, secondarily, the riverbank, where active subaqueous dunes are remobilized. As for the changes in the percentage of mid-channel bars, G3 increased immediately after the construction of the Xingó dam. However, with successive flow reductions, the result of prolonged drought since 2013, and reduction of river transport capacity, the sediments were deposited in regions increasingly nearer the dam, indicating that future flow reductions can lead to further accumulation in these reaches.

Climate and hydrological changes in the LSFR course contributed to the effects caused by the regulation of flow rates downstream of the Xingó reservoir, with a reduction of 3% in rainfall and 40.4% in water discharge during the post-Xingó period relative to the 1941 and 1961 average. Prolonged drought events worsened since 2013, registering one of the most severe droughts in a century-scale and the consequent reduction of 55% in water discharge in the last decade compared to the mid-last century responsible for the increase in bedforms in the Lower São Francisco River. Therefore, the morphological adjustments derived from that in the last decades in the Lower São Francisco River greatly fit the significant climate changes in the Northeast and Southeast of Brazil and not with water storage in the large reservoirs. In this sense, the decrease in precipitation was responsible for reducing the volume of the dam's reservoirs, which began to reduce effluent to maintain their operational volume. This is a consequence, not the reason for the decrease in LSFR flow.

However, much of the reduction in water discharges are due to anthropogenic effects resulting from the diversion of water used for various purposes throughout the basin. In addition, the growing demand for water resources throughout the basin contributes to an even more significant reduction in the quantity of water reaching Lower São Francisco. Due to low precipitation, water demand for irrigation and livestock has increased over the last few decades. Moreover, future precipitation forecasts indicate a remarkable decrease in the entire basin, further reducing streamflow and may continue to alter river morphology. In this sense, public policies are needed for the use of water resources in the basin, as this resource may become increasingly scarce and minimum flows cannot be practiced in the Lower São Francisco, as the effective

discharges of 1873 m^3/s and 2238 m^3/s to the Pão de Açúcar and Propriá stations, respectively. For this, a more accurate determination of the effective discharge values and the individualization of the human impacts on the water discharge in the LSFR is vital for future climate and anthropogenic impact scenarios. For this, the systematic collection of data such as the amount of bottom load, tributary flows, and the construction of a more robust sedimentary load historical series may be an essential aid for reducing uncertainties for the management of the São Francisco river.

Acknowledgments

The current work has been carried out with the support of the Coordination for the Improvement of Higher Education Personnel - Brazil (CAPES) - Funding Code 001. We appreciate their scholarship. We are thankful for the Graduate Program in Geoscience and Basin Analysis and the Federal University of Sergipe (PGAB-UFS), which provided financial and logistical support during field trips. We also thank Aracaju Civil Defense for the acquisition of low-altitude pictures. We are grateful for the reviews and comments of Ana C. S. Andrade, Cristiano P. Galeazzi, and Paulo S. R. Nascimento, who helped improve the document.

References

Ashworth, P.J., 1996. Mid-channel bar growth and its relationship to local flow strength and direction. Earth Surface Process and Landforms. 21 (2), 103-123. https://doi.org/10.1002/(SICI)1096-9837(199602)21:2<103::AID-ESP569>3.0.CO;2-O..

Ashworth, P.J., Best, J.L., Roden, J.E., Bristow, C.S., Klaassen, G.J., 2000. Morphological evolution and dynamics of a large, sand braid-bar, Jamuna River, Bangladesh. Sedimentology. 47 (3), 533-555. https://doi.org/10.1046/j.1365-3091.2000.00305.x.

Ashworth, P.J., Sambrook Smith, G.H., Best, J.L., Bridge, J.S., Lane, S.N., Lunt, I.A., Reesink, A.J.H., Simpson, C.J., Thomas, R.E., 2011. Evolution and sedimentology of a channel fill in the sandy braided South Saskatchewan River and its comparison to the deposits of an adjacent compound bar. Sedimentology, 58(7), 1860-1883. https://doi.org/10.1111/j.1365-3091.2011.01242.x.

Assis, J.M.O., Werônica, M.S., Sobral, M.C., 2015. Climate Analysis of the Rainfall on Sub-medium Part of the São Francisco River Basin Based on the Rain Anomaly Index. Brazilian Journal of Environmental Sciences. 36, 115-127. https://doi.org/10.5327/Z2176-947820151012.

Bandeira, A.A., 2005. Evolução do processo erosivo na margem direita do rio São Francisco e eficiência dos enrocamentos no controle da erosão. MS Dissertation, Pós-Graduação em Desenvolvimento e Meio Ambiente, Universidade Federal de Sergipe, São Cristóvão.

Bandeira, J.V., Salim, L.H., Calisto Acosta, O.E., 2008. Long-term morphological impacts on the coastline of Sergipe State, Brazil, caused by the construction of dams in the São Francisco River Basin. In. In Seventh International Conference on Coastal and Port Engineering in Developing Countries–COPEDEC VII, Dubai, UAE.

Bandeira, J.V., Farias, E.G.G., Lorenzetti, J.A., Salim, L.H., 2013. Resposta morfológica da foz do Rio São Francisco, devido à retenção de sedimentos nos reservatórios.

Bernardes, L.M.C., 1951. Notas sobre o clima da bacia do Rio são Francisco. Revista Brasileira de Geografia. 13, 473-489, 1951.

Benn, P.C., Erskine, W.D., 1994. Complex channel response to flow regulation: Cudgegong River below Windermere Dam, Australia. Applied Geography. 14, 153–168.

Best, J., 2019. Anthropogenic stresses on the world's big rivers. Nature Geoscience. 12 (1), 7-21. https://doi.org/10.1038/s41561-018-0262-x.

Biedenharn, D.S., Thorne, C.R., Soar, P.J., Hey, R.D., Watson, Ch.C., 1999. A practicalguide to effective discharge calculation (Appendix A). in: Watson, C.C., Biedenharn, D.S., Torne, C.R. (Eds.), Demonstration Erosion Control-Design Manual. U.S.Army Corps of Eng, Vicksburg, pp. 239-274.

Borges, C.Z., 2004. Erosão marginal no rio Paraná após a conclusão do reservatório da UHE Sérgio Motta (Porto Primavera) a jusante da barragem. Master Thesis, Universidade Estadual de Maringá.

Brando, P.M., Balch, J.K., Nepstad, D.C., Morton, D.C., Putz, F.E., Coe, M.T., Silvério, D., Macedo, M.N., Davidson, E.A., Nóbrega, C.C., Alencar, A., Soares-Filho, B.S., 2014. Abrupt increases in Amazonian tree mortality due to drought–fire interactions. Proceedings of the National Academy of Sciences, 111(17), 6347-6352. https://doi.org/10.1073/pnas.1305499111.

Brandt, S.A., 2000. Classification of geomorphological effects downstream of dams. Catena. 40 (4), 375-401. https://doi.org/10.1016/S0341-8162(00)00093-X.

Bridge, J.S. 1993. The interaction between channel geometry, water flow, sediment transport and deposition in braided rivers. Geological Society of London, Special Publication. 75, 13-71. https://doi.org/10.1144/GSL.SP.1993.075.01.02.

Carling, P.A., 1988. Channel change and sediment transport in regulated UK rivers. Regulated Rivers: Res. Manage. 2, 369–387. https://doi.org/10.1002/rrr.3450020313.

Casado, A.P.B., Holanda, F.S.R. Araújo-Filho, F.A.G., Yaguiu, P., 2002. Revista Brasileira de Ciência do Solo. 26, 231-239.

Cavalcante, A.D.J.B.D., 2011. Impactos nos processos morfológicos do baixo curso do rio São Francisco, decorrentes da construção de barragens. PhD Thesis, Universidade Federal do Rio de Janeiro, Rio de janeiro.

Cavalcanti, I.F.A., 2004a. Boletim de Monitoramento e Análise Climática. CPTEC/INPE, São Paulo. 19(1).

Cavalcanti, I.F.A., 2004b. Boletim de Monitoramento e Análise Climática. CPTEC/INPE, São Paulo. 19(2).

Cavalcanti, I.F.A., 2007a. Boletim de Monitoramento e Análise Climática. CPTEC/INPE, São Paulo. 22(1).

Cavalcanti, I.F.A., 2007b. Boletim de Monitoramento e Análise Climática. CPTEC/INPE, São Paulo. 22(2).

Chen, Z.Y., Wang, Z.H., Finlayson, B., Chen, J., Yin, D.W., 2010. Implications of flow control by the Three Gorges Dam on sediment and channel dynamics of the middle Yangtze (Changjiang) River, China. Geology. 38, 1043–1046. https://doi.org/10.1130/G31271.1.

Choi, S.U., Yoon, B., Woo, H., 2005. Effects of dam-induced flow regime change on downstream river morphology and vegetation cover in the Hwang River, Korea. River Research and Applications. 21 (2-3), 315-325. https://doi.org/10.1002/rra.849.

Colby, B.R., 1957. Relationship of unmeasured sediment discharge to mean velocity. Eos, Transactions American Geophysical Union. 38 (5), 708-717. https://doi.org/10.1029/TR038i005p00708.

Dai, Z., Liu, J.T., 2013. Impacts of large dams on downstream fluvial sedimentation: An example of the Three Gorges Dam (TGD) on the Changjiang (Yangtze River). Journal of Hydrology, 480, 10-18. https://doi.org/10.1016/j.jhydrol.2012.12.003.

De Jong, P., Tanajura, C.A.S., Sánchez, A.S., Dargaville, R., Kiperstok, A., Torres, E.A., 2018. Hydroelectric production from Brazil's São Francisco River could cease due to climate change and inter-annual variability. Science of the Total Environment. 634, 1540-1553. https://doi.org/10.1016/j.scitotenv.2018.03.256.

Dominguez, J.M.L., Guimarães, J.K., 2021. Effects of Holocene climate changes and anthropogenic river regulation in the development of a wave-dominated delta: The São Francisco River (eastern Brazil). Marine Geology. 435, 106456. https://doi.org/10.1016.j.margeo.2021.106456.

Fontes, L.C.S., 2003. Estudo do processo erosivo das margens do Baixo São Francisco e seus efeitos na dinâmica de sedimentação do rio. Relatório Final Projeto GEF São Francisco, Aracaju.

Fontes, L.C.S., Latrubesse, E., Holanda, F.S.R., Aquino, S., 2009. Major hydrological changes and bank erosion in the lower Sao Francisco River, Brazil, as a consequence of dams, in: Vionnet, C.A., García, M.H., Latrubesse, E.M., Perillo, G.M.E. (Eds.), River, Coastal and Estuarine Morphdynamics. London, pp. 131-136.

Fontes, L.C.S., 2015. Da fonte à bacia: interação continente-oceano no sistema sedimentar Rio São Francisco, Brasil. PhD Thesis, Universidade Estadual Paulista (UNESP) – Instituto de Biociências.

França, A.M.C. 1979. Geomorfologia da margem continental leste brasileira e das bacias oceânica adjacentes. In: Chave Haf (Ed.). Geomorfologia da margem continental brasileira e das áreas oceânicas adjacentes. Série Projeto REMAC, v. 7, p. 89-114. PETROBRAS, DNPM, CPRM, DHN, CNPq.

Friend, P.F., Sinha, R., 1993. Braiding and meandering parameters. Geological Society, London, Special Publications. 75, 105-111. https://doi.org/10.1144.GSL.SP.1993.075.01.05.

Genz, F., Luz, L.D., 2012. Distinguishing the effects of climate on discharge in a tropical river highly impacted by large dams. Hydrological Sciences Journal. 57 (5), 1020-1034. https://doi.org/10.1080/02626667.2012.690880.

Getirana, A., 2016. Extreme Water Defict in Brazil Detected from Space. Journal of Hydrometeorology. 17 (2), 591-599. https://doi.org/10.1175/JHM-D-15-0096.1.

Giardino, J.R., Lee, A.A., 2011. Rates of Channel Migration on the Brazos River. Final Report Submitted to the Texas Water Development Board. Texas A and M University, pp. 8–9.

Grams, P.E., Schmidt, J.C., 2005. Equilibrium or indeterminate? Where sediment budgets fail: Sediment mass balance and adjustment of channel form, Green River downstream from Flaming Gorge Dam, Utah and Colorado. Geomorphology. 71 (1-2), 156-181. https://doi.org/10.1016/j.geomorph.2004.10.012.

Gregory, K.J., Park, C.C., 1974. Adjustment of river channel capacity downstream from a reservoir. Water Resources Research. 10, 870–873.

Grill, G., Lehner, B., Lumsdon, A.E., MacDonald, G.K., Zarfl, C., Liermann, C. R., 2015. An index-based framework for assessing patterns and trends in river fragmentation and flow regulation by global dams at multiple scales. Environmental Research Letters, 10(1), 015001. https:// doi:10.1088/1748-9326/10/1/015001.

Gupta, A., 2007. Introduction, in: Gupta, A. (Eds.), Large Rivers: Geomorphology and Management. The Atrium, Southern Gate, Chichester, pp. 1-6.

Gupta, H., Kao, S.J., Dai, M., 2012. The role of mega dams in reducing sediment fluxes: A case study of large Asian rivers. Journal of Hydrology, 464, 447-458. https://doi.org/10.1016/j.jhydrol.2012.07.038.

Harmar, O. P., Clifford, N.J., Thorne, C.R., Biedenharn, D.S., 2005. Morphological changes of the Lower Mississippi River: geomorphological response to engineering intervention. River Research and Applications, 21(10), 1107-1131. https://doi.org/10.1002/rra.887.

Heimann, D.C., Sprague, L.A., Blevins, D. W., 2011. Trends in suspended-sediment loads and concentrations in the Mississippi River Basin, 1950-2009. US Department of the Interior, US Geological Survey.

Higgs, G., Petts, G., 1988. Hydrological changes and river regulation in the UK. Regulated Rivers: Res. Manage. 2, 349–368. https://doi.org/10.1002/rrr.3450020312.

Holanda, F.S.R., Santos, L.G.D.C., Santos, C.M.D., Casado, A.P.B., Pedrotti, A., Ribeiro, G.T., 2005. Riparian vegetation affected by bank erosion in the Lower São Francisco River, Northeastern Brazil. Revista Árvore. 29 (2), 327-336. https://doi.org/10.1590/S0100-67622005000200016.

Jacobson, R.B., Blevins, D.W. Bitner, C.J., 2009. Sedimet regime constraints on river restoration – An example from the lower Missouri River. Geological Society of America Special papers, p. 1-22.

Jenkins, K., Warren, R., 2015. Quantifying the impact of climate change on drought regimes using the Standardised Precipitation Index. Theoretical and Applied Climatology, 120(1), 41-54. https://doi.org/10.1007/s00704-014-1143-x.

Jiongxin, X., 1990a. An experimental study of complex response in river channel adjustment downstream from a reservoir. Earth Surf. Processes Landforms. 15, 43–53. https://doi.org/10.1002/esp.3290150105.

Jiongxin, X., 1990b. Complex response in adjustment of the Weihe River channel to the construction of the Sanmenxia Reservoir. Zeitschrift für Geomorphologie. 34 (2), 233–245.

Kesel, R. H., 2003. Human modifications to the sediment regime of the Lower Mississippi River flood plain. Geomorphology, 56(3-4), 325-334. https://doi.org/10.1016/S0169-555X(03)00159-.4

Knight, J.R., Folland, C.K., Scaife, A.A., 2006. Climate impacts of the Atlantic multidecadal oscillation. Geophysical Research Letters. 33 (17). https://doi.org/10.1029/2006GL026242.

Knoppers, B., Medeiros, P.R., de Souza, W.F., Jennerjahn, T., 2005. The São Francisco Estuary, Brazil. Estuaries. 5, 51-70. https://doi.org/10.1007/698_5_026.

Kong, D., Latrubesse, E.M., Miao, C., Zhou, R., 2020. Morphological response of the Lower Yellow River to the operation of Xiaolangdi Dam, China. Geomorphology. 350, 106931. https://doi.org/10.1016/j.geomorph.2019.106931.

Kuwajima, J.I., Fan, F.M., Schwanenberg, D., Reis, A.A., Niemann, A., Mauad, F.F., 2019. Climate change, water-related disasters, flood control and rainfall forecasting: a case study in river São Francisco, Brazil. Geological Society, London, Special Publications. 488 (1), 259-276. https://doi.org/10.1144/SP488-2018-128.

Latrubesse, E.M., 2008. Patterns of anabranching channels: The ultimate end-member adjustment of mega rivers. Geomorphology. 101 (1-2), 130-145. https://doi.org/10.1016/j.geomorph.2008.05.035.

Lehner, B., Liermann, C.R., Revenga, C., Vörösmarty, C., Fekete, B., Crouzet, P., Döll, P, Endejan, M, Frenken, K., Magome, J, Nilsson, C., Robertson, J.C., Rödel, R, Sindorf, N., Wisser, D., 2011. Global reservoir and dam (grand) database. Technical Documentation, Version 1.1, 1, 1-14.

Lesk, C., Rowhani, P., Ramankutty, N., 2016. Influence of extreme weather disasters on global crop production. Nature, 529(7584), 84-87. https://doi.org/10.1038/nature16467.

Lima, E.F.W.L., Santos, P.M.C., Chaves, A.G.M, Scilewski, L.R., 2001. Diagnóstico do fluxo de sedimentos em suspensão na Bacia do Rio São Francisco. Embrapa Cerrados, Brasília, 108p.

Lucena, A.F.P., Szklo, A.S., Schaeffer, R., Souza, R.R., Borba, B.S.M.C., Costa, I.V.L., Preira Júnior, A.O., Cunha, S.H F., 2009. The vulnerability of renewable energy to climate change in Brazil. Energy Policy, 37(3), 879-889. https://doi.org/10.1016/j.enpol.2008.10.029

Ma, Y.X., Huang, H.Q., Nanson, G.C., Li, Y., Yao, W.Y., 2012. Channel adjustments in response to the operation of large dams: the upper reach of the lower Yellow River. Geomorphology. 147, 35-48. http://dx.doi.org/10.1016/j.geomorph.2011.07.032.

Magilligan, F.J., Nislow, K.H., 2001. Long-term changes in regional hydrologic regime following impoundment in a humid-climate watershed. Journal of the American Water Resources Association 37, 1551–1569. https://doi.org/10.1111/j.1752-1688.2001.tb03659.x.

Magilligan, F.J., Nislow, K.H., 2005. Changes in hydrologic regime by dams. Geomorphology, 71, 61–78. https://doi.org/10.1016/j.geomorph.2004.08.017.

Marengo, J.A., Chou, S.C., Kay, G., Alves, L.M., Pesquero, J.F., Soares, W.R., Santos, D.C., Lyra, A.A., Sueiro, G., Betts, R., Chagas, D.J., Gomes, J.L., Bustamante, J.F., Tavares, P., 2012. Development of regional future climate change scenarios in South America using Eta CPTEC/HadCM3 climate change projections: climatology and regional analyses for the Amazon, São Francisco and Paraná River basins. Climate Dynamics. 38 (9-10), 1829-1848. https://doi.org/10.1007/s00382-011-1155-5.

Meade. R.H., 1996. River-sediment inputs to major deltas, in: Milliman, J.D., Haq, B.U. (Eds), Sea-level Rise and Coastal Subsidence: Causes, Consequences, and Strategies. Kluwer, Dordrecht, pp. 63–85.

Meade, R.H., Moody, J.A., 2010. Causes for the decline of suspended-sediment discharge in the Mississippi River system, 1940–2007. Hydrological Processes: An International Journal, 24(1), 35-49. https://doi.org/10.1002/hyp.7477.

Medeiros, P.R.P., 2003. Aporte fluvial, transformação e dispersão da matéria em suspensão e nutrientes no estuário do Rio São Francisco, após a construção da Usina Hidroelétrica do Xingó (AL/SE). UFF: Niterói, 2003a.

Medeiros, P.R.P., Knoppers, B., Souza, W.F.L., Oliveira, E.N., 2011. Aporte de material em suspensão no baixo rio São Francisco (SE/AL) em diferentes condições hidrológicas. Brazilian Journal of Aquatic Science and Technology. 15, 42-53. https://doi.org/10.14210/bjast.v15n1.p42-53.

Medeiros, P.P., Santos, M.M., Cavalcante, G.H., Souza, W.F.L., Silva, W.F., 2014. Características ambientais do Baixo São Francisco (AL/SE): efeitos de barragens no transporte de materiais na interface continente-oceano. Geochimica Brasiliensis. 28, 65-78. http://dx.doi.org/10.21715/gb.v28i1.384.

Merrit, D.M., Cooper, D.J., 2000. Riparian vegetation and channel change in response to river regulation: a comparative study of regulated and unregulated streams in the Green River Basin, USA. Regulated Rivers: Research & Management: An International Journal Devoted to River Research and Management. 16 (6), 543-564. https://doi.org/10.1002/1099-1646(200011/12)16:6<543::AID-RRR590>3.0.CO;2-N.

Miall, A.D. 1996. The geology of fluvial deposits. Springer-Verlag, New-York.

Milliman, J.D., 1997. Blessed dams or damned dams? Nature. 386, 325-326. https://doi.org/10.1038/386325a0.

Milliman, J.D., Farnsworth, K.L., Jones, P.D., Xu, K.H., Smith, L.C., 2008. Climatic and anthropogenic factors affecting river discharge to the global ocean, 1951-2000. Global an Planetary Change. 62 (3-4), 187-194. https://doi.org/10.1016/j.gloplacha.2008.03.001.

Morris, G.L., Fan, J., 1997. Reservoir Sedimentation Handbook: Design and Management of Dams, Reservoirs, and Watersheds for Sustainable Use. McGraw-Hill, New York, 805 pp.

Moura, M.M., Fontes, C.S., Santos, M.H., Araujo Filho, R.N., Holanda, F.S.R., 2017. Estimativa de perda de solo no Baixo São Francisco sergipano. Scientia Agraria, 18(2), 126-135.

Nakicenovic, N., Alcamo, J., Davis, G., Vries, B., Fenhann, J., Gaffin, S., Gregory, K., Grübler, A., Jung, T.Y., Kram, T., Rovere, E.L., Michaelis, L., Mori, S., Morita, T., Pepper, W., Pitcher, H., Price, L.,Riahi, K., Roehrl, A., Rogner, H., Sankovski, A., Schlesinger, M., Shukla, P., Smith, S., Swart, R., Rooijen, S., Victor, N, Dadi, Z., 2000. Emissions scenarios – special report of the Intergovernamental Panel on climate Change.

Nelson, N.C., Erwin, S.O., Schmidt, J.C., 2013. Spatial and temporal patterns in channel change on the Snake River downstream from Jackson Lake dam, Wyoming. Geomorphology. 200, 132-142. https://doi.org/10.1016/j.geomorph.2013.03.019.

Nouh, M., 1990. The flow regime downstream of dams in arid areas: development and effects of channel stability. Hydrology of Mountainous Regions—II: Artificial Reservoirs, Water and Slopes. IAHS Publication, 194.

Novello, V.F., Cruz, F.W., Karmann, I., Burns, S.J., Stríkis, N.M., Vuille, M., Cheng, H., Edwards, R.L., Santos, R.V., Frigo, E., Barreto, E. A., 2012. Multidecadal climate variability in Brazil's Nordeste during the last 3000 years based on speleothem isotope records. Geophysical Research Letters. 39, 1-6. https://doi.org/10.1029/2012GL053936.

Oliveira, A.M., Júnior, R.C.S., Hernandez, A.O., Segundo, G.H.C., Araújo, A.E.M. 2003. A morte do Delta do Rio São Francisco. In: Anais do II Congresso sobre Planejamento e Gestão das Zonas Costeiras dos Países de Expressão Portuguesa IX Congresso da Associação Brasileira de Estudos do Quaternário, II Congresso do Quaternário dos Países de Língua Ibéricas.

Petts, G.E., 1979. Complex response of river channel morphology subsequent to reservoir construction. Progress in Physical Geography. 3, 329–362. https://doi.org/10.1177/030913337900300302.

Petts, G.E., Gurnell, A.M., 2005. Dams and geomorphology: research progress and future directions. Geomorphology. 71, 27–47. https://doi.org/10.1016/j.geomorph.2004.02.015.

Petts, G.E., Gurnell, A.M., 2021. Hydrogeomorphic Effects of Reservoirs, Dams, and Diversions, Reference Module in Earth Systems and Environmental Sciences, Elsevier, https://doi.org/10.1016/B978-0-12-818234-5.00034-1.

Roman, P., 2017). The São Francisco inter-basin water transfer in Brazil: Tribulations of a megaproject through constraints and controversy. Water Alternatives, 10(2), 395.

Rustomji, P., Zhang, X.P., Hairsine, PB., Zhang, L., Zhao, J., 2008. River sediment load and concentration responses to changes in hydrology and catchment management in the Loess Plateau region of China. Water Resources Research, 44(7). https://doi.org/10.1029/2007WR006656.

Santos, H.A., Pompeu, P.S., Kenji, D.O.L., 2012. Changes in the flood regime of São Francisco River (Brazil) from 1940 to 2006. Regional Environment Change. 12, 123-132. https://doi.org/10.1007/s10113-011-0240-y.

Santos, C.A.G., Neto, R.M.B., Passos, J.S.A., Silva, R.M., 2017. Drought assessment using a TRMM-derived standardized precipitation index for the upper São Francisco River basin, Brazil. Environmental Monitoring and Assessment. 189 (6), 250. https://doi.org/10.1007/s10661-017-5948-9.

Santos, C.A.G., Neto, R.M.B., Silva, R.M., Passos, J.S.A., 2018. Integrated spatiotemporal trends using TRMM 3B42 data for the Upper São Francisco River basin, Brazil. Environmental Monitoring and Assessment. 190(3), 1-20. https://doi.org/10.1007/s10661-018-6536-3.

Schmidt, J.C., Rubin, D.M., 1995. Regulated streamflow, fine-grained deposits, and effective discharge in canyons with abundant debris fans. Natural and anthropogenic influences in fluvial geomorphology, 89, 177-195. https://doi.org/10.1029/GM089p0177.

Schmidt, J.C., Wilcock, P.R., 2008. Metrics for assessing the downstream effects of dams. Water Resources Research, 44(4). https://doi.org/10.1029/2006WR005092

Schumm, S.A., Lichty, R.W., 1965. Time, space and causality in geomorphology, American Journal of Science. 263 (2), 110-119. https://doi.org/10.2475/ajs.263.2.110.

Sherrard, J.J.; Erskine, W.D., 1991. Complex response of a sand-bed stream to upstream impoundment. Regulated Rivers: Research & Management. 6 (1), 53-70. https://doi.org/10.1002/rrr.3450060106.

Silva, W.F.; Medeiros, P.R.P.; Viana, F.G.B. 2010. Quantificação preliminar do aporte de sedimentos no baixo São Francisco e seus principais impactos. X Simpósio de Recursos Hídricos do Nordeste. Fortaleza, Brazil, p. 1-14.

Silva, V.P.R., Silva, M. T., Souza, E.P. 2016. Influence of land use change on sediment yield: a case study of the sub-middle of the São Francisco River Basin. Engenharia Agrícola. Vol 36 (6).

Skalak, K.J., Benthem, A.J., Schenk, E.R., Hupp, C.R., Galloway, J.M., Nustad, R.A., Wiche, G.J., 2013. Large dams and alluvial rivers in the Anthropocene: The impacts of the Garrison and Oahe Dams on the Upper Missouri River. Anthropocene. 2, 51-64. https://doi.org/10.1016/j.ancene.2013.10.002.

Souza Filho, E.E., Rocha, P.C., Comunello, E., Stevaux, J.C., 2004. Effects of the Porto Primavera Dam on physical environmental of the downstream floodplain. In: Thomaz, S.M., Agostinho, A.A., Hahn, N.S. (eds.), The Upper Paraná River and its Floodplain: Physical Aspects, Ecology and Conservation. Backhuys Publisher, Lieden, The Netherland, pp. 55-74.

Stevaux, J.C., Martins, D.P., & Meurer, M., 2009. Changes in a large regulated tropical river: The Paraná River downstream from the Porto Primavera Dam, Brazil. Geomorphology, 113(3-4), 230-238. https://doi.org/10.1016/j.geomorph.2009.03.015

Stevaux, J.C. and Latrubesse, E.M., 2017. Geomorfologia fluvial, ed. Oficina de Textos, São Paulo.

Surian, N. (1999). Channel changes due to river regulation: the case of the Piave River, Italy. Earth Surface Processes and Landforms: The Journal of the British Geomorphological Research Group, 24(12), 1135-1151. https://doi.org/10.1002/(SICI)1096-9837(199911)24:12<1135::AID-ESP40>3.0.CO;2-F.

Syvitski, J.P., Vörösmarty, C.J., Kettner, A.J., Green, P., 2005. Impact of humans on the flux of terrestrial sediment to the global coastal ocean. Science, 308(5720), 376-380. https://doi.org/10.1126/science.1109454.

Stríkis, N.M., Cruz, F.W., Cheng, H., Karmann, I., Edwards, R.L., Vuille, Wang, X., Paula, M.S., Novello, V.F., M., Auler, A. S., 2011. Abrupt variations in South American monsoon rainfall during the Holocene based on a speleothem record from central-eastern Brazil. Geology. 39 (11), 1075-1078. https://doi.org/10.1130/G32098.1.

Sun, T., Ferreira, V.G., He, X., Andam-Akorful, S.A., 2016. Water Availability of São Francisco River Basin Based on a Space-Borne Geodetic Sensor. Water. 8 (5), 213. https://doi.org/10.3390/w8050213.

Syvitski, J.P., Kettner, A.J., Overeem, I., Hutton, E.W., Hannon, M.T., Brakenridge, G.R., Day, J., Vörösmarty, C., Saito, Y., Giosan, L., Nicholls, R. J., 2009. Sinking deltas due to human activities. Nature Geoscience. 2 (10), 681-686. https://doi.org/10.1038/ngeo629.

Thoms, M.C., Walker, K.F., 1993. Channel changes associated with two adjacent weirs on a regulated lowland alluvial river. Regulated rivers: Res. Manage. 8 (3), 271–284. https://doi.org/10.1002/rrr.3450080306.

Traini, C., Schrottke, K., Stattegger, K., Dominguez, J.M.L., Guimaraes, J.K., Vital, H., D'avila Beserra, D., Silva, A.G.A., 2012. Morphology of subaqueous dunes at the mouth of the dammed River São Francisco (Brazil). Journal of Coastal Research. 28 (6), 1580-1590. https://doi.org/10.2112/JCOASTRES-D-10-00195.1.

Trenberth, K.E., Dai, A., Van Der Schrier, G., Jones, P.D., Barichivich, J., Briffa, K.R., Sheffield, J., 2014. Global warming and changes in drought. Nature Climate Change, 4(1), 17-22. https://doi.or/10.1038/NCLIMATE2067.

United States Fish and Wildlife Service and Hooja Valley Tribe, 1999. Trinity River Flow Evaluation, Final Report. June 1999. 307 pp.

Vericat, D., Batalla, R.J., Garcia, C.,2 006. Breakup and reestablishment of the armour layer in a large gravel-bed river below dams: The lower Ebro. Geomorphology, 76(1-2), 122-136. https://doi.org/10.1016/j.geomorph.2005.10.005.

Viviroli, D., Weingartner, R., 2004. The hydrological significance of mountains: from regional to global scale. Hydrology and earth system sciences. 8 (6), 1017-1030. https://doi.org/10.5194/hess-8-1017-2004.

Wallick, R.J., Grant, G.E., Lancaster, S.T., Bolte, J.P. Denlinger, R.P., 2007. Patterns and Controls on Historical Channel Change in the Willamete River, Oregon, USA, in: Gupta (Eds.), Large Rivers: Geomorphology and Management. The Atrium, Southern Gate, Chichester, pp. 491-516.

Walling, D.E., 2006. Human impact on land–ocean sediment transfer by the world's rivers. Geomorphology, 79(3-4), 192-216. https://doi.org/10.1016/j.geomorph.2006.06.019.

Wang, W., Wang, T., Cui, W., Yao, Y., Ma, F., Chen, B., Wu, J., 2021. Change of Flow and Sediment Transport in the Lower Min River in Southeastern China under the Impacts of Climate Variability and Human Activities. Water, 13(5), 673. https://doi.org/10.3390/w13050673.

Williams, G.P., Wolman, M.G., 1984. Downstream effects of dams on alluvial rivers, Washington, DC.

Wohl, E.E., 2007. Hydrology and Discharge, in: Gupta, A. (Eds.) Large Rivers: Geomorphology and Management. The Atrium, Southern Gate, Chichester, 29-44.

Wolman, M.G., Miller, J.P., 1960. Magnitude and frequency of forces in geomorphic processes. The Journal of Geology. 68 (1), 54-74. http://dx.doi.org/10.1086/626637.

Wu, X., Bi, N.S., Yuan, P., Li, S., Wang, H.J., 2015. Sediment dispersal and accumulation off the present Huanghe (Yellow River) delta as impacted by the Water-Sediment Regulation Scheme. Cont. Shelf Res. 111, 126–138. http://dx.doi.org/10.1016/j.csr.2015.11.003.

Yang, S.L., Milliman, J.D., Xu, K.H., Deng, B., Zhang, X.Y., Luo, X.X., 2014. Downstream sedimentary and geomorphic impacts of the Three Gorges Dam on the Yangtze River. Earth-Science Reviews, 138, 469-486. https://doi.org/10.1016/j.earscirev.2014.07.006.

Yang, S.L., Xu, K.H., Milliman, J.D., Yang, H.F., Wu, C.S.; 2015. Decline of Yangtze River water and sediment discharge: Impact from natural and anthropogenic changes. Scientific reports, 5(1), 1-14. https://doi.org/10.1038/srep12581.

Zahar, Y., GhoRbel, A., Albergel, G., 2008. Impacts of large dams on downstream flow conditions of rivers: aggradation and reduction of the Medjerda channel capacity downstream of the Sidi Salem dam (Tunisia). Journal of Hydrology. 351, 318–330. https://doi.org/10.1016/j.jhydrol.2007.12.019.

Zhou, Z., 1996. Impact of reservoirs on fluvial processes and environment of alluvial rivers. Reservoir Sedimentation, Proceedings of the St Petersburg Workshop May 1994, IHP-V., Paris, France, pp. 273–290.

Zhou, Y.Y., Huang, H.Q., Nanson, G.C., Huang, C., Liu, G.H., 2015. Progradation of theYellow (Huanghe) River delta in response to the implementation of a basin-scale water regulation program. Geomorphology. 243, 65–74, http://dx.doi.org/10.1016/j.geomorph.2015.04.023.

Zhou, M., Xia, J., Lu, J., Deng, S., Lin. F. 2017. Morphological adjustments in a meandering reach of the middle Yangtze River caused by severe human activities, Geomorphology, 285, 325-332, https://doi.org/10.1016/j.geomorph.2017.02.022.

Appendix

Table 1: Percentage of mid-channel bar

Year of satellite image	Reaches																
	R1	R2	R3	R4	R5	R6	R7	R8	R9	R10	R11	R12	R13	R14	R15	R16	R17
1985	1.3	0.0	0.2	0.4	0.4	26.7	5.6	14.7	8.9	0.0	1.6	12.4	26.0	26.2	30.9	35.7	25.2
1992	0.7	0.0	0.2	0.3	2.2	26.3	7.5	13.7	5.3	2.1	1.8	14.4	25.6	19.0	28.9	39.0	27.5
1996	0.6	0.0	0.7	1.2	1.4	19.3	8.5	14.9	10.9	3.6	7.6	9.1	32.8	25.1	30.7	38.0	28.7
1998	1.0	0.0	0.5	0.8	1.5	17.3	6.8	12.9	5.3	2.8	6.9	17.7	32.1	24.7	31.1	39.5	28.4
2001	1.9	0.1	1.1	2.8	3.1	19.5	3.3	14.5	11.6	0.8	10.8	10.1	33.6	27.9	30.7	39.4	29.3
2003	0.9	1.0	1.7	2.8	3.0	20.6	3.2	8.1	10.7	2.6	14.4	15.6	35.7	30.8	34.5	44.3	30.2
2004	1.8	0.2	1.7	3.1	3.4	21.1	4.6	9.1	11.4	2.8	14.3	12.2	33.3	30.7	30.5	39.5	26.8
2009	0.3	0.9	1.2	1.2	1.8	20.9	5.0	13.4	8.4	12.2	12.8	9.8	30.4	31.0	36.4	45.1	31.4
2011	0.4	0.8	1.5	2.0	1.9	22.3	5.9	14.0	12.6	14.7	15.0	12.6	32.6	29.8	35.0	46.1	33.3
2013	3.3	0.2	2.0	4.1	4.2	24.2	12.0	10.8	19.0	19.0	17.5	19.5	26.9	37.8	29.7	46.2	33.4
2018	6.8	1.2	4.0	3.3	13.7	34.7	20.0	14.5	23.1	22.5	30.8	26.2	39.4	32.9	16.5	49.5	35.4
2020	0.5	0.4	0.5	0.1	1.6	25.5	5.0	12.9	16.1	18.0	14.9	22.2	31.9	32.2	35.2	51.4	34.7

Table 2: Channel sinuosity

Year of satellite image	Reaches																
	R1	R2	R3	R4	R5	R6	R7	R8	R9	R10	R11	R12	R13	R14	R15	R16	R17
1985	1.1	1.0	1.0	1.0	1.0	1.1	1.1	1.1	1.0	1.2	1.2	1.1	1.1	1.1	1.1	1.4	1.1
1992	1.1	1.0	1.0	1.0	1.0	1.1	1.1	1.1	1.0	1.2	1.2	1.1	1.1	1.1	1.1	1.4	1.1
1996	1.1	1.0	1.0	1.0	1.0	1.1	1.1	1.1	1.1	1.2	1.2	1.1	1.1	1.2	1.1	1.4	1.1
1998	1.1	1.0	1.0	1.0	1.0	1.0	1.1	1.1	1.1	1.2	1.2	1.1	1.1	1.1	1.1	1.4	1.1
2001	1.1	1.0	1.0	1.0	1.0	1.1	1.1	1.1	1.1	1.2	1.2	1.1	1.1	1.2	1.1	1.4	1.1
2003	1.1	1.0	1.0	1.0	1.0	1.1	1.1	1.1	1.1	1.2	1.2	1.1	1.1	1.2	1.1	1.4	1.1
2004	1.1	1.0	1.0	1.0	1.0	1.0	1.1	1.1	1.1	1.2	1.2	1.1	1.1	1.2	1.1	1.4	1.1
2009	1.1	1.0	1.0	1.0	1.0	1.1	1.1	1.1	1.1	1.2	1.2	1.1	1.1	1.2	1.1	1.4	1.1
2011	1.1	1.0	1.0	1.0	1.0	1.1	1.1	1.1	1.0	1.2	1.2	1.1	1.1	1.2	1.1	1.3	1.1
2013	1.1	1.0	1.0	1.0	1.1	1.1	1.1	1.1	1.0	1.2	1.3	1.1	1.1	1.2	1.1	1.4	1.1
2018	1.1	1.1	1.0	1.0	1.1	1.1	1.2	1.1	1.1	1.2	1.3	1.1	1.2	1.2	1.2	1.4	1.1
2020	1.1	1.0	1.0	1.0	1.1	1.1	1.1	1.1	1.1	1.2	1.3	1.1	1.1	1.2	1.2	1.4	1.1

Table 3: Braid-channel ratio

Year of satellite image	Reaches																
	R1	R2	R3	R4	R5	R6	R7	R8	R9	R10	R11	R12	R13	R14	R15	R16	R17
1985	1.3	1.0	1.2	1.1	1.2	2.6	1.5	1.8	1.9	1.0	1.6	2.2	2.7	2.9	2.7	2.8	2.7
1992	1.2	1.0	1.2	1.2	1.5	2.8	2.0	2.0	1.9	1.2	1.5	2.1	2.4	2.6	2.5	2.4	2.5
1996	1.1	1.0	1.2	1.2	1.2	2.3	2.2	2.0	2.1	1.4	2.4	2.0	2.8	3.3	2.8	2.3	2.6
1998	1.3	1.1	1.3	1.2	1.3	2.3	1.8	1.8	1.9	1.3	2.4	2.4	2.8	3.3	2.5	2.3	2.6
2001	1.3	1.1	1.2	1.3	1.2	2.8	1.8	1.9	2.1	1.6	2.7	1.9	3.0	3.1	2.7	2.3	2.7
2003	1.2	1.2	1.3	1.4	1.3	2.5	2.0	1.5	2.1	1.5	2.4	2.3	2.9	3.0	2.3	2.5	2.8
2004	1.2	1.1	1.2	1.3	1.3	2.7	2.1	1.8	2.3	1.6	2.4	2.0	2.6	3.0	2.4	2.4	2.3
2009	1.1	1.1	1.3	1.3	1.2	2.7	2.0	2.0	2.6	2.5	2.4	2.0	3.0	3.4	2.7	2.8	2.6
2011	1.1	1.1	1.2	1.3	1.3	2.6	2.0	1.8	2.4	2.2	2.5	2.2	2.7	3.0	2.7	2.8	2.9
2013	1.3	1.1	1.2	1.4	1.4	2.5	2.3	1.9	2.9	2.3	2.2	2.1	2.9	3.3	2.6	2.9	2.9
2018	1.2	1.2	1.4	1.4	1.9	3.3	2.6	2.1	2.3	2.1	2.6	1.8	2.4	2.2	2.3	3.0	2.9
2020	1.1	1.1	1.2	1.2	1.7	3.0	2.4	2.4	3.1	2.7	2.4	2.4	2.9	3.1	2.6	2.9	2.8

Table 4: Channel width

Year of satellite image	Reaches																
	R1	R2	R3	R4	R5	R6	R7	R8	R9	R10	R11	R12	R13	R14	R15	R16	R17
1985	335	351	586	664	763	1296	919	916	919	737	905	1018	1427	1473	1528	1599	1506
1992	333	349	587	664	787	1308	988	901	932	820	899	1041	1340	1316	1391	1581	1487
1996	283	339	577	655	742	1100	970	875	891	774	876	935	1322	1325	1406	1577	1440
1998	309	350	580	663	754	1123	986	878	925	789	892	1034	1322	1316	1384	1589	1488
2001	280	323	552	629	714	1105	895	855	884	739	874	967	1312	1300	1401	1605	1483
2003	240	320	559	644	728	1097	891	765	895	746	864	895	1294	1282	1360	1586	1478
2004	237	324	557	647	726	1110	924	792	886	752	879	913	1328	1318	1418	1567	1507
2009	298	342	566	646	732	1094	913	863	893	856	858	902	1328	1227	1391	1612	1464
2011	295	338	563	638	739	1093	916	864	918	861	870	891	1329	1246	1411	1638	1464
2013	217	313	543	626	684	1063	850	780	876	827	785	856	1065	1194	1170	1579	1444
2018	171	304	525	579	648	1038	742	661	679	680	698	729	921	769	818	1561	1427
2020	277	346	578	661	738	1058	858	795	873	825	774	844	1050	1014	1090	1558	1423

Table 5: Lateral migration rate

Year of satellite image	Reaches																
	R1	R2	R3	R4	R5	R6	R7	R8	R9	R10	R11	R12	R13	R14	R15	R16	R17
1985-1992	2.5	1.6	1.1	1.1	3.5	2.1	5.6	2.6	2.9	13.1	2.4	4.7	2.4	12.2	19.7	4.3	4.3
1992-1996	4.9	3.1	2.6	2.1	9.7	28.6	3.2	3.7	5.5	11.0	6.3	21.9	3.0	11.3	5.2	3.1	6.6
1996-1998	8.1	6.3	4.8	4.7	6.9	9.1	7.4	5.3	10.7	9.8	7.3	41.2	4.6	7.8	8.6	6.6	12.2
1998-2001	4.4	5.8	3.9	3.8	6.1	5.1	14.2	3.6	7.2	12.5	5.4	22.3	3.4	3.5	4.8	5.5	12.9
2001-2003	8.6	7.6	4.3	4.3	9.8	4.7	8.8	26.9	5.6	5.4	7.5	16.8	66.2	7.1	11.1	8.8	12.9
2003-2004	12.1	15.2	8.7	9.9	17.6	9.6	13.2	20.1	15.8	23.1	16.5	20.8	9.3	18.6	24.1	12.7	13.6
2004-2009	3.9	4.3	3.6	2.6	3.0	2.0	2.8	10.0	3.8	17.3	6.2	3.9	29.7	8.7	11.2	6.0	24.2
2009-2011	8.7	9.8	7.7	5.7	7.3	5.2	4.8	4.7	7.0	9.6	17.7	10.2	9.5	12.9	17.5	15.8	11.3
2011-2013	10.1	8.0	6.8	4.8	7.8	4.0	10.0	28.8	5.2	5.8	28.2	21.6	66.1	6.5	41.0	6.9	5.9
2013-2018	2.9	2.0	1.5	4.3	2.8	4.8	9.1	10.3	18.9	17.5	9.7	11.9	15.0	45.8	29.5	6.3	2.6
2018-2020	11.7	9.4	8.9	13.6	8.6	11.7	21.7	28.6	37.3	37.9	15.0	29.1	34.8	62.7	74.1	12.5	8.9

CAPÍTULO 3 – CONCLUSÃO

Sistemas fluviais barrados podem apresentar variações em seus regimes hidrológicos e sedimetológicos e uma grande complexidade para sua quantificação e comparação desses ajustes. Em vista diso, esse trabalho tem como objetivo analizar os processos e resultados dos fatores de controle de descarga de água significativos e como isso impactou o Baixo São Fancisco. Nossas análises de imagens de satélite mostraram uma predominância de ajustes internos para o canal principal (diminuição da largura e aumento da porcentagem de barras de meio de canal) em vez de ajustes externos para o canal (baixa taxa de migração lateral e uma ligeira variação da sinuosidade do canal).

O processo de estreitamento do canal (aproximadamente 20%) no canal principal prevaleceu em vez de alargamento nos últimos 35 anos. Nesse quesito, o G1 tem redução de 40%, principalmente devido à deposição de leques na confluência de pequenos rios tributários. G2 e G3 exibiram o pior cenário. A transformação do canal ativo em planície de inundação se deve ao abandono dos canais secundários que responderam rapidamente após a construção de Xingó com a expansão de barras de meio do canal e a fixação dessas barras às margens. Os processos de estreitamento do canal no G2 sugerem que a erosão das margens é local e parte da dinâmica fluvial, prevalecendo a transformação de áreas ocupadas pelo canal em planíe de inundação, corroborada pela redução da largura média de 22% em 33 anos (1985-2018). O G3 (trechos 13, 14 e 15) sofreu as maiores reduções na largura do canal (30%, 42% e 42%) após a construção do Xingó e é o grupo mais crítico.

Os modos deposicionais que melhor explicam o acúmulo de sedimentos em LSFR indicam que novas áreas de acreção são originadas por sedimentos erodidos do leito do canal à montante e, secundariamente, da margem do rio, onde dunas subaquosas são remobilizadas. Quanto à variação do percentual de barras médias do canal, o G3 aumentou imediatamente após a construção da barragem de Xingó. Porém, com sucessivas reduções de vazão, fruto da prolongada seca desde 2013, e a redução da capacidade de transporte fluvial, os sedimentos foram depositados em regiões cada vez mais próximas de Xingó, indicando que futuras reduções de vazão podem levar ao maior acúmulo nessas áreas.

Mudanças climáticas e hidrológicas no curso do LSFR contribuíram para os efeitos da regulação das vazões a jusante do reservatório de Xingó, com redução de 3% nas chuvas e 40,4% na vazão de água no período pós-Xingó em relação à média dos anos entre 1941 e 1961. Os eventos de seca prolongada se agravaram desde 2013, registrando uma das mais severas secas em desde o último século e a consequente redução de 55% na descarga de água na última década em relação a meados do século passado responsável pelo aumento de formas de leito no Baixo São Francisco. Portanto, os ajustes morfológicos derivados das últimas décadas no Baixo São

Francisco se ajustam muito às mudanças climáticas significativas no Nordeste e Sudeste do Brasil e não com o armazenamento de água nos grandes reservatórios. Nesse sentido, a diminuição da precipitação foi responsável pela redução do volume dos reservatórios da barragem, que passou a reduzir o efluente para manter seu volume operacional. Esta é uma consequência, não a razão para a diminuição das vazões no trecho final do rio São Francisco.

No entanto, grande parte da redução nas descargas de água ainda deve-se a intervenções antropogênicas resultantes do desvio de água usada para diversos fins ao longo da bacia. Além disso, a crescente demanda por recursos hídricos em toda a bacia contribui para uma redução ainda mais significativa na quantidade de água que chega ao Baixo São Francisco. Devido à baixa precipitação, a demanda de água para irrigação e pecuária aumentou nas últimas décadas. Além disso, as previsões de precipitação futura indicam uma diminuição significativa em toda a bacia, o que reduzirá ainda mais a vazão do rio e pode continuar a alterar a sua morfologia. Nesse sentido, são necessárias políticas públicas mais severas para o uso dos recursos hídricos da bacia, visto que esse pode se tornar cada vez mais escasso e vazões mínimas podem ser possíveis de serem praticadas no Baixo São Francisco, como as descargas efetivas de 1873 m^3/s e 2238 m^3/s para as estações Pão de Açúcar e Propriá, respectivamente. Para isso, uma determinação mais precisa dos valores efetivos de descarte e a individualização dos impactos humanos sobre a descarga de água no LSFR é vital para futuros cenários climáticos e de impacto antrópico. Para isso, a coleta sistemática de dados como quantidade de carga de sedimento de fundo, vazões de tributários para a construção de uma série histórica mais robusta pode ser um auxílio essencial para reduzir as incertezas para o gerenciamento do rio São Francisco.

.

ANEXO I

Normas de submissão da revista *Geomorphology*

GUIDE FOR AUTHORS

Your Paper Your Way

We now differentiate between the requirements for new and revised submissions. You may choose to submit your manuscript as a single Word or PDF file to be used in the refereeing process. Only when your paper is at the revision stage, will you be requested to put your paper in to a 'correct format' for acceptance and provide the items required for the publication of your article.
To find out more, please visit the Preparation section below.

INTRODUCTION

Geomorphology publishes peer-reviewed works across the full spectrum of the discipline from fundamental theory and science to applied research of relevance to sustainable management of the environment. Our journal's scope includes geomorphic themes of: tectonics and regional structure; glacial processes and landforms; fluvial sequences, Quaternary environmental change and dating; fluvial processes and landforms; mass movement, slopes and periglacial processes; hillslopes and soil erosion; weathering, karst and soils; aeolian processes and landforms, coastal dunes and arid environments; coastal and marine processes, estuaries and lakes; modelling, theoretical and quantitative geomorphology; DEM, GIS and remote sensing methods and applications; hazards, applied and planetary geomorphology; and volcanics.

Types of paper

Research Papers that meet the Aims and Scope of the journal, with typical length of text in the 5000-10000 word range. Research papers may include specific case studies if these studies demonstrate theoretical significance and broad systemic relevance.

Review Articles provide a comprehensive and novel assessment of an issue or significant region in geomorphological research and should be of interest to a wide readership. A Review Article should provide a balanced, integrated and critical summary of previous work, possibly supported by some new findings, and should evaluate potential controversial issues. Illustrations should where possible integrate existing data into new comprehensive figures rather than duplicating published work. Length should not normally exceed 25000 words. Potential authors are encouraged to consult informally with one of the Editors before preparing a Review Article. From time to time, authors may be approached by the Editors to contribute an **Invited Review** to the journal. Such invited articles are expected to be of particularly high quality and consequently tend to be well used and/or well cited.

Short Communications are primarily intended to be compact versions of Full Length Articles, and must still report new and original research of high quality that meet the criteria of being of broad international interest, significant and novel. Other matters of general interest to the community will be considered for occasional publication as a Short Communication; an example could be a short contribution that addresses one very specific technical issue. Short Communications should be no more than 5000 words in length and contain no more than 5 figures.

Geomorphology publishes **Book Reviews**. Please contact the Book Review Editor Professor Kimberly Meitzen kmm218@txstate.edu for more information.

It is possible to submit a **Comment** about a recently published article in Geomorphology. It must be brief and directed only towards the main issue(s) that are being questioned in the original paper. It is not a vehicle for extensive review or for publishing the author's new findings, and should typically be no more than 3000 words. The original author(s) will be invited to write a **Reply** which must likewise be brief and directed only at the issues in question. Both parties are limited to one Comment and Reply each. These comments and replies must be submitted within six months of publication of the original article; the author of the Reply must submit it within one month of being notified of the Comment.

Information for prospective guest editors intending to submit a proposal for a special issue in the journal can be found here. Authors contributing to special issues should ensure that they select the appropriate special issue article type when submitting their manuscript.

Submission checklist

You can use this list to carry out a final check of your submission before you send it to the journal for review. Please check the relevant section in this Guide for Authors for more details.

Ensure that the following items are present:

One author has been designated as the corresponding author with contact details:
• E-mail address
• Full postal address

All necessary files have been uploaded:
Manuscript:
• Include keywords
• All figures (include relevant captions)
• All tables (including titles, description, footnotes)
• Ensure all figure and table citations in the text match the files provided
• Indicate clearly if color should be used for any figures in print
Graphical Abstracts / Highlights files (where applicable)
Supplemental files (where applicable)

Further considerations
• Manuscript has been 'spell checked' and 'grammar checked'
• All references mentioned in the Reference List are cited in the text, and vice versa
• Permission has been obtained for use of copyrighted material from other sources (including the Internet)
• A competing interests statement is provided, even if the authors have no competing interests to declare
• Journal policies detailed in this guide have been reviewed
• Referee suggestions and contact details provided, based on journal requirements

For further information, visit our Support Center.

BEFORE YOU BEGIN

Ethics in publishing

Please see our information pages on Ethics in publishing and Ethical guidelines for journal publication.

Declaration of interest

All authors must disclose any financial and personal relationships with other people or organizations that could inappropriately influence (bias) their work. Examples of potential conflicts of interest include employment, consultancies, stock ownership, honoraria, paid expert testimony, patent applications/ registrations, and grants or other funding. Authors should complete the declaration of interest statement using this template and upload to the submission system at the Attach/Upload Files step. If there are no interests to declare, please choose: 'Declarations of interest: none' in the template. This statement will be published within the article if accepted. More information.

Submission declaration and verification

Submission of an article implies that the work described has not been published previously (except in the form of an abstract, a published lecture or academic thesis, see 'Multiple, redundant or concurrent publication' for more information), that it is not under consideration for publication elsewhere, that its publication is approved by all authors and tacitly or explicitly by the responsible authorities where the work was carried out, and that, if accepted, it will not be published elsewhere in the same form, in English or in any other language, including electronically without the written consent of the copyright-holder. To verify originality, your article may be checked by the originality detection service Crossref Similarity Check.

Preprints
Please note that preprints can be shared anywhere at any time, in line with Elsevier's sharing policy. Sharing your preprints e.g. on a preprint server will not count as prior publication (see 'Multiple, redundant or concurrent publication' for more information).

Use of inclusive language

Inclusive language acknowledges diversity, conveys respect to all people, is sensitive to differences, and promotes equal opportunities. Articles should make no assumptions about the beliefs or commitments of any reader, should contain nothing which might imply that one individual is superior to another on the grounds of race, sex, culture or any other characteristic, and should use inclusive

language throughout. Authors should ensure that writing is free from bias, for instance by using 'he or she', 'his/her' instead of 'he' or 'his', and by making use of job titles that are free of stereotyping (e.g. 'chairperson' instead of 'chairman' and 'flight attendant' instead of 'stewardess').

Changes to authorship

Authors are expected to consider carefully the list and order of authors **before** submitting their manuscript and provide the definitive list of authors at the time of the original submission. Any addition, deletion or rearrangement of author names in the authorship list should be made only **before** the manuscript has been accepted and only if approved by the journal Editor. To request such a change, the Editor must receive the following from the **corresponding author**: (a) the reason for the change in author list and (b) written confirmation (e-mail, letter) from all authors that they agree with the addition, removal or rearrangement. In the case of addition or removal of authors, this includes confirmation from the author being added or removed.
Only in exceptional circumstances will the Editor consider the addition, deletion or rearrangement of authors **after** the manuscript has been accepted. While the Editor considers the request, publication of the manuscript will be suspended. If the manuscript has already been published in an online issue, any requests approved by the Editor will result in a corrigendum.

Copyright

Upon acceptance of an article, authors will be asked to complete a 'Journal Publishing Agreement' (see more information on this). An e-mail will be sent to the corresponding author confirming receipt of the manuscript together with a 'Journal Publishing Agreement' form or a link to the online version of this agreement.

Subscribers may reproduce tables of contents or prepare lists of articles including abstracts for internal circulation within their institutions. Permission of the Publisher is required for resale or distribution outside the institution and for all other derivative works, including compilations and translations. If excerpts from other copyrighted works are included, the author(s) must obtain written permission from the copyright owners and credit the source(s) in the article. Elsevier has preprinted forms for use by authors in these cases.

For gold open access articles: Upon acceptance of an article, authors will be asked to complete an 'Exclusive License Agreement' (more information). Permitted third party reuse of gold open access articles is determined by the author's choice of user license.

Author rights

As an author you (or your employer or institution) have certain rights to reuse your work. More information.

Elsevier supports responsible sharing
Find out how you can share your research published in Elsevier journals.

Role of the funding source

You are requested to identify who provided financial support for the conduct of the research and/or preparation of the article and to briefly describe the role of the sponsor(s), if any, in study design; in the collection, analysis and interpretation of data; in the writing of the report; and in the decision to submit the article for publication. If the funding source(s) had no such involvement then this should be stated.

Open access

Please visit our Open Access page for more information.

Elsevier Researcher Academy
Researcher Academy is a free e-learning platform designed to support early and mid-career researchers throughout their research journey. The "Learn" environment at Researcher Academy offers several interactive modules, webinars, downloadable guides and resources to guide you through the process of writing for research and going through peer review. Feel free to use these free resources to improve your submission and navigate the publication process with ease.

Language (usage and editing services)
Please write your text in good English (American or British usage is accepted, but not a mixture of these). Authors who feel their English language manuscript may require editing to eliminate possible grammatical or spelling errors and to conform to correct scientific English may wish to use the English Language Editing service available from Elsevier's Author Services.

Submission

Submission to this journal proceeds totally online and you will be guided stepwise through the creation and uploading of your files. The system automatically converts source files to a single PDF file of the article, which is used in the peer-review process. Please note that even though manuscript source files are converted to PDF files at submission for the review process, these source files are needed for further processing after acceptance. All correspondence, including notification of the Editor's decision and requests for revision, takes place by e-mail removing the need for a paper trail. Please submit your paper with double line spacing and line number.
Authors are encouraged to additionally embed low res versions of their images and captions at appropriate places within the main body of their text.

Submit your article

Please submit your article via http://ees.elsevier.com/geomor

Referees

Please submit the names and institutional e-mail addresses of several potential referees. For more details, visit our Support site. Note that the editor retains the sole right to decide whether or not the suggested reviewers are used.

PREPARATION

NEW SUBMISSIONS

Submission to this journal proceeds totally online and you will be guided stepwise through the creation and uploading of your files. The system automatically converts your files to a single PDF file, which is used in the peer-review process.
As part of the Your Paper Your Way service, you may choose to submit your manuscript as a single file to be used in the refereeing process. This can be a PDF file or a Word document, in any format or lay-out that can be used by referees to evaluate your manuscript. It should contain high enough quality figures for refereeing. If you prefer to do so, you may still provide all or some of the source files at the initial submission. Please note that individual figure files larger than 10 MB must be uploaded separately.

References

There are no strict requirements on reference formatting at submission. References can be in any style or format as long as the style is consistent. Where applicable, author(s) name(s), journal title/ book title, chapter title/article title, year of publication, volume number/book chapter and the article number or pagination must be present. Use of DOI is highly encouraged. The reference style used by the journal will be applied to the accepted article by Elsevier at the proof stage. Note that missing data will be highlighted at proof stage for the author to correct.

Formatting requirements

There are no strict formatting requirements but all manuscripts must contain the essential elements needed to convey your manuscript, for example Abstract, Keywords, Introduction, Materials and Methods, Results, Conclusions, Artwork and Tables with Captions.
If your article includes any Videos and/or other Supplementary material, this should be included in your initial submission for peer review purposes.
Divide the article into clearly defined sections.

Figures and tables embedded in text

Please ensure the figures and the tables included in the single file are placed next to the relevant text in the manuscript, rather than at the bottom or the top of the file. The corresponding caption should be placed directly below the figure or table.

Peer review

This journal operates a single blind review process. All contributions will be initially assessed by the editor for suitability for the journal. Papers deemed suitable are then typically sent to a minimum of two independent expert reviewers to assess the scientific quality of the paper. The Editor is responsible for the final decision regarding acceptance or rejection of articles. The Editor's decision is final. More information on types of peer review.

REVISED SUBMISSIONS

Use of word processing software
Regardless of the file format of the original submission, at revision you must provide us with an editable file of the entire article. Keep the layout of the text as simple as possible. Most formatting codes will be removed and replaced on processing the article. The electronic text should be prepared in a way very similar to that of conventional manuscripts (see also the Guide to Publishing with Elsevier). See also the section on Electronic artwork.
To avoid unnecessary errors you are strongly advised to use the 'spell-check' and 'grammar-check' functions of your word processor.

LaTeX
You are recommended to use the Elsevier article class elsarticle.cls to prepare your manuscript and BibTeX to generate your bibliography.
Our LaTeX site has detailed submission instructions, templates and other information.

Article structure

Subdivision - numbered sections
Divide your article into clearly defined and numbered sections. Subsections should be numbered 1.1 (then 1.1.1, 1.1.2, ...), 1.2, etc. (the abstract is not included in section numbering). Use this numbering also for internal cross-referencing: do not just refer to 'the text'. Any subsection may be given a brief heading. Each heading should appear on its own separate line.

Please ensure the text of your paper is double-spaced and has consecutive line numbering this is an essential peer review requirement.

Introduction
State the objectives of the work and provide an adequate background, avoiding a detailed literature survey or a summary of the results.
Regional setting:
For papers that focus on an area, provide a brief synopsis of the physical and geological characteristics of the area, sufficient to give the new work context, but again avoid a detailed literature survey.

Material and methods
Provide sufficient details to allow the work to be reproduced by an independent researcher. Methods that are already published should be summarized, and indicated by a reference. If quoting directly from a previously published method, use quotation marks and also cite the source. Any modifications to existing methods should also be described.

Results
Results should be clear and concise. This should highlight the key results (and not repeat material already in figures or tables) and summarise the direct implications of these results.

Discussion
This should explore the significance of the results of the work, not repeat them. A combined Results and Discussion section is often appropriate. Avoid extensive citations and discussion of published literature.It may include limited speculation, that will not appear in the conclusions.

Conclusions
The main conclusions of the study may be presented in a short Conclusions section, which may stand alone or form a subsection of a Discussion or Results and Discussion section.

Acknowledgements
Collate acknowledgements in a separate section at the end of the article before the references and do not, therefore, include them on the title page, as a footnote to the title or otherwise. List here those individuals who provided help during the research (e.g., providing language help, writing assistance or proof reading the article, etc.). Place acknowledgements, including information on grants received, before the references, in a separate section.

Data Availability
Authors are encouraged to include a 'Data Availability' section within the text of their manuscript which is visible in ALL reading formats and may refer to data hosted in ANY repository. It should be placed before the references to provide readers with information about where they can obtain the research data required to reproduce the work reported in the manuscript, and typically consists of a simple sentence giving the URL(s) of and citation(s) to the dataset(s). Full information can be found here.

Appendices
If there is more than one appendix, they should be identified as A, B, etc. Formulae and equations in appendices should be given separate numbering: Eq. (A.1), Eq. (A.2), etc.; in a subsequent appendix, Eq. (B.1) and so on. Similarly for tables and figures: Table A.1; Fig. A.1, etc.

Essential title page information

• ***Title.*** Concise and informative. Titles are often used in information-retrieval systems. Avoid abbreviations and formulae where possible.
• ***Author names and affiliations.*** Please clearly indicate the given name(s) and family name(s) of each author and check that all names are accurately spelled. You can add your name between parentheses in your own script behind the English transliteration. Present the authors' affiliation addresses (where the actual work was done) below the names. Indicate all affiliations with a lower-case superscript letter immediately after the author's name and in front of the appropriate address. Provide the full postal address of each affiliation, including the country name and, if available, the e-mail address of each author.
• ***Corresponding author.*** Clearly indicate who will handle correspondence at all stages of refereeing and publication, also post-publication. This responsibility includes answering any future queries about Methodology and Materials. **Ensure that the e-mail address is given and that contact details are kept up to date by the corresponding author.**
• ***Present/permanent address.*** If an author has moved since the work described in the article was done, or was visiting at the time, a 'Present address' (or 'Permanent address') may be indicated as a footnote to that author's name. The address at which the author actually did the work must be retained as the main, affiliation address. Superscript Arabic numerals are used for such footnotes.

Highlights

Highlights are mandatory for this journal as they help increase the discoverability of your article via search engines. They consist of a short collection of bullet points that capture the novel results of your research as well as new methods that were used during the study (if any). Please have a look at the examples here: example Highlights.

Highlights should be submitted in a separate editable file in the online submission system. Please use 'Highlights' in the file name and include 3 to 5 bullet points (maximum 85 characters, including spaces, per bullet point).

Abstract

A concise and factual abstract is required. The abstract should state briefly the purpose of the research, the principal results and major conclusions. An abstract is often presented separately from the article, so it must be able to stand alone. For this reason, References should be avoided, but if essential, then cite the author(s) and year(s). Also, non-standard or uncommon abbreviations should be avoided, but if essential they must be defined at their first mention in the abstract itself.

Graphical abstract
Although a graphical abstract is optional, its use is encouraged as it draws more attention to the online article. The graphical abstract should summarize the contents of the article in a concise, pictorial form designed to capture the attention of a wide readership. Graphical abstracts should be submitted as a separate file in the online submission system. Image size: Please provide an image with a minimum of 531 × 1328 pixels (h × w) or proportionally more. The image should be readable at a size of 5 × 13 cm using a regular screen resolution of 96 dpi. Preferred file types: TIFF, EPS, PDF or MS Office files. You can view Example Graphical Abstracts on our information site.
Authors can make use of Elsevier's Illustration Services to ensure the best presentation of their images and in accordance with all technical requirements.

Keywords

Immediately after the abstract, provide a maximum of 6 keywords, using American spelling and avoiding general and plural terms and multiple concepts (avoid, for example, 'and', 'of'). Be sparing with abbreviations: only abbreviations firmly established in the field may be eligible. These keywords will be used for indexing purposes.

Abbreviations
Define abbreviations that are not standard in this field in a footnote to be placed on the first page of the article. Such abbreviations that are unavoidable in the abstract must be defined at their first mention there, as well as in the footnote. Ensure consistency of abbreviations throughout the article.

Formatting of funding sources
List funding sources in this standard way to facilitate compliance to funder's requirements:

Funding: This work was supported by the National Institutes of Health [grant numbers xxxx, yyyy]; the Bill & Melinda Gates Foundation, Seattle, WA [grant number zzzz]; and the United States Institutes of Peace [grant number aaaa].

It is not necessary to include detailed descriptions on the program or type of grants and awards. When funding is from a block grant or other resources available to a university, college, or other research institution, submit the name of the institute or organization that provided the funding.

If no funding has been provided for the research, please include the following sentence:

This research did not receive any specific grant from funding agencies in the public, commercial, or not-for-profit sectors.

Units
Follow internationally accepted rules and conventions: use the international system of units (SI). If other units are mentioned, please give their equivalent in SI.

Math formulae

Present simple formulae in the line of normal text where possible and use the solidus (/) instead of a horizontal line for small fractional terms, e.g., X/Y. In principle, variables are to be presented in italics. Powers of e are often more conveniently denoted by exp. Number consecutively any equations that have to be displayed separately from the text (if referred to explicitly in the text).

Occasionally authors may experience problems with the conversion of equations in their Word file to PDF. If your submission contains equations created using Microsoft Word 2007, please use the link https://service.elsevier.com/app/answers/detail/a_id/302/ ,which will help you to solve the problem.

Footnotes
Footnotes should be used sparingly. Number them consecutively throughout the article. Many word processors build footnotes into the text, and this feature may be used. Should this not be the case, indicate the position of footnotes in the text and present the footnotes themselves separately at the end of the article.

Artwork

Electronic artwork
General points
• Make sure you use uniform lettering and sizing of your original artwork.
• Preferred fonts: Arial (or Helvetica), Times New Roman (or Times), Symbol, Courier.
• Number the illustrations according to their sequence in the text.
• Use a logical naming convention for your artwork files.
• Indicate per figure if it is a single, 1.5 or 2-column fitting image.
• For Word submissions only, you may still provide figures and their captions, and tables within a single file at the revision stage.
• Please note that individual figure files larger than 10 MB must be provided in separate source files.

A detailed guide on electronic artwork is available.
You are urged to visit this site; some excerpts from the detailed information are given here.
Formats
Regardless of the application used, when your electronic artwork is finalized, please 'save as' or convert the images to one of the following formats (note the resolution requirements for line drawings, halftones, and line/halftone combinations given below):
EPS (or PDF): Vector drawings. Embed the font or save the text as 'graphics'.
TIFF (or JPG): Color or grayscale photographs (halftones): always use a minimum of 300 dpi.
TIFF (or JPG): Bitmapped line drawings: use a minimum of 1000 dpi.
TIFF (or JPG): Combinations bitmapped line/half-tone (color or grayscale): a minimum of 500 dpi is required.
Please do not:
• Supply files that are optimized for screen use (e.g., GIF, BMP, PICT, WPG); the resolution is too low.
• Supply files that are too low in resolution.

• Submit graphics that are disproportionately large for the content.

Color artwork
Please make sure that artwork files are in an acceptable format (TIFF, EPS or MS Office files) and with the correct resolution. If, together with your accepted article, you submit usable color figures then Elsevier will ensure, at no additional charge, that these figures will appear in color on the Web (e.g., ScienceDirect and other sites) regardless of whether or not these illustrations are reproduced in color in the printed version. **For color reproduction in print, you will receive information regarding the costs from Elsevier after receipt of your accepted article**. Please indicate your preference for color in print or on the Web only. For further information on the preparation of electronic artwork, please see https://www.elsevier.com/artworkinstructions.

Please note:Figures should be designed in a form that will reproduce in greyscale in the print version of the journal. Captions and statements in the text relating to figures should be written with this in mind. Material submitted in colour will be reproduced in colour on the web version free of charge, but if authors wish to have colour in the print version, page charges will be applicable."

For the journal Geomorphology, the need to have useful colour and greyscale figures is especially acute. During the submission process, authors will be asked to upload both colour and greyscale versions of their figures, and so should be prepared to create both versions accordingly. Authors may need to print or view their images in greyscale to assess their meaningfulness in this format. In special circumstances, where it is impossible for an author to prepare a meaningful greyscale version of a colour figure, Editors will be able to arrange for print colour charges to be waived.

Figure captions
Ensure that each illustration has a caption. A caption should comprise a brief title (**not** on the figure itself) and a description of the illustration. Keep text in the illustrations themselves to a minimum but explain all symbols and abbreviations used.

Text graphics
Text graphics may be embedded in the text at the appropriate position. See further under Electronic artwork.

Tables

Please submit tables as editable text and not as images. Tables can be placed either next to the relevant text in the article, or on separate page(s) at the end. Number tables consecutively in accordance with their appearance in the text and place any table notes below the table body. Be sparing in the use of tables and ensure that the data presented in them do not duplicate results described elsewhere in the article. Please avoid using vertical rules and shading in table cells.

References

Citation in text
Please ensure that every reference cited in the text is also present in the reference list (and vice versa). Any references cited in the abstract must be given in full. Unpublished results and personal communications are not recommended in the reference list, but may be mentioned in the text. If these references are included in the reference list they should follow the standard reference style of the journal and should include a substitution of the publication date with either 'Unpublished results' or 'Personal communication'. Citation of a reference as 'in press' implies that the item has been accepted for publication.

Web references
As a minimum, the full URL should be given and the date when the reference was last accessed. Any further information, if known (DOI, author names, dates, reference to a source publication, etc.), should also be given. Web references can be listed separately (e.g., after the reference list) under a different heading if desired, or can be included in the reference list.

Data references
This journal encourages you to cite underlying or relevant datasets in your manuscript by citing them in your text and including a data reference in your Reference List. Data references should include the following elements: author name(s), dataset title, data repository, version (where available), year, and global persistent identifier. Add [dataset] immediately before the reference so we can properly identify it as a data reference. The [dataset] identifier will not appear in your published article.

References in a special issue
Please ensure that the words 'this issue' are added to any references in the list (and any citations in the text) to other articles in the same Special Issue.

Reference management software
Most Elsevier journals have their reference template available in many of the most popular reference management software products. These include all products that support Citation Style Language styles, such as Mendeley. Using citation plug-ins from these products, authors only need to select the appropriate journal template when preparing their article, after which citations and bibliographies will be automatically formatted in the journal's style. If no template is yet available for this journal, please follow the format of the sample references and citations as shown in this Guide. If you use reference management software, please ensure that you remove all field codes before submitting the electronic manuscript. More information on how to remove field codes from different reference management software.

Users of Mendeley Desktop can easily install the reference style for this journal by clicking the following link:
http://open.mendeley.com/use-citation-style/geomorphology
When preparing your manuscript, you will then be able to select this style using the Mendeley plug-ins for Microsoft Word or LibreOffice.

Reference formatting
There are no strict requirements on reference formatting at submission. References can be in any style or format as long as the style is consistent. Where applicable, author(s) name(s), journal title/ book title, chapter title/article title, year of publication, volume number/book chapter and the article number or pagination must be present. Use of DOI is highly encouraged. The reference style used by the journal will be applied to the accepted article by Elsevier at the proof stage. Note that missing data will be highlighted at proof stage for the author to correct. If you do wish to format the references yourself they should be arranged according to the following examples:

Reference style
Text: All citations in the text should refer to:
1. *Single author:* the author's name (without initials, unless there is ambiguity) and the year of publication;
2. *Two authors:* both authors' names and the year of publication;
3. *Three or more authors:* first author's name followed by 'et al.' and the year of publication.
Citations may be made directly (or parenthetically). Groups of references can be listed either first alphabetically, then chronologically, or vice versa.
Examples: 'as demonstrated (Allan, 2000a, 2000b, 1999; Allan and Jones, 1999)…. Or, as demonstrated (Jones, 1999; Allan, 2000)… Kramer et al. (2010) have recently shown …'
List: References should be arranged first alphabetically and then further sorted chronologically if necessary. More than one reference from the same author(s) in the same year must be identified by the letters 'a', 'b', 'c', etc., placed after the year of publication.
Examples:
Reference to a journal publication:
Van der Geer, J., Hanraads, J.A.J., Lupton, R.A., 2010. The art of writing a scientific article. J. Sci. Commun. 163, 51–59. https://doi.org/10.1016/j.Sc.2010.00372.
Reference to a journal publication with an article number:
Van der Geer, J., Hanraads, J.A.J., Lupton, R.A., 2018. The art of writing a scientific article. Heliyon. 19, e00205. https://doi.org/10.1016/j.heliyon.2018.e00205.
Reference to a book:
Strunk Jr., W., White, E.B., 2000. The Elements of Style, fourth ed. Longman, New York.
Reference to a chapter in an edited book:
Mettam, G.R., Adams, L.B., 2009. How to prepare an electronic version of your article, in: Jones, B.S., Smith , R.Z. (Eds.), Introduction to the Electronic Age. E-Publishing Inc., New York, pp. 281–304.
Reference to a website:
Cancer Research UK, 1975. Cancer statistics reports for the UK. http://www.cancerresearchuk.org/aboutcancer/statistics/cancerstatsreport/ (accessed 13 March 2003).
Reference to a dataset:
[dataset] Oguro, M., Imahiro, S., Saito, S., Nakashizuka, T., 2015. Mortality data for Japanese oak wilt disease and surrounding forest compositions. Mendeley Data, v1. https://doi.org/10.17632/xwj98nb39r.1.

Journal abbreviations source
Journal names should be abbreviated according to the List of Title Word Abbreviations.

Video
Elsevier accepts video material and animation sequences to support and enhance your scientific research. Authors who have video or animation files that they wish to submit with their article are strongly encouraged to include links to these within the body of the article. This can be done in the same way as a figure or table by referring to the video or animation content and noting in the body text where it should be placed. All submitted files should be properly labeled so that they directly relate to the video file's content. In order to ensure that your video or animation material is directly usable, please provide the file in one of our recommended file formats with a preferred maximum size of 150 MB per file, 1 GB in total. Video and animation files supplied will be published online in the electronic version of your article in Elsevier Web products, including ScienceDirect. Please supply 'stills' with your files: you can choose any frame from the video or animation or make a separate image. These will be used instead of standard icons and will personalize the link to your video data. For more detailed instructions please visit our video instruction pages. Note: since video and animation cannot be embedded in the print version of the journal, please provide text for both the electronic and the print version for the portions of the article that refer to this content.

Data visualization
Include interactive data visualizations in your publication and let your readers interact and engage more closely with your research. Follow the instructions here to find out about available data visualization options and how to include them with your article.

Supplementary material
Supplementary material such as applications, images and sound clips, can be published with your article to enhance it. Submitted supplementary items are published exactly as they are received (Excel or PowerPoint files will appear as such online). Please submit your material together with the article and supply a concise, descriptive caption for each supplementary file. If you wish to make changes to supplementary material during any stage of the process, please make sure to provide an updated file. Do not annotate any corrections on a previous version. Please switch off the 'Track Changes' option in Microsoft Office files as these will appear in the published version.

Research data
This journal requires and enables you to share data that supports your research publication where appropriate, and enables you to interlink the data with your published articles. Research data refers to the results of observations or experimentation that validate research findings. To facilitate reproducibility and data reuse, this journal also encourages you to share your software, code, models, algorithms, protocols, methods and other useful materials related to the project.

Below are a number of ways in which you can associate data with your article or make a statement about the availability of your data when submitting your manuscript. When sharing data in one of these ways, you are expected to cite the data in your manuscript and reference list. Please refer to the "References" section for more information about data citation. For more information on depositing, sharing and using research data and other relevant research materials, visit the research data page.

Data linking
If you have made your research data available in a data repository, you can link your article directly to the dataset. Elsevier collaborates with a number of repositories to link articles on ScienceDirect with relevant repositories, giving readers access to underlying data that gives them a better understanding of the research described.

There are different ways to link your datasets to your article. When available, you can directly link your dataset to your article by providing the relevant information in the submission system. For more information, visit the database linking page.

For supported data repositories a repository banner will automatically appear next to your published article on ScienceDirect.

In addition, you can link to relevant data or entities through identifiers within the text of your manuscript, using the following format: Database: xxxx (e.g., TAIR: AT1G01020; CCDC: 734053; PDB: 1XFN).

Mendeley Data
This journal supports Mendeley Data, enabling you to deposit any research data (including raw and processed data, video, code, software, algorithms, protocols, and methods) associated with your manuscript in a free-to-use, open access repository. During the submission process, after uploading your manuscript, you will have the opportunity to upload your relevant datasets directly to *Mendeley Data*. The datasets will be listed and directly accessible to readers next to your published article online.

For more information, visit the Mendeley Data for journals page.

To maximise the visibility of your data, authors are invited to add a citation to their datasets by including a data reference in their Reference List as per the 'Data References' instructions elsewhere on this page.

Data in Brief
You have the option of converting any or all parts of your supplementary or additional raw data into one or multiple data articles, a new kind of article that houses and describes your data. Data articles ensure that your data is actively reviewed, curated, formatted, indexed, given a DOI and publicly available to all upon publication. You are encouraged to submit your article for *Data in Brief* as an additional item directly alongside the revised version of your manuscript. If your research article is accepted, your data article will automatically be transferred over to *Data in Brief* where it will be editorially reviewed and published in the open access data journal, *Data in Brief*. Please note an open access fee of 600 USD is payable for publication in *Data in Brief*. Full details can be found on the Data in Brief website. Please use this template to write your Data in Brief.

MethodsX
You have the option of converting relevant protocols and methods into one or multiple MethodsX articles, a new kind of article that describes the details of customized research methods. Many researchers spend a significant amount of time on developing methods to fit their specific needs or setting, but often without getting credit for this part of their work. MethodsX, an open access journal, now publishes this information in order to make it searchable, peer reviewed, citable and reproducible. Authors are encouraged to submit their MethodsX article as an additional item directly alongside the revised version of their manuscript. If your research article is accepted, your methods article will automatically be transferred over to MethodsX where it will be editorially reviewed. Please note an open access fee is payable for publication in MethodsX. Full details can be found on the MethodsX website. Please use this template to prepare your MethodsX article.

Data statement
To foster transparency, we require you to state the availability of your data in your submission if your data is unavailable to access or unsuitable to post. This may also be a requirement of your funding body or institution. You will have the opportunity to provide a data statement during the submission process. The statement will appear with your published article on ScienceDirect. For more information, visit the Data Statement page..

AFTER ACCEPTANCE

Online proof correction

To ensure a fast publication process of the article, we kindly ask authors to provide us with their proof corrections within two days. Corresponding authors will receive an e-mail with a link to our online proofing system, allowing annotation and correction of proofs online. The environment is similar to MS Word: in addition to editing text, you can also comment on figures/tables and answer questions from the Copy Editor. Web-based proofing provides a faster and less error-prone process by allowing you to directly type your corrections, eliminating the potential introduction of errors.
If preferred, you can still choose to annotate and upload your edits on the PDF version. All instructions for proofing will be given in the e-mail we send to authors, including alternative methods to the online version and PDF.
We will do everything possible to get your article published quickly and accurately. Please use this proof only for checking the typesetting, editing, completeness and correctness of the text, tables and figures. Significant changes to the article as accepted for publication will only be considered at this stage with permission from the Editor. It is important to ensure that all corrections are sent back to us in one communication. Please check carefully before replying, as inclusion of any subsequent corrections cannot be guaranteed. Proofreading is solely your responsibility.

Offprints

The corresponding author will, at no cost, receive a customized Share Link providing 50 days free access to the final published version of the article on ScienceDirect. The Share Link can be used for sharing the article via any communication channel, including email and social media. For an extra charge, paper offprints can be ordered via the offprint order form which is sent once the article is accepted for publication. Both corresponding and co-authors may order offprints at any time via Elsevier's Author Services. Corresponding authors who have published their article gold open access do not receive a Share Link as their final published version of the article is available open access on ScienceDirect and can be shared through the article DOI link.

AUTHOR INQUIRIES

Visit the Elsevier Support Center to find the answers you need. Here you will find everything from Frequently Asked Questions to ways to get in touch.
You can also check the status of your submitted article or find out when your accepted article will be published.

ANEXO II

Comprovante de submissão do artigo

Geomorphology

Multitemporal analysis of morphological adjustments in the Lower São Francisco River (Northeast, Brazil): impacts of the Xingó dam on river dynamics

--Manuscript Draft--

Manuscript Number:	
Article Type:	Research Paper
Keywords:	Dam rivers; Fluvial Morphology; Effective Discharge; Climate Changes
Corresponding Author:	Pedro Gomes BRAZIL
First Author:	Pedro Gomes
Order of Authors:	Pedro Gomes
	Felipe Torres Figueiredo
	Gelson Luís Fambrini
	Carlos Henrique Grohmann
	Luiz Alberto Vedana
	Luisa Sampaio Franco
Abstract:	After successive big dams were built throughout the last hundred years, and particularly after the facility of Xingó became operational, the lower course of the São Francisco River (LSFR) suffered a reduction in the average water discharge and is no longer capable of transporting most of the sandy bedload downstream. Nevertheless, assessing the role of dams or climate change on the São Francisco River morphological adjustments is difficult and scarce in the literature. In order to fulfill that gap and evaluate the role of Xingó's reservoir on morphological adjustments, we focused on the characterization and quantification of the morphological adjustments in the LSFR. A time series of satellite images, water, and sediment discharge data were used along seventeen reaches between Xingó and Penedo. To assess the influence of climate change along the drainage basin, we carried out a linear regression approach using a pre and post-dam time series comparison. Our satellite image analysis demonstrates a predominance of internal adjustments to the channel over external ones, with low values of lateral migration rate and slight variation in channel sinuosity. After the construction of the Xingó dam, the percentage of sandy bars remained constant in the groups closest to the dam (G1 and G2), while G3 presented an increase in bedforms. However, with the decrease in water discharges accompanied by rainfall in the river basin, sediments settled closer to the dam. This process is also responsible for increasing the channel interlace rate in the LSFR. During the prolonged drought (2013-present), the most significant decreases in channel width occurred in all LSFR reaches. This dry period was responsible for a 40.4% decrease in discharges in the post-Xingó period, representing the primary control over the decrease in water discharge affecting fluvial morphological elements downstream of Xingó. Thus, the reduction of Xingó's and other upstream dam outflows is essentially a consequence of lower rainfall in the whole drainage basin.
Suggested Reviewers:	José Cândido Stevaux josecstevaux@gmail.com Specialist in geomorphology of Brazilian rivers with articles and book published on the subject.
	Edgardo Manuel Latrubesse latrubesse@austin.utexas.edu Specialist in fluvial geomorphology with international recognition. It has relevant works on Brazilian rivers and also on the São Francisco river, object of study of this work.

ANEXO III

Justificativa da participação dos coautores

Em acordo à resolução 01/2018 do colegiado do PGAB, segue a justificativa da participação dos coautores no artigo submetido à revista *Geomorphology*,

Gelson Luís Fambrini: o coautor contribuiu com materiais de consultorias realizadas pelo mesmo no rio São Francisco, assim como no debate sobre rios barrados e sobre os impactos que a barragem de Xingó causou no baixo curso do rio.

Carlos Henrique Grohmann: o coautor contribui com a tradução para a língua inglesa do manuscrito e foi fundamental no debate e ajustes sobre os métodos aplicados nesse trabalho, garantindo que estes fossem utilizados com uma melhor acurácia.

Luís Alberto Vedana: o coautor foi fundamental no debate e ajustes sobre os métodos aplicados nesse trabalho, garantindo que estes fossem utilizados com uma melhor acurácia.

Luisa Sampaio Franco: a coautora viabilizou e foi responsável pela aquisição de parte dos dados cd campo, mais precisamente fotografias aéreas na área de estudo, também contribuiu com extração de dados de imagens de satélite, edição de figuras e na discussão sobre resultados obtidos.

APÊNDICES

Porcentagem de barras de meio de canal

Ano das imagens de satélite	Trechos																
	R1	R2	R3	R4	R5	R6	R7	R8	R9	R10	R11	R12	R13	R14	R15	R16	R17
1985	1.3	0.0	0.2	0.4	0.4	26.7	5.6	14.7	8.9	0.0	1.6	12.4	26.0	26.2	30.9	35.7	25.2
1992	0.7	0.0	0.2	0.3	2.2	26.3	7.5	13.7	5.3	2.1	1.8	14.4	25.6	19.0	28.9	39.0	27.5
1996	0.6	0.0	0.7	1.2	1.4	19.3	8.5	14.9	10.9	3.6	7.6	9.1	32.8	25.1	30.7	38.0	28.7
1998	1.0	0.0	0.5	0.8	1.5	17.3	6.8	12.9	5.3	2.8	6.9	17.7	32.1	24.7	31.1	39.5	28.4
2001	1.9	0.1	1.1	2.8	3.1	19.5	3.3	14.5	11.6	0.8	10.8	10.1	33.6	27.9	30.7	39.4	29.3
2003	0.9	1.0	1.7	2.8	3.0	20.6	3.2	8.1	10.7	2.6	14.4	15.6	35.7	30.8	34.5	44.3	30.2
2004	1.8	0.2	1.7	3.1	3.4	21.1	4.6	9.1	11.4	2.8	14.3	12.2	33.3	30.7	30.5	39.5	26.8
2009	0.3	0.9	1.2	1.2	1.8	20.9	5.0	13.4	8.4	12.2	12.8	9.8	30.4	31.0	36.4	45.1	31.4
2011	0.4	0.8	1.5	2.0	1.9	22.3	5.9	14.0	12.6	14.7	15.0	12.6	32.6	29.8	35.0	46.1	33.3
2013	3.3	0.2	2.0	4.1	4.2	24.2	12.0	10.8	19.0	19.0	17.5	19.5	26.9	37.8	29.7	46.2	33.4
2018	6.8	1.2	4.0	3.3	13.7	34.7	20.0	14.5	23.1	22.5	30.8	26.2	39.4	32.9	16.5	49.5	35.4
2020	0.5	0.4	0.5	0.1	1.6	25.5	5.0	12.9	16.1	18.0	14.9	22.2	31.9	32.2	35.2	51.4	34.7

Sinuosidade do canal

Ano das imagens de satélite	Trechos																
	R1	R2	R3	R4	R5	R6	R7	R8	R9	R10	R11	R12	R13	R14	R15	R16	R17
1985	1.1	1.0	1.0	1.0	1.0	1.1	1.1	1.1	1.0	1.2	1.2	1.1	1.1	1.1	1.1	1.4	1.1
1992	1.1	1.0	1.0	1.0	1.0	1.1	1.1	1.1	1.0	1.2	1.2	1.1	1.1	1.1	1.1	1.4	1.1
1996	1.1	1.0	1.0	1.0	1.0	1.1	1.1	1.1	1.1	1.2	1.2	1.1	1.1	1.2	1.1	1.4	1.1
1998	1.1	1.0	1.0	1.0	1.0	1.0	1.1	1.1	1.1	1.2	1.2	1.1	1.1	1.1	1.1	1.4	1.1
2001	1.1	1.0	1.0	1.0	1.0	1.1	1.1	1.1	1.1	1.2	1.2	1.1	1.1	1.2	1.1	1.4	1.1
2003	1.1	1.0	1.0	1.0	1.0	1.1	1.1	1.1	1.1	1.2	1.2	1.1	1.1	1.2	1.1	1.4	1.1
2004	1.1	1.0	1.0	1.0	1.0	1.0	1.1	1.1	1.1	1.2	1.2	1.1	1.1	1.2	1.1	1.4	1.1
2009	1.1	1.0	1.0	1.0	1.0	1.1	1.1	1.1	1.1	1.2	1.2	1.1	1.1	1.2	1.1	1.4	1.1
2011	1.1	1.0	1.0	1.0	1.0	1.1	1.1	1.1	1.0	1.2	1.2	1.1	1.1	1.2	1.1	1.3	1.1
2013	1.1	1.0	1.0	1.0	1.1	1.1	1.1	1.1	1.0	1.2	1.3	1.1	1.1	1.2	1.1	1.4	1.1
2018	1.1	1.1	1.0	1.0	1.1	1.1	1.2	1.1	1.1	1.2	1.3	1.1	1.2	1.2	1.2	1.4	1.1
2020	1.1	1.0	1.0	1.0	1.1	1.1	1.1	1.1	1.1	1.2	1.3	1.1	1.1	1.2	1.2	1.4	1.1

Taxa de entrelaçamento do canal

Ano das imagens de satélite	Trechos																
	R1	R2	R3	R4	R5	R6	R7	R8	R9	R10	R11	R12	R13	R14	R15	R16	R17
1985	1.3	1.0	1.2	1.1	1.2	2.6	1.5	1.8	1.9	1.0	1.6	2.2	2.7	2.9	2.7	2.8	2.7
1992	1.2	1.0	1.2	1.2	1.5	2.8	2.0	2.0	1.9	1.2	1.5	2.1	2.4	2.6	2.5	2.4	2.5
1996	1.1	1.0	1.2	1.2	1.2	2.3	2.2	2.0	2.1	1.4	2.4	2.0	2.8	3.3	2.8	2.3	2.6
1998	1.3	1.1	1.3	1.2	1.3	2.3	1.8	1.8	1.9	1.3	2.4	2.4	2.8	3.3	2.5	2.3	2.6
2001	1.3	1.1	1.2	1.3	1.2	2.8	1.8	1.9	2.1	1.6	2.7	1.9	3.0	3.1	2.7	2.3	2.7
2003	1.2	1.2	1.3	1.4	1.3	2.5	2.0	1.5	2.1	1.5	2.4	2.3	2.9	3.0	2.3	2.5	2.8
2004	1.2	1.1	1.2	1.3	1.3	2.7	2.1	1.8	2.3	1.6	2.4	2.0	2.6	3.0	2.4	2.4	2.3
2009	1.1	1.1	1.3	1.3	1.2	2.7	2.0	2.0	2.6	2.5	2.4	2.0	3.0	3.4	2.7	2.8	2.6
2011	1.1	1.1	1.2	1.3	1.3	2.6	2.0	1.8	2.4	2.2	2.5	2.2	2.7	3.0	2.7	2.8	2.9
2013	1.3	1.1	1.2	1.4	1.4	2.5	2.3	1.9	2.9	2.3	2.2	2.1	2.9	3.3	2.6	2.9	2.9
2018	1.2	1.2	1.4	1.4	1.9	3.3	2.6	2.1	2.3	2.1	2.6	1.8	2.4	2.2	2.3	3.0	2.9
2020	1.1	1.1	1.2	1.2	1.7	3.0	2.4	2.4	3.1	2.7	2.4	2.4	2.9	3.1	2.6	2.9	2.8

Largura do canal

Ano das imagens de satélite	Trechos																
	R1	R2	R3	R4	R5	R6	R7	R8	R9	R10	R11	R12	R13	R14	R15	R16	R17
1985	335	351	586	664	763	1296	919	916	919	737	905	1018	1427	1473	1528	1599	1506
1992	333	349	587	664	787	1308	988	901	932	820	899	1041	1340	1316	1391	1581	1487
1996	283	339	577	655	742	1100	970	875	891	774	876	935	1322	1325	1406	1577	1440
1998	309	350	580	663	754	1123	986	878	925	789	892	1034	1322	1316	1384	1589	1488
2001	280	323	552	629	714	1105	895	855	884	739	874	967	1312	1300	1401	1605	1483
2003	240	320	559	644	728	1097	891	765	895	746	864	895	1294	1282	1360	1586	1478
2004	237	324	557	647	726	1110	924	792	886	752	879	913	1328	1318	1418	1567	1507
2009	298	342	566	646	732	1094	913	863	893	856	858	902	1328	1227	1391	1612	1464
2011	295	338	563	638	739	1093	916	864	918	861	870	891	1329	1246	1411	1638	1464
2013	217	313	543	626	684	1063	850	780	876	827	785	856	1065	1194	1170	1579	1444
2018	171	304	525	579	648	1038	742	661	679	680	698	729	921	769	818	1561	1427
2020	277	346	578	661	738	1058	858	795	873	825	774	844	1050	1014	1090	1558	1423

Taxa de migração lateral

Ano das imagens de satélite	Trechos																
	R1	R2	R3	R4	R5	R6	R7	R8	R9	R10	R11	R12	R13	R14	R15	R16	R17
1985-1992	2.5	1.6	1.1	1.1	3.5	2.1	5.6	2.6	2.9	13.1	2.4	4.7	2.4	12.2	19.7	4.3	4.3
1992-1996	4.9	3.1	2.6	2.1	9.7	28.6	3.2	3.7	5.5	11.0	6.3	21.9	3.0	11.3	5.2	3.1	6.6
1996-1998	8.1	6.3	4.8	4.7	6.9	9.1	7.4	5.3	10.7	9.8	7.3	41.2	4.6	7.8	8.6	6.6	12.2
1998-2001	4.4	5.8	3.9	3.8	6.1	5.1	14.2	3.6	7.2	12.5	5.4	22.3	3.4	3.5	4.8	5.5	12.9
2001-2003	8.6	7.6	4.3	4.3	9.8	4.7	8.8	26.9	5.6	5.4	7.5	16.8	66.2	7.1	11.1	8.8	12.9
2003-2004	12.1	15.2	8.7	9.9	17.6	9.6	13.2	20.1	15.8	23.1	16.5	20.8	9.3	18.6	24.1	12.7	13.6
2004-2009	3.9	4.3	3.6	2.6	3.0	2.0	2.8	10.0	3.8	17.3	6.2	3.9	29.7	8.7	11.2	6.0	24.2
2009-2011	8.7	9.8	7.7	5.7	7.3	5.2	4.8	4.7	7.0	9.6	17.7	10.2	9.5	12.9	17.5	15.8	11.3
2011-2013	10.1	8.0	6.8	4.8	7.8	4.0	10.0	28.8	5.2	5.8	28.2	21.6	66.1	6.5	41.0	6.9	5.9
2013-2018	2.9	2.0	1.5	4.3	2.8	4.8	9.1	10.3	18.9	17.5	9.7	11.9	15.0	45.8	29.5	6.3	2.6
2018-2020	11.7	9.4	8.9	13.6	8.6	11.7	21.7	28.6	37.3	37.9	15.0	29.1	34.8	62.7	74.1	12.5	8.9